ACTA PROTOZOOLOGICA

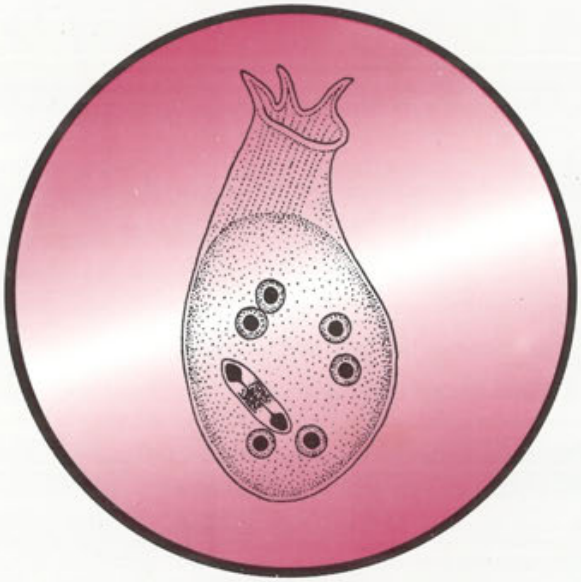

NENCKI INSTITUTE OF EXPERIMENTAL BIOLOGY
WARSAW, POLAND
1996
VOLUME 35 NUMBER 4
ISSN 0065-1583

Polish Academy of Sciences
Nencki Institute of Experimental Biology

ACTA PROTOZOOLOGICA

International Journal on Protistology

ACTA PROTOZOOLOGICA appears quarterly.

The price (including Air Mail postage) of subscription to ACTA PROTOZOOLOGICA at 1997 is: US $ 180.- by institutions and US $ 120.- by individual subscribers. Limited number of back volumes at reduced rate are available. TERMS OF PAYMENT: Cheque, money oder or payment to be made to the Nencki Institute of Experimental Biology. Account Number: 370044-3522-2700-1-73 at Państwowy Bank Kredytowy XIII Oddz. Warszawa, Poland. WITH NOTE: ACTA PROTOZOOLOGICA! For matters regarding ACTA PROTOZOOLOGICA, contact Managing Editor, Nencki Institute of Experimental Biology, ul. Pasteura 3, 02-093 Warszawa, Poland; Fax: 48-22 225342; E-mail: jurek@ameba.nencki.gov.pl

Front cover: *Stephanopogon colpoda.* In: I. B. Raikov - Kariologiya prosteishikh. Izd. Nauka, Leningrad 1967

Printed at the MARBIS, ul. Kombatantów 60, 05-070Sulejówek, Poland

Acta Protozoologica (1996) 35: 257 - 280

ACTA
PROTOZOOLOGICA

Morphology and Morphogenesis of *Lamtostyla edaphoni* Berger and Foissner and *Onychodromopsis flexilis* Stokes, Two Hypotrichs (Protozoa: Ciliophora) from Antarctic Soils

Wolfgang PETZ and Wilhelm FOISSNER

Universität Salzburg, Institut für Zoologie, Salzburg, Austria

Summary. The morphology and morphogenesis of *Lamtostyla edaphoni* Berger and Foissner, 1987 and *Onychodromopsis flexilis* Stokes, 1887 were investigated using silver impregnation and scanning electron microscopy. Stomatogenesis of *L. edaphoni* commences apokinetally near the leftmost transverse cirrus, like in *L. perisincirra*, *L. hyalina* and *L. australis* nov. comb. This distinguishes *Lamtostyla* from *Amphisiella*, whose oral primordium originates parakinetally from the amphisiellid median cirral row (ACR). Five cirral anlagen develop. In the proter, the undulating membranes, the buccal cirrus and the cirrus left of the ACR each provides one streak, two anlagen derive from the ACR. In the opisthe, the oral primordium produces the anlage for the undulating membranes and very likely three cirral streaks; one anlage develops at the posterior end of the ACR. The new ACR is formed by alignment of the two rightmost cirral anlagen, proving that *Lamtostyla* belongs to the Amphisiellidae. Based on these data, improved definitions are given for all amphisiellid genera. *Onychodromopsis flexilis* is redescribed emphasizing somatic variation and the fine structure of the oral apparatus. It has cortical granules and an oxytrichid FVT-cirral pattern but two to three right and one to two left marginal rows. The morphogenetic processes are very similar to those of *Oxytricha granulifera*. In the opisthe, cirrus IV/2, V/3 and V/4 each provides one streak (anlagen 4-6), and three streaks (anlagen 1-3) originate from the oral primordium and/or the posterior ends of anlagen 4-6. The anlagen of the proter originate from the paroral membrane, cirri II/2, III/2 and IV/3, and by splitting of the opisthe's anlagen 5 and 6. Two marginal anlagen each develop in the outer right and inner left marginal row; the inner right and outer left row remain unchanged and are later resorbed. Physiological regeneration resembles development in the proter. However, cirrus V/3 is inactive and the anlagen 5 and 6 originate from cirri IV/2 and V/4, respectively. The data show that *O. flexilis* belongs to the Oxytrichidae and is closely related to *Oxytricha*.

Key words: *Amphisiella*, Antarctica, *Lamtostyla*, morphogenesis, *Onychodromopsis*, soil ciliates.

INTRODUCTION

The interphasic cirral pattern is a rather ambiguous character for the generic classification of hypotrichs because similar patterns may originate by different ontogenetic processes (Eigner and Foissner 1994, Eigner 1995). Therefore, morphogenetic features are increasingly used for distinguishing genera, families and orders (e.g. Borror 1972, 1979; Wicklow 1982; Eigner and Foissner 1994; Eigner 1995). In the present study, we describe the morphogenesis of *Lamtostyla edaphoni*, an amphisiellid hypotrich formerly assigned to the

Address for correspondence: Wolfgang Petz, Universität Salzburg, Institut für Zoologie, Hellbrunnerstrasse 34, A-5020 Salzburg, Austria; FAX: +43 (0) 662 8044 5698; E-mail: WOLFGANG.PETZ@MH.SBG.AC.AT

oxytrichids, and *Onychodromopsis flexilis*, a rather poorly known oxytrichid ciliate.

MATERIALS AND METHODS, TYPE SLIDES

Lamtostyla edaphoni, population I, was collected on 14.11.1993 in the 0-0.5 cm soil layer at Casey Station, Budd Coast, Wilkes Land, continental Antarctica, 66°17'S, 110°32'E, *ca.* 40 m NN. The ice-free surface is a cold-desert soil consisting of weathered charnockitic, granitic and gneissic debris (feelfield) containing very little organic material, mainly from epilithic algae and lichens; macroscopic vegetation is almost lacking. Daytime temperature is generally distinctly higher in soil than in air, i.e. often above freezing; it is usually below zero at night. In winter the area is covered with snow and ice.

Immediately after collection, the soil was saturated with deionized water in glass Petri dishes of 20 cm diameter, providing raw cultures. Morphogenesis was studied in pure cultures initiated with a few specimens from the raw cultures; a mixture of indigenous bacteria and snow algae (*Parmellopsis* sp., *Stichococcus* sp., *Macrochloris* sp.) from cultures was used as food.

Population II was found in moss collected by Dr R. I. L. Smith (British Antarctic Survey) on 23.03.1981 at Charlotte Bay, Andrée Island, maritime Antarctic, 64°31'S, 61°30'W. The air-dried sample was treated with the non-flooded Petri dish method (Foissner 1987).

Onychodromopsis flexilis was found on 18.01.1993 in moss collected by Dr J. Cooper (University of Cape Town) at the coast of Core Bay, Prince Edward Island, Prince Edward Islands, Subantarctic, 46°35'S, 37°56'E (Foissner 1996). A raw culture was established following the non-flooded Petri dish method (Foissner 1987). Morphogenesis was studied in pure cultures using a few crushed wheat grains to support growth of bacteria and small ciliates which served as food organisms.

Live observations and measurements are mostly from field material (*L. edaphoni*) and raw cultures (*O. flexilis*). The live measurements provide only rough estimates but are valuable because specimens usually shrink or contract during fixation and preparation. Biomass was estimated from biovolume using a conversion factor of 1 μm^3 = 1 pg protoplasm (Finlay 1982); volume was calculated using *in vivo* dimensions and applying standard geometric figures to cells. Specimens from raw and/or pure cultures were impregnated with protargol according to Wilbert (1975) or Foissner's Protocol A (1991; population II of *L. edaphoni*), and used for morphometry; counts and measurements were performed at x 1000 magnification (1 measuring unit = 1.3 µm). Drawings were made using a camera lucida. Statistics were calculated according to textbooks. Terminology mainly follows Kahl (1932), Wallengren (1900) and Eigner and Foissner (1994).

Soil pH (in deionized water) was measured using an electrode, humidity and loss-on-ignition (unsifted soil) were assessed after air-drying and heating to 550°C, respectively.

Neotype slides of *O. flexilis* and voucher slides of *L. edaphoni* are deposited in the collection of microscopic slides of the Oberösterreichische Landesmuseum in Linz (LI), Austria.

RESULTS

Morphology and morphogenesis of *Lamtostyla edaphoni* Berger and Foissner, 1987

Morphology (Figs. 1-4, Table 1)

The Antarctic populations are very similar to the type specimens found in a bundle of straw in Austria. Thus, only supplementary observations of population I and a comprehensive morphometric characterization are provided. *In vivo* 55-80 (rarely up to 120) x 18-25 µm, flexible, usually rather transparent at low magnification. Macronuclear nodules *in vivo* 15-18 x 7-8 µm. One to four micronuclei, 2.5-3 µm across *in vivo*, in variable position attached to macronuclear nodules. Contractile vacuole slightly anterior to or in mid-body, on left margin, without collecting canals (Fig. 1). Food vacuoles contained dark and bright green debris (flagellates, algae), rarely fungi. Crawls moderately fast, quickly going back and forth; thigmotactic, i.e. not easy to take with pipette.

Frontal cirri composed of 2-3, all other cirri of 2 basal body rows; however, bases of frontal cirri, buccal cirrus and cirrus left of amphisiellid median cirral row (ACR, Eigner and Foissner 1994; formerly frontal row) slightly elongated and thus also larger (Fig. 2). Very rarely (in 2 out of about 70 specimens), a short second row of 3-4 cirri left of ACR's posterior portion, possibly remnants from last division (Fig. 4). Number of marginal cirri distinctly higher in cultured specimens, but other characters similar to field material (Table 1).

Buccal field very narrow. Adoral zone of membranelles about 30% of body length, cilia about 16 µm long. Undulating membranes often almost parallel, posterior portions rarely optically intersecting; each membrane possibly composed of single basal body row, cilia *in vivo* 5-6µm long. Pharyngeal fibres 9-12µm long in protargol impregnated specimens (Fig. 2).

Occurrence and ecology: *Lamtostyla edaphoni* was found at two sites of the Budd Coast, viz. in mineral debris overgrown with *Usnea sphacelata* (lichen) at Casey Station and in mineral debris covered with *Prasiola crispa* (alga) at the margin of a small melt pool on Shirley Island (Windmill Islands, 66°17'S, 110°29'E, about 15 m NN). At these sites, *L. edaphoni* occurred together with nematodes, rotifers, tardigrades, green flagellates and ciliates, viz. *Colpoda cucullus*, *Colpoda inflata*, *Euplotes* sp.,

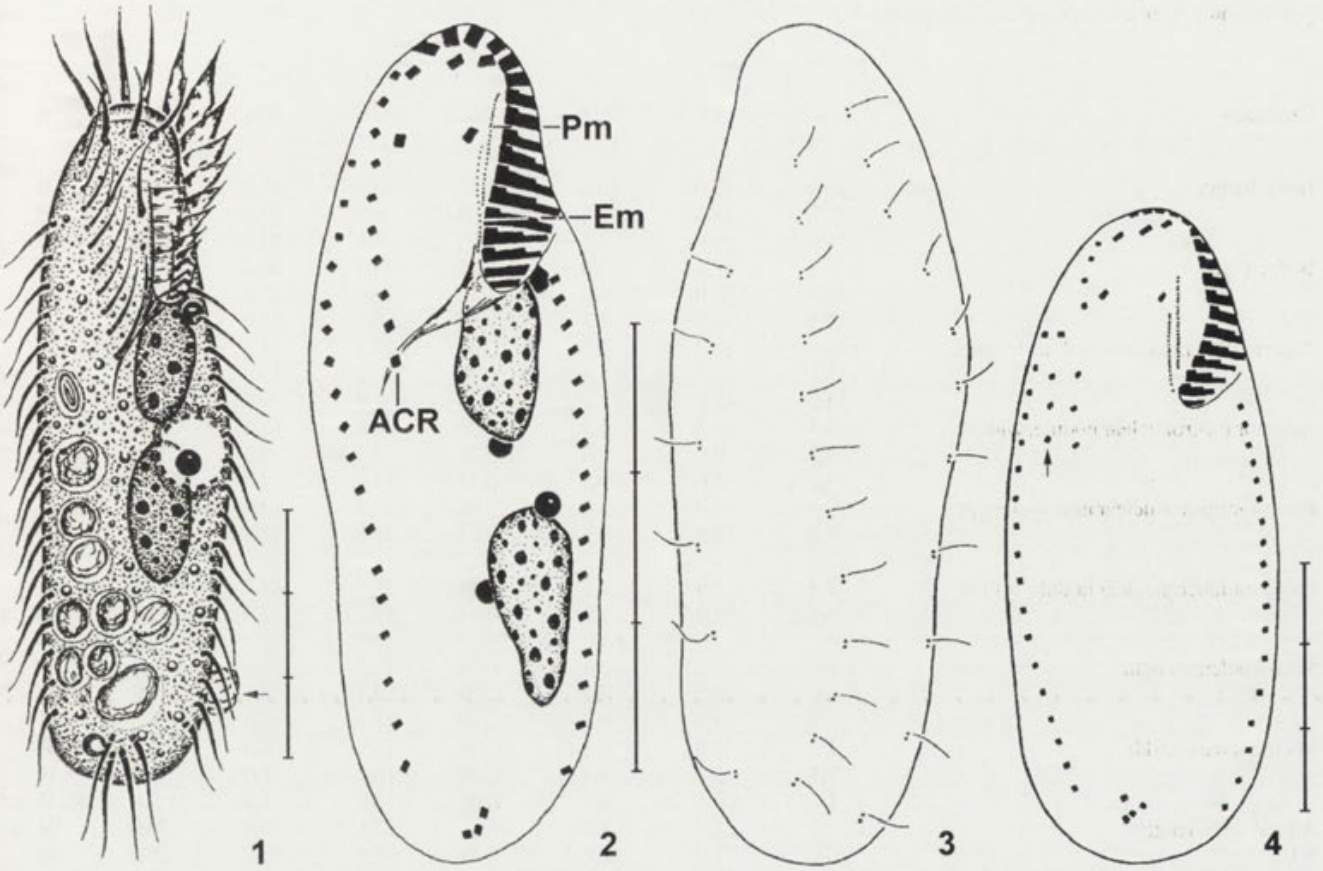

Figs. 1-4. *Lamtostyla edaphoni* from life (1) and after protargol impregnation (2-4). 1 - ventral view of a typical specimen. Arrow marks cytopyge; 2, 3 - infraciliature of ventral and dorsal side of same specimen; 4 - ventral view showing surplus cirral row (arrow) adjacent to ACR. ACR - amphisiellid median cirral row, Em - endoral membrane, Pm - paroral membrane. Scale bar division 10 μm

Holosticha sigmoidea, *Keronopsis muscicola*, *Leptopharynx costatus*, *Odontochlamys* sp., *Pseudochilodonopsis mutabilis*, *Pseudoholophrya terricola*, *Pseudoplatyophrya nana*, *Sathrophilus muscorum*, *Spathidium* sp n. and *S. claviforme*. Environmental parameters in soil: humidity up to 26.6% of wet mass, loss-on-ignition <1-7.8% of dry mass, pH 5.1-6.6. Biomass of 10^6 individuals: 16 mg.

Population II was associated with the moss *Brachythecium austro-salebrosum*.

Comparison with type specimens and related species: The Antarctic specimens are very similar to those of the type population (Berger and Foissner 1987). The most conspicuous difference is the slightly higher number of cirri composing the median cirral row in population I ($\bar{x}$ = 9.5 vs. 8.0), which thus extends slightly beyond the proximal buccal vertex. This number matches that of *L. lamottei* Buitkamp, 1977 which has, however, three cirri left of the ACR, suggesting that it develops six frontoventral anlagen. Other minor differences to the type specimens concern the size of the macronuclear nodules (about 16-17 vs. 9-10 μm) and the position of the contractile vacuole, viz. on left margin vs. displaced towards the midline (Berger and Foissner 1987, 1988).

These differences are considered to be site-specific variations insufficient for separating population I as a distinct taxon. This is sustained by the significantly changed numbers of marginal cirri in specimens from pure cultures (Table 1). Furthermore, the ACR of population II also extends slightly beyond the proximal buccal vertex although its cirral number is the same as in the type specimens (Table 1).

Morphogenesis (Figs. 5-16)

Ontogenesis is very difficult to study in *L. edaphoni* because it is small and all cirri and primordia are very

Table 1. Morphometric characteristics from *Lamtostyla edaphoni*[1]. First line: raw culture of population I; second line: pure culture of population I; third line: raw culture of population II

Character	$\bar{X}$	M	SD	SE	CV	Min	Max	n
Body, length	76.8	78.0	10.4	1.87	13.5	55.0	109.0	31
	79.8	81.0	7.4	2.05	9.3	62.0	92.0	13
	57.5	56.0	3.5	1.06	6.1	52.0	63.0	11
Body, width	27.4	27.0	5.0	0.90	18.3	20.0	39.0	31
	30.8	30.0	4.0	1.12	13.1	25.0	38.0	13
	17.3	17.0	1.9	0.56	10.7	15.0	20.0	11
Anterior macronuclear nodule, length	16.4	16.0	3.6	0.65	22.2	11.0	25.0	31
	18.1	17.8	2.2	0.59	12.2	13.0	22.5	14
	11.8[2]	12.0	1.2	0.35	9.9	9.0	13.0	11
Anterior macronuclear nodule, width	7.4	7.5	1.3	0.22	16.8	5.0	10.0	31
	9.2	9.0	0.9	0.24	9.7	8.0	11.0	14
	4.8[2]	5.0	0.8	0.23	15.6	4.0	6.0	11
Posterior macronuclear nodule, length	17.4	16.0	3.8	0.68	21.7	12.0	26.0	31
	18.5	18.8	3.9	1.03	21.0	11.5	26.0	14
	-[3]	-	-	-	-	-	-	-
Posterior macronuclear nodule, width	7.5	7.0	1.8	0.33	24.6	4.5	12.0	31
	9.4	9.0	1.8	0.47	18.7	7.0	13.0	14
	-[3]	-	-	-	-	-	-	-
Micronucleus, length	2.9	3.0	0.4	0.08	12.9	2.0	4.0	31
	2.6	2.5	0.4	0.09	14.5	2.0	3.0	16
	2.1	2.0	0.3	0.10	15.1	2.0	3.0	11
Micronucleus, width	2.9	3.0	0.4	0.08	12.9	2.0	4.0	31
	2.4	2.5	0.4	0.10	16.3	2.0	3.0	16
	1.6	1.5	0.2	0.06	12.9	1.5	2.0	11
Adoral zone, length	23.2	24.0	3.0	0.55	13.1	16.0	29.0	31
	20.9	21.0	1.8	0.44	8.4	18.0	25.0	16
	17.0	17.0	1.3	0.40	7.9	16.0	20.0	11
Paroral membrane, length	10.3	10.0	1.8	0.33	17.5	7.0	13.5	30
	9.0	9.0	0.9	0.24	10.5	7.0	10.0	15
	-[3]	-	-	-	-	-	-	-
Endoral membrane, length	9.2	9.0	1.1	0.21	12.3	7.0	11.0	28
	7.8	8.0	0.9	0.24	11.4	6.5	9.0	14
	-[3]	-	-	-	-	-	-	-
Apex to posterior end of ACR, distance	29.2	30.0	6.0	1.07	20.4	19.0	38.0	31
	28.0	27.5	3.4	0.88	12.2	23.0	35.0	15
	19.5	19.0	1.6	0.49	8.4	17.0	22.0	11
Macronuclear nodules, number	2.0	2.0	0.2	0.03	8.8	2.0	3.0	31
	2.0	2.0	0	0	0	2.0	2.0	18
	2.0	2.0	0	0	0	2.0	2.0	11
Micronuclei, number	2.0	2.0	0.5	0.09	25.8	1.0	4.0	31
	1.9	2.0	0.5	0.12	25.8	1.0	3.0	17
	2.3	2.0	0.6	0.19	28.5	1.0	3.0	11
Adoral membranelles, number	16.8	17.0	1.0	0.18	6.0	14.0	19.0	31
	17.4	17.0	0.7	0.13	4.1	16.0	19.0	31
	16.1	16.0	0.5	0.16	3.4	15.0	17.0	11
Left marginal cirri, number	17.7	18.0	2.9	0.52	16.4	13.0	26.0	31
	25.4	24.5	3.6	1.05	14.3	20.0	31.0	12
	15.3	15.0	1.9	0.57	12.5	13.0	20.0	11
Right marginal cirri, number	18.2	18.0	1.7	0.31	9.6	15.0	21.0	31
	24.4	24.5	1.7	0.47	7.1	21.0	27.0	14
	15.5	16.0	1.6	0.49	10.5	13.0	18.0	11
Frontal cirri, number	3.0	3.0	0.2	0.03	6.1	2.0	3.0	31
	3.0	3.0	0	0	0	3.0	3.0	18
	3.0	3.0	0	0	0	3.0	3.0	11
Buccal cirri, number	1.0	1.0	0.2	0.03	17.4	1.0	2.0	31
	1.0	1.0	0	0	0	1.0	1.0	20
	1.0	1.0	0	0	0	1.0	1.0	11

Table 1 (con.)

Cirri in ACR, number[4]	9.5	9.0	1.3	0.21	13.3	7.0	13.0	35
	9.9	10.0	1.2	0.32	12.2	8.0	12.0	14
	7.8	7.0	1.1	0.33	13.8	7.0	10.0	11
Transverse cirri, number[5]	4.3	4.0	0.7	0.12	15.1	3.0	6.0	31
	4.4	4.0	0.8	0.19	18.1	3.0	6.0	17
	4.0	4.0	0.6	0.19	15.8	3.0	5.0	11
Dorsal kineties, number	3.0	3.0	0	0	0	3.0	3.0	30
	3.0	3.0	0	0	0	3.0	3.0	15
	3.0	3.0	0	0	0	3.0	3.0	11

[1] Based on randomly selected, protargol impregnated and mounted non-dividers. Measurements in µm. Abbreviations: CV - coefficcient of variation in %, M - median, Max - maximum, Min - minimum, SD - standard deviation, SE - standard error of arithmetic mean, $\bar{x}$ - arithmetic mean. [2] Not discriminated between anterior and posterior nodule. [3] Not determined. [4] Without cirrus left of it. [5] Including ventral cirri ahead of transverse cirri

close together. Thus, the origin of some anlagen could not be clarified unambiguously.

Oral primordium and cirral streaks (Figs. 5-9, 11-13, 15): Stomatogenesis commences with the apokinetal proliferation of basal bodies close above the left transverse cirrus (four cases observed; Fig. 5). The anarchic field then elongates anteriorly to the parental adoral zone. Simultaneously, the posteriormost cirrus of the amphisiellid median cirral row (ACR) disintegrates and a small patch of basal bodies develops posteriorly (Fig. 6). Whether this patch derives from a dedifferentiated ACR-cirrus or originates de novo could not be clarified. Furthermore, we could not determine whether this field is incorporated into the oral primordium or remains independent, forming only cirral anlagen (Figs. 6, 7). The same problems exist in *L. australis* and *L. perisincirra* (Berger et al. 1984, Voss 1992).

Subsequently, the buccal cirrus and the cirrus left of the ACR disaggregate, becoming proter's anlagen 2 and 3, respectively (Figs. 7, 8). Simultaneously, additional cirri dedifferentiate at the posterior end of the ACR, forming opisthe's anlage 5, which terminates near the oral primordium and, respectively, the basal body patch mentioned above (Figs. 7, 8). A further ACR-cirrus then disintegrates anterior to anlage 5, providing streak 4 of the proter (Fig. 8, arrow). The oral anarchic field differentiates membranelles from right to left in a posteriad direction (Fig. 8). Basal bodies right of these align to the primordium for the undulating membranes (anlage 1) and also form cirral anlagen 2 and 3 of the opisthe; some of the anlagen occasionally contact the posterior end of the proter's corresponding streaks (Figs. 8, 9, 11). The origin of the opisthe's anlage 4 could not be clarified unambiguously; very likely, it evolves from the oral primordium as stated in *L. australis* (Voss 1992).

The parental paroral membrane dedifferentiates next and the endoral very likely becomes double-rowed, possibly incorporating basal bodies from the disaggregating paroral, which appears as a loose row extending to the opisthe's oral primordium. Finally, a conspicuous, double-rowed anlage is recognizable, the anterior portion of which becomes the leftmost frontal cirrus, while the posterior portion develops to the new undulating membranes (Figs. 9, 11, 12). Streak 5 of the proter develops anterior to anlage 4, very likely from a dissolving cirrus of the parental ACR (Figs. 9, 11). The streaks subsequently elongate by basal body proliferation and five anlagen each are recognizable in the proter and opisthe (Fig. 11). Cirri differentiate in a posteriad direction as follows (Fig. 12): left frontal cirrus and undulating membranes from anlage 1; middle frontal, buccal and sometimes also one transverse cirrus from anlage 2; right frontal, enlarged cirrus (rarely two) left of ACR and one transverse cirrus from anlage 3; a variable number of ACR-cirri and usually one, respectively, two transverse cirri from anlagen 4 and 5.

When the new transverse cirri organize, anlage 4 migrates backwards and aligns behind streak 5, both forming the new ACR (Figs. 12, 13, 15). Some surplus basal body pairs in the anlagen are apparently resorbed, as are all parental cirri not involved in primordia formation. However, we cannot exclude that some cirri at the anterior end of the old ACR remain because these are always very close to anlage 5 (Figs. 12, 13, 15). The parental adoral zone is apparently not renewed, but the pharyngeal fibres are resorbed and rebuilt during cytokinesis and in postdividers.

Marginal and dorsal anlagen (Figs. 10, 12-16): Most marginal cirri dissolve, forming two separate anlagen in

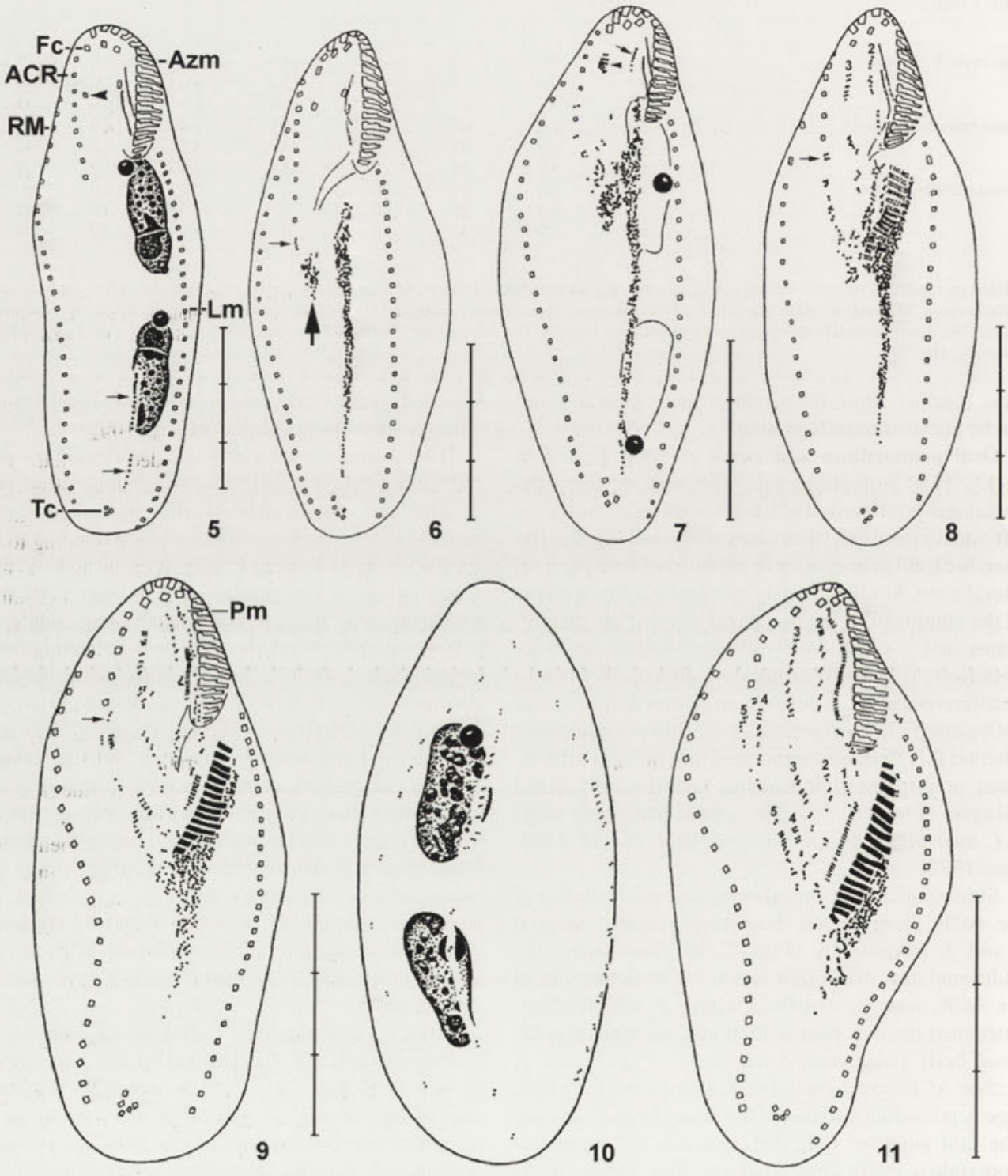

Figs. 5-11. Morphogenesis of *Lamtostyla edaphoni*, protargol impregnation. 5 - very early divider showing origin of oral primordium (arrows). Arrowhead marks cirrus left of ACR; 6, 7 - early dividers showing basal body patch (thick arrow) right of oral primordium. Thin arrows mark disintegrating ACR- and buccal cirrus, respectively; arrowhead denotes disaggregating cirrus left of ACR; 8, 9 - early dividers showing organization of cirral anlagen. Arrows mark anlagen for proter's streak 4 (Fig. 8) and 5 (Fig. 9); 10 - dorsal view of specimen shown in Fig. 9; 11 - middle divider showing five streaks each in proter and opisthe. ACR - amphisiellid median cirral row, Azm - adoral zone of membranelles, Fc - frontal cirri, Lm - left marginal row, Pm - disintegrated paroral membrane, Rm - right marginal row, Tc - transverse cirri; numbers denote cirral anlagen. Scale bar division 10µm

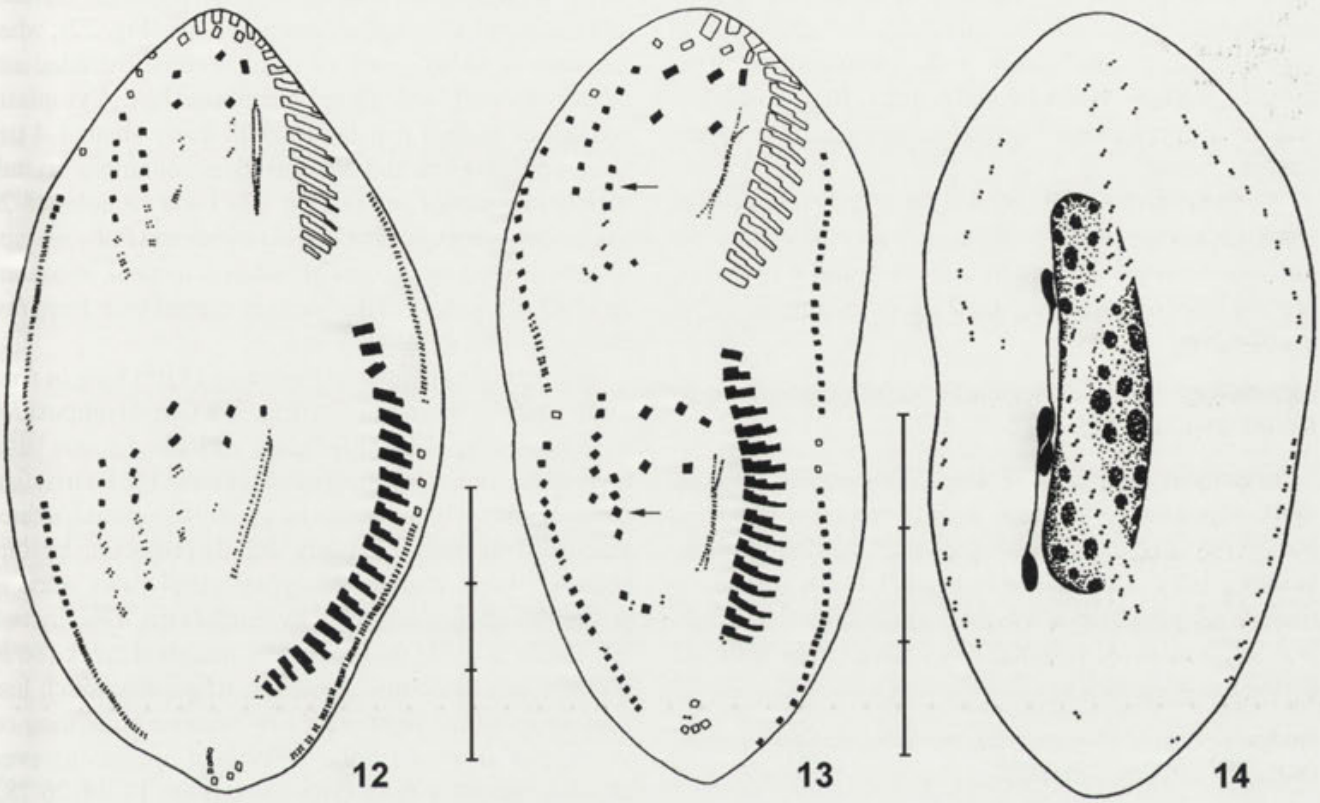

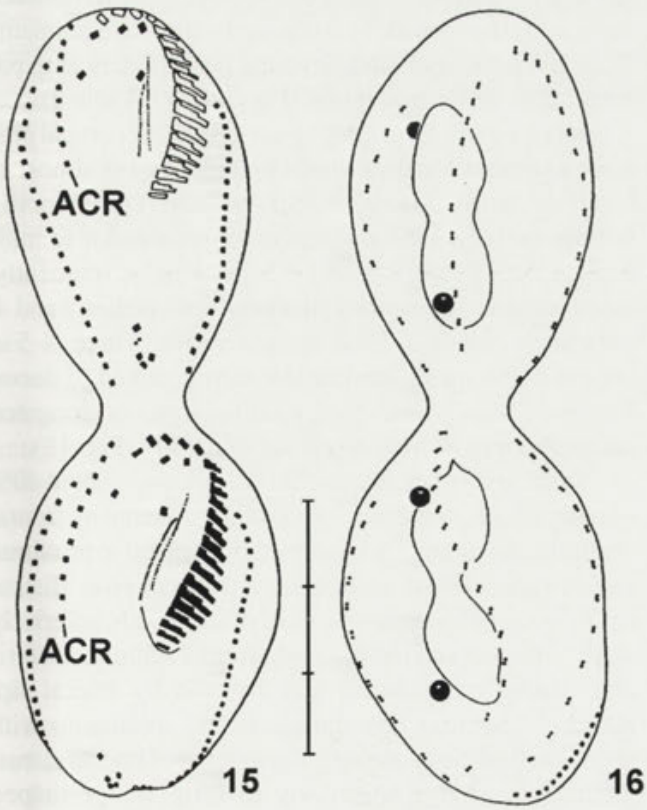

Figs. 12-16. Morphogenesis of *Lamtostyla edaphoni*, protargol impregnation. 12 - middle divider showing segregation of cirri and development of marginal primordia; 13, 14 - ventral and dorsal view of a late divider. Arrows mark migrating anlage 4; 15, 16 - ventral and dorsal view of a very late divider. Anlagen 4 and 5 have aligned one behind the other, producing the amphisiellid median cirral row (ACR). Scale bar division 10μm

each row (Figs. 12, 13). The dorsal kineties develop by intrakinetal basal body proliferation, i.e. according to type 1 of Foissner and Adam (1983), commencing in the anterior portions of rows 2 and 3 (Figs. 10, 14, 16). The anlagen in dorsal kinety 1 appear distinctly later. No caudal cirri are formed.

Nuclear division (Figs. 14, 16): This proceeds as usual, i.e. the micronuclei split once, very rarely twice; the macronuclear nodules first fuse and then divide twice, the second fission being completed after cytokinesis, i.e. in postdividers.

Morphology and morphogenesis of *Onychodromopsis flexilis* Stokes, 1887

Improved diagnosis of *Onychodromopsis* Stokes, 1887: Flexible Oxytrichidae with 18 frontal, ventral and transverse cirri; caudal cirri present. Undulating membranes side by side. Several right and left marginal cirral rows developing from at least two anlagen in a single right and left row each; parental rows completely resorbed during morphogenesis.

Redescription of *Onychodromopsis flexilis* Stokes, 1887 (Figs. 17-32, 70a, Table 2)

Improved diagnosis: Field populations *in vivo* about 90-125 x 40-70 µm, cultured stocks 100-200 x 40-80 µm. Cortical granules colourless, arranged in longitudinal rows. 2-3 right and 1-2 left marginal cirral rows. On average 33 adoral membranelles, 5 transverse cirri, 3 caudal cirri, 6 dorsal kineties, 2 macronuclei and 2 micronuclei. In freshwater and soil.

Redescription (Figs. 17-32, 70a, Table 2): Specimens in pure culture on average 24% larger than in raw culture (mean length 112.8 µm, SD 7.8, CV 6.9, extremes 98, 127 µm; mean width 55.4 µm, SD 6.0, CV 10.8, extremes 41, 70 µm; n = 30). Body very flexible, broadly elliptical and dorsoventrally flattened up to 2:1 (Figs. 17, 20, 21). Macronuclear nodules ellipsoidal; nucleoli spherical to ellipsoidal, 1-4 µm across in protargol slides. Micronuclei almost globular, usually one each in variable position in indentation of macronuclear nodules. Contractile vacuole with two collecting canals in mid-body near left margin. Cortical granules 0.8-1 µm across, arranged in rather narrowly spaced rows underneath entire cell surface as in *Oxytricha granulifera* Foissner and Adam, 1983, colourless and rather compact, stain blue but become not extruded when methyl green-pyronin is added (Figs. 22, 70a), impregnate faintly to intensely with protargol depending on method and bleaching time (Fig. 30). A second type of granules, minute (≤ 0.2 µm) and invisible in live specimens, occurs in great numbers between the larger granules and stains red with methyl green-pyronin (Fig. 22); when the stain is added, many of them become extruded and adhere to cirri and adoral membranelles. Cytoplasm colourless, in field populations with many about 1-4 µm sized lipid droplets and 3-5 µm long, colourless crystals mainly in posterior portion (Fig. 23). Food vacuoles 15-20 µm across, often contain *Colpoda steinii* and *Polytoma* sp.; in cultures feeding also on *Cyclidium glaucoma*, starch and up to 45 µm long, slender bacteria carried over from raw culture. Glides moderately fast.

All cirri of field population about 13 µm long *in vivo*, insert in shallow cortical pits (Fig. 31). Cirral composition as shown in Fig. 18, only slightly variable, i.e. one basal body row more or less may occur in most FVT-cirri; first cirrus of inner left marginal row usually composed of three kineties. Transverse cirri only slightly projecting beyond posterior body margin. Marginal cirral rows open at posterior end, gap occupied by caudal cirri. Usually two left (81%, n = 31) and two right marginal rows (86%, n = 80); left outer row, however, frequently much less conspicuous than right inner row because consisting on average of five cirri only, in 19% of specimens even lacking, one cell with short third row (Figs. 17, 18, 26-28). Rarely, a very short third right marginal row is present, namely 1-7 cirri left of inner row (6%) or 2-3 cirri between inner and outer row (8%); very likely, these are remnants from last generation and/or young postdividers with parental cirri still in resorption (Figs. 28, 57, Table 2).

Dorsal cilia 3-5 µm long, insert in shallow cortical pits, arranged in six kineties (Fig. 19): kineties 1-3 almost as long as body, kinety 4 curved and commencing subequatorially, kinety 5 extends from anterior to mid-body, kinety 6 consists of 4-5 bristles only; frequently, some irregularly arranged cilia between kineties 3 and 4, very likely remnants from last generation. Three (4-5 in six out of 34 specimens) caudal cirri attached to dorsal kineties 1, 2 and 4, inconspicuous because not elongated and composed of four, rarely six cilia only (Fig. 18).

Adoral zone of membranelles conspicuous, about 40% of body length, distal portion ventrally covered by frontal scutum, cilia gradually shortened from distal to proximal end of zone; widest bases about 10 µm *in vivo*. Buccal cavity occupying about one third of cell width, anteriorly slightly curved and merging into frontal scutum, posteriorly gradually deepened and covered by buccal lip. Buccal lip hyaline, bent upright to and continuous with frontal cell surface, commences at level of buccal cirrus, gradually widened posteriorly to form wedge-shaped structure obliquely merging into posterior buccal ver-

Table 2. Morphometric characteristics from *Onychodromopsis flexilis* in pure culture[1]

Character	$\bar{x}$	M	SD	SE	CV	Min	Max
Body, length	139.6	139.0	16.2	2.92	11.6	105	194.0
Body, width	63.1	62.0	9.2	1.65	14.6	43	83.0
Anterior macronuclear nodule,							
length	28.2	27.0	4.8	0.86	17.0	22	38.0
width	15.1	15.0	1.4	0.26	9.5	12	17.5
Posterior macronuclear nodule,							
length	26.8	25.0	4.5	0.8	16.7	22	39.0
width	16.6	17.0	2.0	0.36	11.9	13	22.0
Micronucleus, length	4.4	4.5	0.4	0.07	9.5	4	5.0
Micronucleus, width	4.1	4.0	0.4	0.06	8.4	3	5.0
Adoral zone, length	54.0	54.0	3.3	0.60	6.2	47	61.0
Paroral membrane, length	28.3	29.0	2.2	0.39	7.7	25	32.0
Endoral membrane, length	29.2	29.0	2.6	0.47	9.0	25	35.0
Apex to posterior end of inner							
right marginal row, distance	111.1	109.0	14.9	2.68	13.4	72	152.0
Distance between macronuclear nodules	15.5	16.0	5.1	0.92	33.1	4	27.0
Macronuclear nodules, number	2.0	2.0	0	0	0	2	2.0
Micronuclei, number	2.3	2.0	0.6	0.1	25.3	1	4.0
Adoral membranelles, number	33.0	33.0	1.7	0.3	5.0	30	37.0
Marginal cirri, number in							
outer right row	28.8	29.0	2.2	0.39	7.6	24	33.0
inner right row	17.1	17.0	3.5	0.62	20.3	10	25.0
inner left row	25.6	26.0	2.6	0.46	10.1	20	31.0
outer left row	4.6	5.0	3.7	0.65	79.5	0	13.0
Frontal cirri, number	3.0	3.0	0.2	0.03	6.1	2	3.0
Buccal cirri, number	1.0	1.0	0	0	0	1	1.0
Frontoventral cirri, number[2]	4.0	4.0	0	0	0	4	4.0
Ventral cirri, number	5.0	5.0	0	0	0	5	5.0
Transverse cirri, number	5.0	5.0	0	0	0	5	5.0
Caudal cirri, number	3.2	3.0	0.5	0.08	14.9	3	5.0
Dorsal kineties, number	6.1	6.0	0.2	0.05	3.7	6	7.0
Resting cysts, length[3]	41.0	41.0	2.9	0.65	7.1	36	48.0
Resting cysts, width[3]	39.7	40.0	2.9	0.64	7.2	34	44.0

[1] Based on 31 randomly selected, protargol impregnated and mounted non-dividers. Measurements in µm. Abbreviations: CV - coefficient of variation in %, M - median, Max - maximum, Min - minimum, SD - standard deviation, SE - standard error of arithmetic mean, $\bar{x}$ - arithmetic mean. [2] Excluding frontal and buccal cirri. [3] From three-week-old pure culture, measured *in vivo*

tex; longitudinally bipartite by deep cleft containing proximal two thirds of paroral membrane, right sheet narrower than left (Figs. 31, 32). Paroral membrane anteriorly slightly curved, cilia about 8 µm long. Endoral membrane straight, inserts on right wall of buccal cavity, not recognizable in scanning electron micrographs because underneath buccal lip. Paroral and endoral usually side by side in silvered specimens, posterior portions rarely slightly intersecting in surface view of cell, both very likely composed of dikinetids (Fig. 18). Pharyngeal fibres 30-55 µm long in protargol slides, originate from adoral membranelles and paroral and endoral membrane.

Resting cysts globular to slightly ellipsoidal (Figs. 24, 29; Table 2). Cyst wall colourless, about 2 µm thick, compact; surface studded with about 2 µm long, hyaline spines and sometimes separated by narrow, transparent layer from compact part of wall (Figs. 24, 25, 29). Cyst contents (cell) usually conspicuously lobed, does not occupy entire cyst volume (Fig. 29); however, when cyst is slightly pressed, its contents expand, completely filling interior. Cortex distinctly striated. Cytoplasm contains many 1-3 µm sized, colourless globules. Macronuclear nodules and micronuclei do not fuse (Fig. 24).

Occurrence and ecology: *Onychodromopsis flexilis* was found at two sites of the Prince Edward Islands, viz. in a slightly saline and acidic (pH 6.1) grass sward on rock at the seaward limit of vegetation on Marion Island and in a slightly saline and acidic (pH 6.3) moss sample

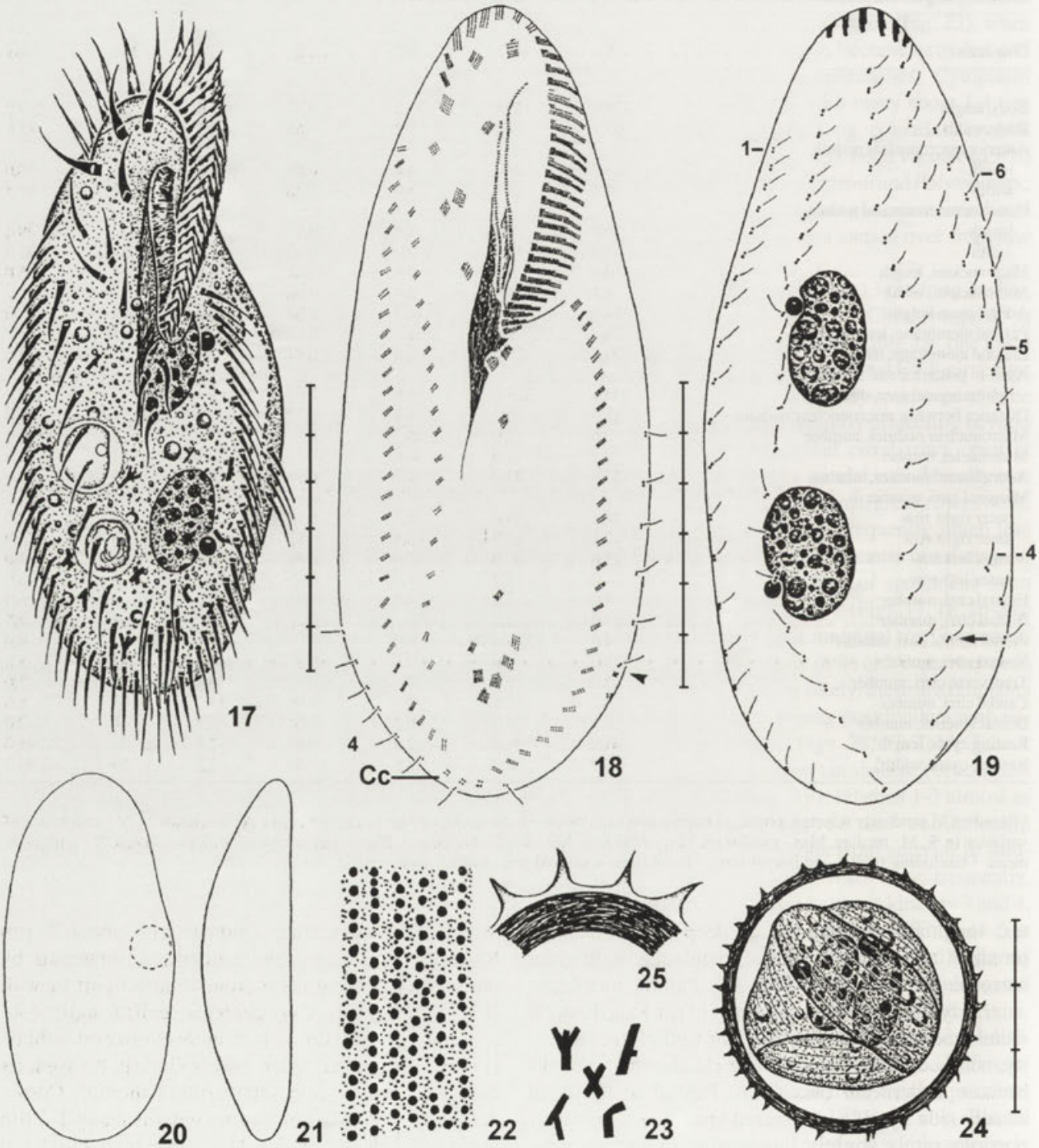

Figs. 17-25. *Onychodromopsis flexilis* from life (17, 20-25) and after protargol impregnation (18, 19). 17 - ventral view of a typical specimen; 18, 19 - infraciliature of ventral and dorsal side of same specimen. Arrowhead marks surplus dorsal kinety seen only in this specimen, arrow denotes interkinetal dorsal dikinetid; 20 - broad specimen; 21 - lateral view; 22 - cortical granulation consisting of small and large granules; 23 - cytoplasmic crystals; 24 - optical section of resting cyst; 25 - detail of cyst wall. Cc - caudal cirri; numbers denote dorsal kineties. Scale bar division 10 µm

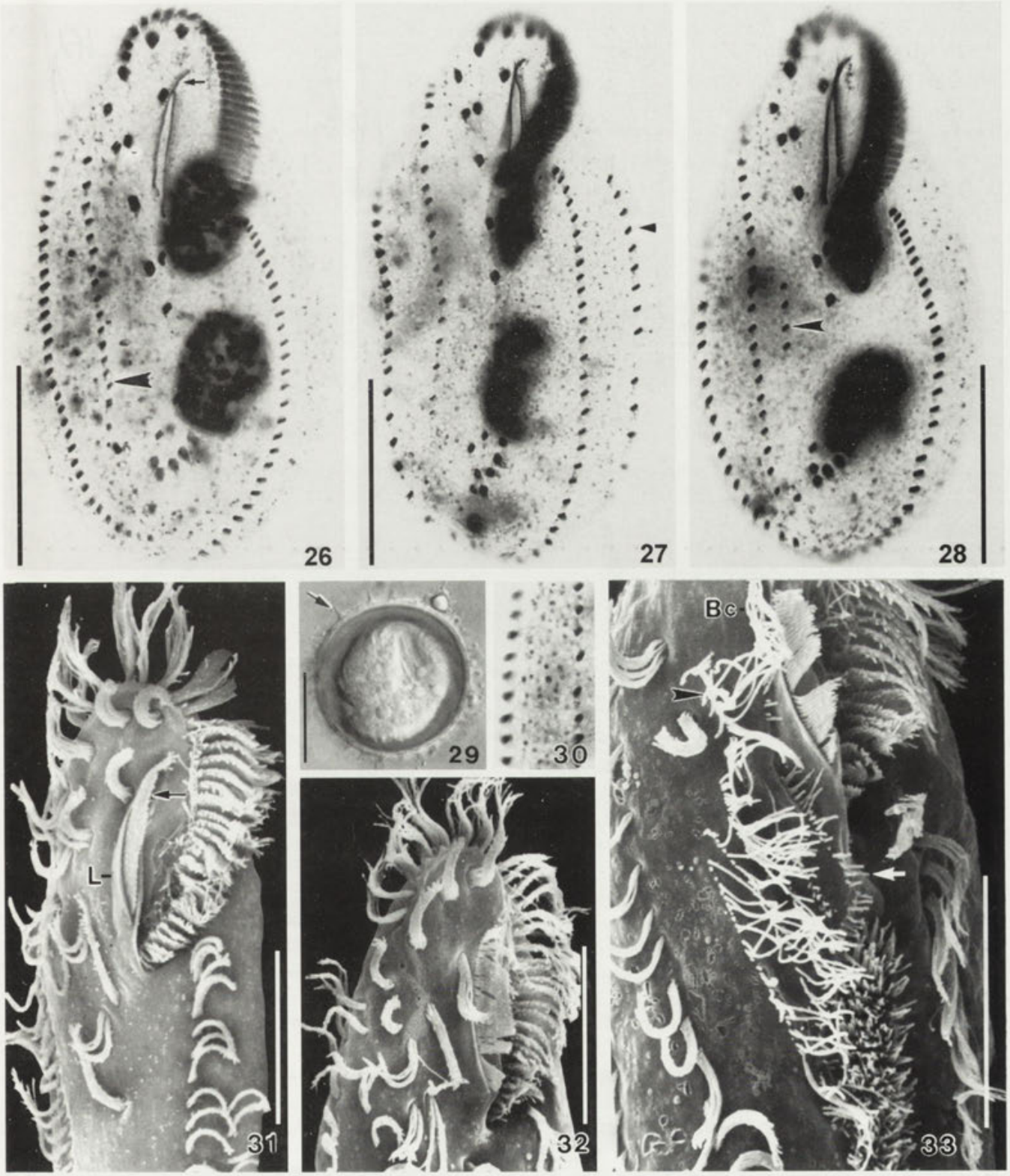

Figs. 26-33. *Onychodromopsis flexilis* from life (29), after protargol impregnation (26-28, 30) and in the scanning electron microscope (31-33). 26, 27, 28 - ventral views. Arrow denotes paroral membrane, black arrowheads mark inner right and outer left marginal row, respectively; white arrowhead indicates surplus right marginal row; 29 - resting cyst, differential interference contrast; 30 - cortical granulation; 31, 32 - ventral views of oral area. Arrow marks paroral membrane inserted in deep furrow of buccal lip; 33 - early divider showing organizing cirral streaks. Opisthe's anlage 2 (arrow) extends anteriad from oral primordium not contacting parental paroral membrane. Arrowhead marks disaggregating cirrus III/2. Bc - dissolving buccal cirrus, L - buccal lip. Bars - 50 µm (Figs. 26-28), 20 µm (Figs. 29, 31-33)

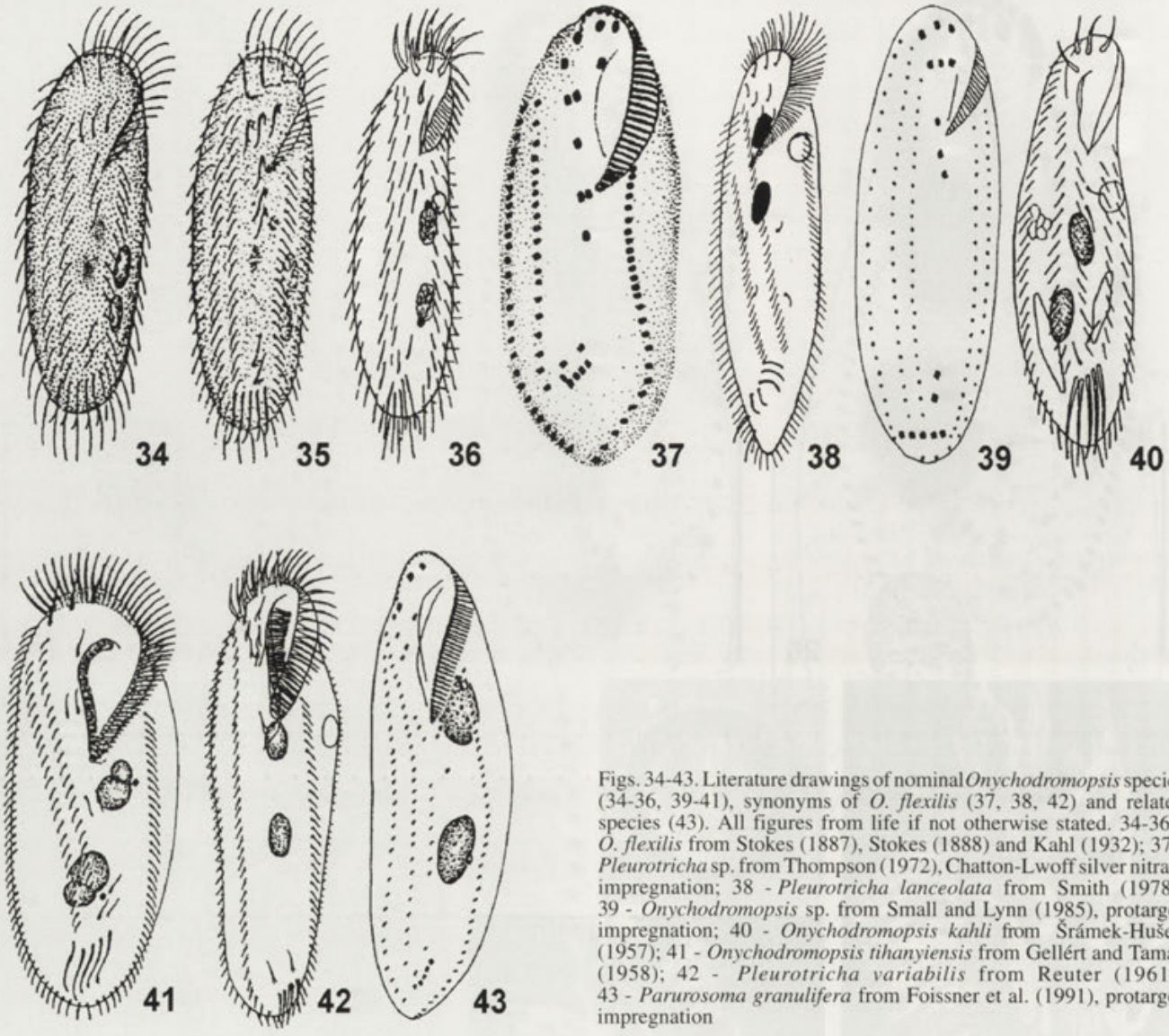

Figs. 34-43. Literature drawings of nominal *Onychodromopsis* species (34-36, 39-41), synonyms of *O. flexilis* (37, 38, 42) and related species (43). All figures from life if not otherwise stated. 34-36 - *O. flexilis* from Stokes (1887), Stokes (1888) and Kahl (1932); 37 - *Pleurotricha* sp. from Thompson (1972), Chatton-Lwoff silver nitrate impregnation; 38 - *Pleurotricha lanceolata* from Smith (1978); 39 - *Onychodromopsis* sp. from Small and Lynn (1985), protargol impregnation; 40 - *Onychodromopsis kahli* from Šrámek-Hušek (1957); 41 - *Onychodromopsis tihanyiensis* from Gellért and Tamás (1958); 42 - *Pleurotricha variabilis* from Reuter (1961); 43 - *Parurosoma granulifera* from Foissner et al. (1991), protargol impregnation

collected between *Poa* and *Callitricha* vegetation near a penguin rookery on Prince Edward Island (Foissner 1996). At these sites, *O. flexilis* occurred together with *Acineria uncinata*, *Colpoda aspera*, *C. cucullus*, *C. inflata*, *C. steinii*, *Cyrtolophosis mucicola*, *Haplocaulus terrenus*, *Leptopharynx costatus*, *Nivaliella plana*, *Platyophrya vorax* and *Pseudoplatyophrya nana*. Biomass of 10^6 individuals: 80 mg.

The type population was found in a freshwater pond with *Lemna* sp. (Stokes 1887). Later, Kahl (1932) reported *O. flexilis* from a sapropelic site near Hamburg together with rhodobacteria and flagellates. Other populations or very similar species were found in a variety of Antarctic and temperate freshwater and brackish habitats (see comparison with related species). Thompson (1972), for instance, described and illustrated (Fig. 37) a *Pleurotricha* sp. from an Antarctic tidal pool with freshwater dilution. However, size and infraciliature of this hypotrich are very similar to those of our specimens. Likewise, Smith (1978) reported a *Pleurotricha lanceolata* (Fig. 38), which is, according to the arrangement of the transverse cirri, very likely *O. flexilis*, too, from Subantarctic (South Georgia) and maritime Antarctic (South Orkney Islands, Elephant Island) moss peats and soils. Sandon and Cutler (1924) mentioned a *Pleurotricha* sp. from soils of Tristan da Cunha (Southern Atlantic), but did not provide a description or figure.

Comparison with related species: The Subantarctic specimens were rather similar to the original description by Stokes (1887), who mentioned, however, three right

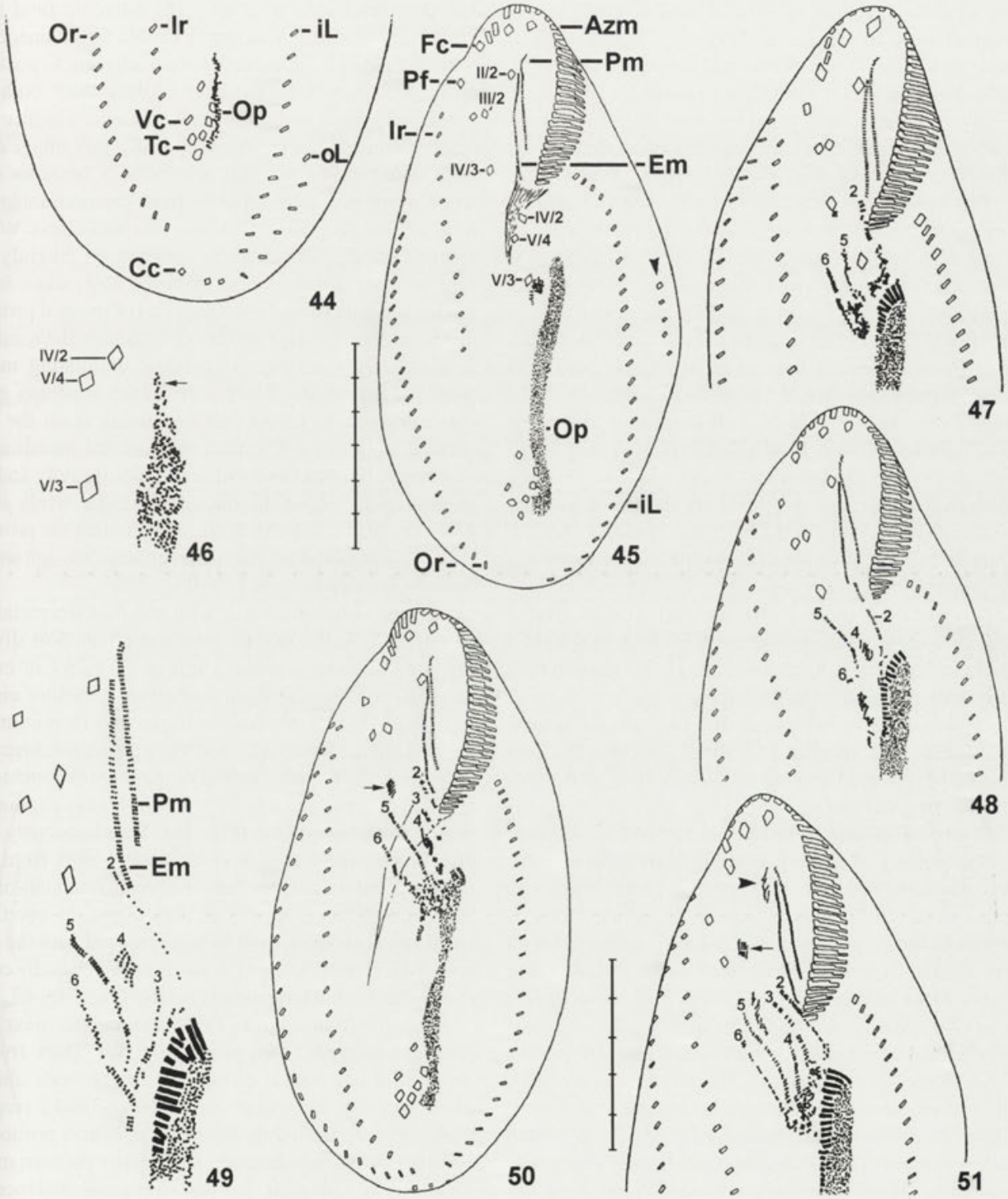

Figs. 44-51. Morphogenesis of *Onychodromopsis flexilis*, protargol impregnation. 44 - very early divider with oral primordium close to the transverse cirri; 45 - early divider showing basal body patch close to postoral cirrus V/3. Arrowhead denotes outer left marginal row; 46 - anlage 2 (arrow) extending anteriorly from oral primordium; 47-49 - early dividers showing development of opisthe's anlagen 2-6; 50, 51 - early dividers. Arrows mark disaggregating cirrus IV/3 (Fig. 50) and III/2 (Fig. 51); arrowhead denotes dedifferentiating buccal cirrus II/2. Azm - adoral zone of membranelles, Cc - caudal cirri, Em - endoral membrane, Fc - anterior frontal cirri, iL, oL - inner and outer left marginal row, respectively, Ir, Or - inner and outer right marginal row, respectively, Op - oral primordium, Pf - posterior frontal cirri, Pm - paroral membrane, Tc - transverse cirri, Vc - ventral cirri; designation of cirri in Figs. 45, 46 according to Wallengren (1900), other numbers denote cirral anlagen. Scale bar division 10 µm

marginal rows (Fig. 34). Nevertheless, we consider our populations to be conspecific because 14% of the specimens (including postdividers) had three right marginal rows, too, and Stokes (1887), not having the advantage of silver impregnation, could not provide data on variability. Furthermore, he did not recognize the cortical granules, very likely because they are colourless.

The subsequent illustration by Stokes (1888) differs from the original in showing a straight row of transverse cirri at right-angles to the main body axis (Fig. 35). This difference appears to be an inaccuracy by Stokes (1888). However, *Onychodromopsis* sp. in Small and Lynn (1985) matches Stokes' (1888) figure of *O. flexilis* in every detail (Fig. 39). Compared with other populations of *O. flexilis* [Thompson 1972 (Fig. 37), Smith 1978 (Fig. 38), Lundin and West 1963], Stokes' (1887, 1888), Kahl's (1932), and Small and Lynn's (1985) drawings (Figs. 34-36, 39) lack some frontal cirri and are thus very likely incomplete or, more likely, influenced by Stokes' (1887) figure. Thus and in the absence of any type material, we fix our population as neotype.

Onychodromopsis kahli Šrámek-Hušek, 1957 (Fig. 40) is obviously based upon his own and Kahl's (1932) incomplete observations of *O. flexilis* and thus cannot be recognized as distinct species.

Onychodromopsis tihanyiensis Gellért and Tamás, 1958 (Fig. 41), the third nominal species, has two obliquely arranged ventral rows indicating that it belongs to another genus.

Pleurotricha variabilis Reuter, 1961 (Fig. 42) has, unlike the type of the genus, a flexible body and transverse cirri not separated into two groups. These characters match those of *Onychodromopsis*, to which Reuter's species is thus transferred: *O. variabilis* (Reuter, 1961) nov. comb. According to Reuter's rather detailed live observations on four cultured clones, his species differs from *O. flexilis* in size (200-220 µm), position of contractile vacuole (in anterior third of body) and in having only a single left marginal row. However, these are weak differences considering the high variability of *O. flexilis* (Table 2). *Parurosoma granulifera* (Fig. 43), a nomen nudum species in Foissner et al. (1991), very likely also belongs to *Onychodromopsis*, although it has distinctly curved and intersecting undulating membranes.

Morphogenesis (Figs. 33, 44-74)

Oral primordium and cirral streaks (Figs. 33, 44-63, 70): Stomatogenesis commences with the apokinetal (?) proliferation of basal bodies close to the left transverse cirri (Fig. 44). The anarchic field then elongates anteriorly in a narrow streak. Simultaneously, a small field of basal bodies appears adjacent to postoral cirrus V/3, which disintegrates slightly later; both the basal body field and the dissolved cirrus produce the opisthe's anlage 6 (Fig. 45). Very likely, this anlage does not contribute to the oral primordium because it is slightly but distinctly separate from the oral anlage in 81% of the cases observed (n = 16) and cirrus V/3 is inactive during physiological regeneration. Slightly before or after disintegration of cirrus V/3, some basal bodies separate from the anterior end of the oral primordium, migrate anteriad and become the opisthe's anlage 2, seemingly touching the parental undulating membranes (Figs. 46, 47, 58, 59). However, scanning electron micrographs reveal that this streak is on the cell surface and does not contact the parental membranes, which are still intact and within the buccal cavity and the longitudinal cleft of the buccal lip, respectively (Fig. 33); very likely, this streak does not contact the proter's anlage 2 (dissolved buccal cirrus) either, although sometimes being rather close to it (Fig. 33).

Almost simultaneously with the dedifferentiation of cirrus V/3, the middle postoral cirrus V/4 disaggregates, forming opisthe's anlage 5; in 28% of cases (n = 18) it even dissolves immediately before cirrus V/3 (Fig. 58). Membranelles begin to differentiate in the oral anlage from right to left in a posteriad direction (Figs. 47, 59). Subsequently, the anterior postoral cirrus IV/2 breaks up into files of basal bodies aligning to anlage 4 of the opisthe (Fig. 48). Simultaneously, the opisthe's anlage 3 develops near, and possibly from, the posterior ends of anlagen 5 and 6 or from remnants of the oral primordium (Fig. 49). At this stage, the opisthe's cirral streaks often appear to be connected with the oral primordium (Fig. 50), which has, however, usually commenced to form adoral membranelles (Figs. 48, 49, 51).

Posterior frontal cirrus IV/3 disintegrates next and produces anlage 4 of the proter (Fig. 50). Then, frontal cirrus III/2 and buccal cirrus II/2 disaggregate almost simultaneously, forming proter's anlagen 3 and 2, respectively (Fig. 51). Slightly later, the opisthe's primordia 5 and 6 separate in midregion. The anterior portions move forward, as indicated by the decreased distance to frontal cirrus VI/3, becoming proter's anlagen 5 and 6 (Figs. 33, 51-53). The origin of the opisthe's anlage 1 (undulating membranes) could not be clarified. It develops rather late from anarchic basal bodies located between the oral primordium and the posterior ends of the cirral streaks. Finally, all primordia of the opisthe

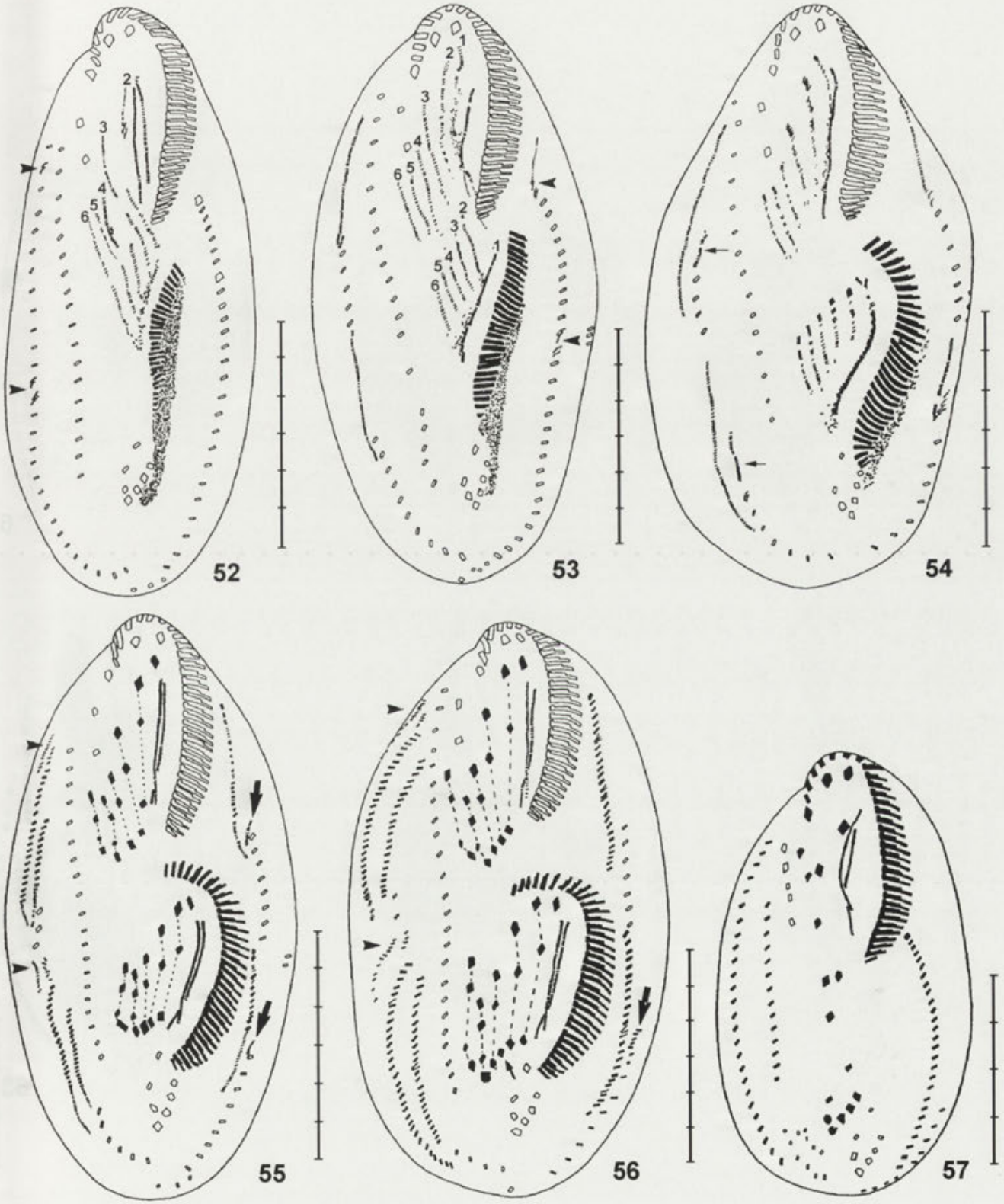

Figs. 52-57. Morphogenesis of *Onychodromopsis flexilis*, protargol impregnation. 52-54 - middle dividers showing separation of cirral streaks 5 and 6 and marginal anlagen formation. Arrowheads denote primordia for outer right and inner left marginal row, respectively; arrows mark anlage for inner right marginal row; 55, 56 - middle dividers showing migration of cirri, development of dorsal kineties 5 and 6 (arrowheads) and origin of outer left marginal row (large arrows). Small arrow marks surplus cirrus; 57 - postdivider (opisthe) still having some parental cirri. Scale bar division 10 µm

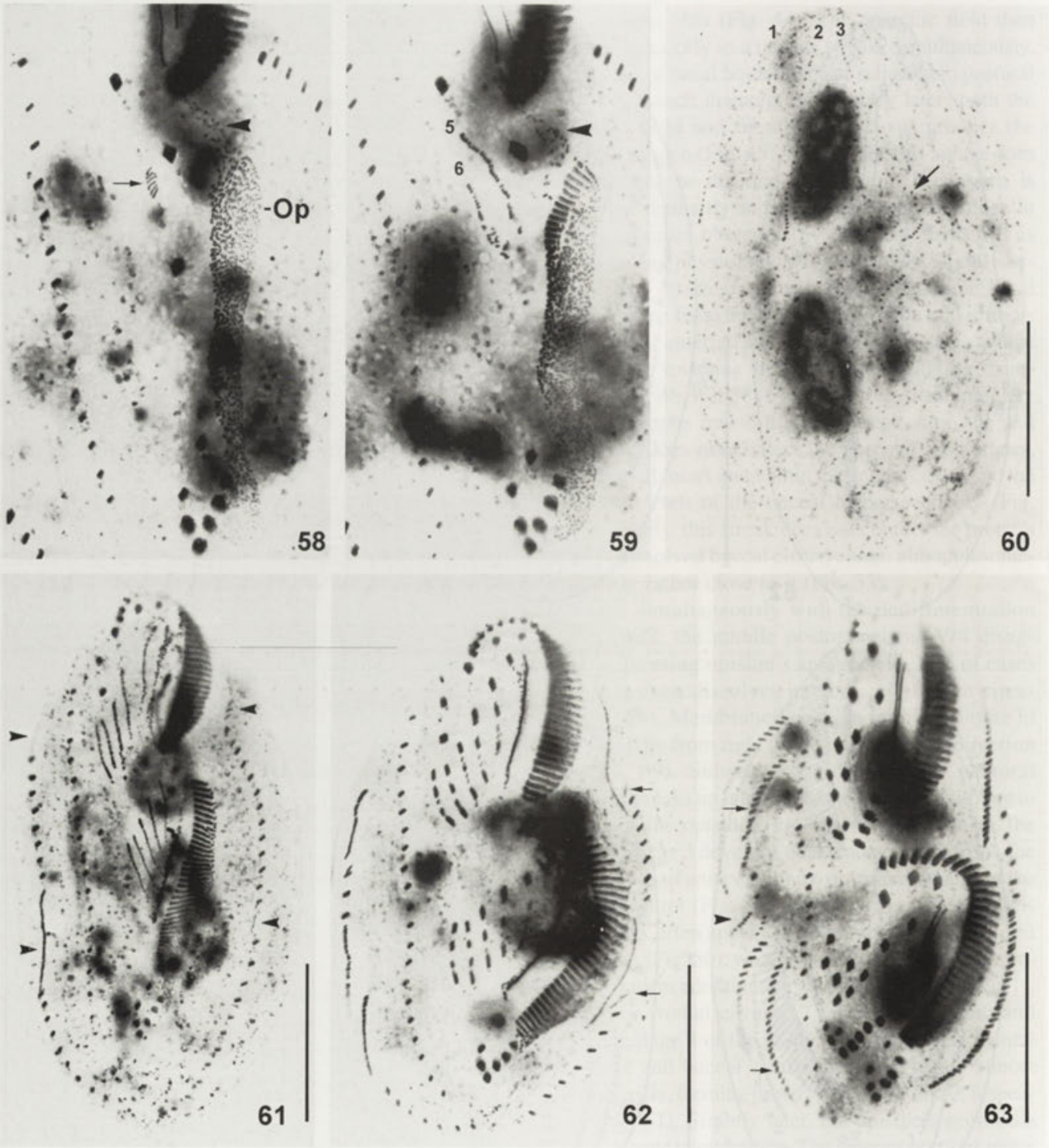

Figs. 58-63. Protargol impregnated dividers of *Onychodromopsis flexilis*. 58 - early divider showing dedifferentiating cirrus V/4 (arrow). Arrowhead marks anlage 2; 59 - early divider showing organizing anlagen 2 (arrowhead), 5 and 6 (compare Fig. 47); 60 - dorsal view of a middle divider showing new kineties 1-3 and separation of kinety 4 (arrow; compare Fig. 65); 61 - middle divider showing marginal primordia (arrowheads) and six cirral anlagen each in proter and opisthe; 62 - middle divider showing segregation of cirri. Arrows mark anlage for outer left marginal row; 63 - late divider showing anlagen for inner right marginal row (arrows) and new dorsal kineties 5 and 6 (arrowhead). Op - oral primordium; numbers denote cirral streaks (Fig. 59) and dorsal kineties (Fig. 60). Bars - 50 µm

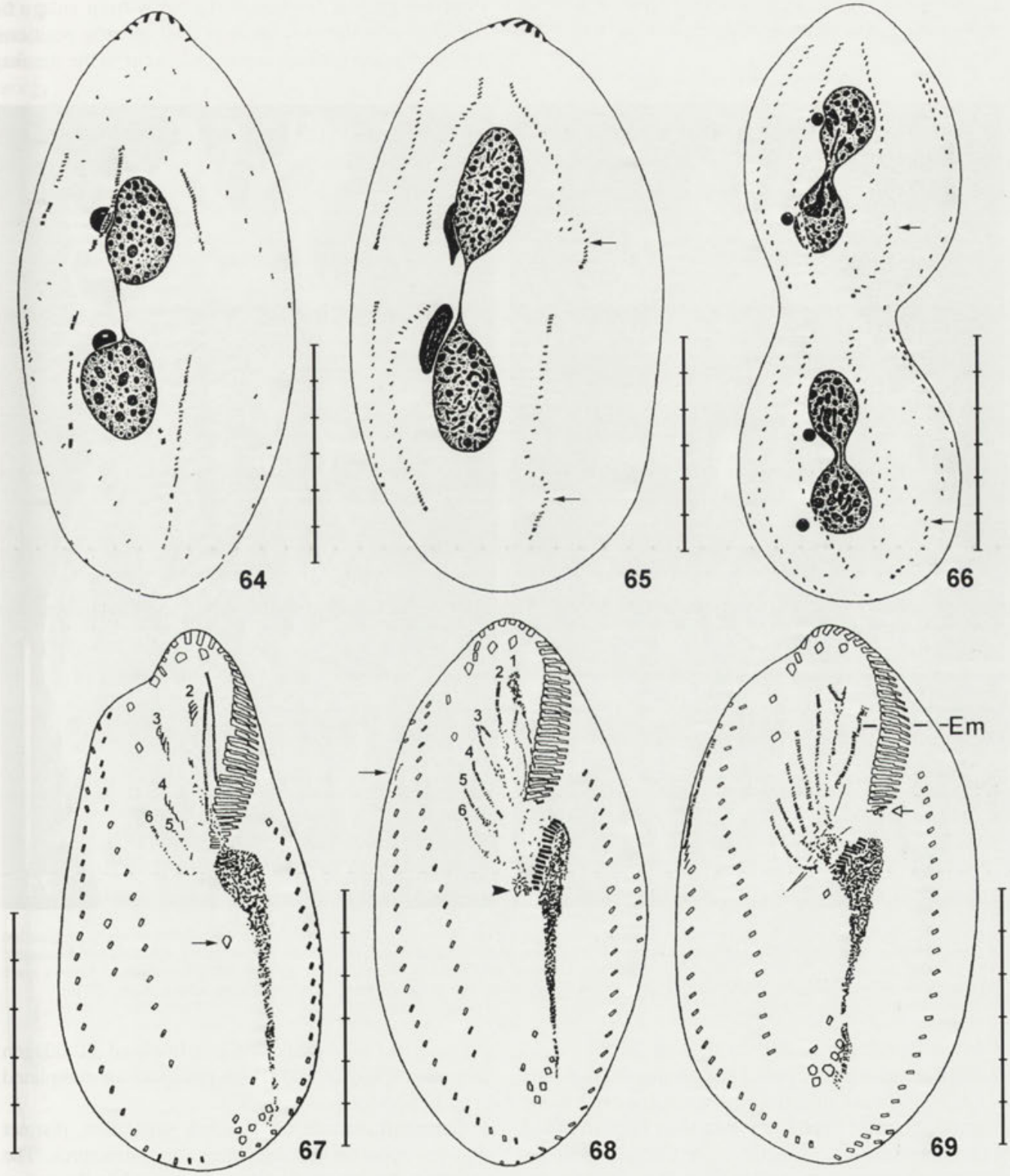

Figs. 64-69. Morphogenesis of dorsal infraciliature (64-66) and physiological regeneration (67-69) of *Onychodromopsis flexilis*, protargol impregnation. 64-66 - middle and late dividers. Dorsal kinety 4 (arrows) splits from kinety 3; 67 - early reorganizer showing organization of cirral anlagen. Arrow marks inactive cirrus V/3; 68, 69 - early reorganizers showing dedifferentiation of undulating membranes and development of outer right marginal primordium (arrow). Arrowhead marks disintegrating cirrus V/3 seen only in this specimen, open arrow marks dissolving adoral membranelles. Em - reorganizing endoral membrane; numbers denote cirral anlagen. Scale bar division 10 µm

distinctly separate from those of the proter due to cell elongation and/or anlagen movement (Figs. 52, 53, 61, 70).

right ventral and one transverse cirrus from anlage 6. Subsequently, the cirri move to their specific positions and surplus cirri, which sometimes occur in the streaks,

Figs. 70-71. *Onychodromopsis flexilis* from life (70a) and in the scanning electron microscope (70, 71). 70 - middle divider showing evagination of buccal cavity, invagination of oral primordium and reorganizing paroral membrane (arrowhead). Arrows mark opisthe's cirral anlagen; 70a - cortical granulation; 71 - late reorganizer showing evaginated buccal cavity and reorganizing undulating membranes. Arrows mark cirral anlagen, arrowhead denotes reorganizing adoral membranelles. L - left marginal anlage, Op - oral primordium. Bars - 20 µm

In the broadened middle dividers, six cirral streaks each are recognizable in proter and opisthe (Figs. 54-56, 62). Cirri differentiate from anterior to posterior in the classical oxytrichid pattern: leftmost frontal cirrus and paroral membrane from anlage 1; one frontal, the buccal and one transverse cirrus from anlage 2; two frontal and one transverse cirrus from anlage 3; one frontal, one postoral (anteriormost) and one transverse cirrus from anlage 4; two postoral cirri, the left ventral and one transverse cirrus from anlage 5; two frontal cirri, the

are resorbed as are all cirri not involved in anlagen formation (Figs. 56, 63). These processes are completed in early postdividers (Fig. 57).

Concomitant with cirral streak separation, distinct changes occur in the daughters' oral structures. The opisthe's oral primordium invaginates, while the parental adoral zone and buccal cavity evaginate (Fig. 70). The evagination is accompanied by a dedifferentiation of the parental paroral membrane, which proliferates basal bodies at least at its anterior end (Figs. 53, 54, 61,

62). This anlage forms the leftmost frontal cirrus. The endoral membrane, which is always separate from the paroral anlage, is very likely also partially or completely reorganized as indicated by its slightly loosened kinetids; a special primordium is, however, not formed. When the buccal cavity evaginates, the undulating membranes become more narrowly spaced and optically intersect in their posterior third. When the buccal field invaginates in early postdividers, the membranes move apart and thus do not intersect any longer (Figs. 55-57). While the buccal cavity is restored, the pharyngeal fibres are resorbed and rebuilt.

Marginal anlagen (Figs. 52-57, 61-63): Differentiation commences in middle dividers. The second (47% of cases), third (35%) or, rarely, first (18%) cirrus of the outer right row and, slightly later, invariably the first cirrus of the inner left row commence anlagen formation in the proter; the primordia for the opisthe originate from parental cirri at about mid-body (Figs. 52, 53). A few cirri each disintegrate into files of basal bodies which align longitudinally to form a row. These primordia subsequently become double-rowed and elongate by basal body proliferation and incorporation of additional cirri at their posterior ends (Figs. 53, 54, 61). The inner right and outer left marginal row are morphogenetically inactive but originate from primordia formed at the anterior ends of the remaining parental outer right and inner left marginal rows, respectively (Figs. 54, 62). The primordia in the left marginal row are distinctly smaller than those in the right row and thus produce fewer cirri.

The parental inner right marginal row is completely resorbed only after cytokinesis. Therefore, specimens having three right marginal kineties are very likely postdividers (Fig. 57).

Dorsal anlagen (Figs. 60, 64-66): The dorsal ciliature forms according to type 4 of Foissner and Adam (1983). Kineties 1-3 develop anlagen anterior and posterior to the prospective division furrow. Kineties 5 and 6 originate very close to or from the anterior end of the primordium for the outer right marginal row. Kinety 4 forms by posterior fragmentation of the new dorsal kinety 3 (Figs. 60, 65). Usually one, rarely two, caudal cirri each differentiate at the posterior ends of kineties 1, 2 and 4 (Fig. 66).

Nuclear division (Figs. 64-66): This proceeds as usual, i.e. the macronuclear nodules first fuse and then split twice, the last macronuclear division being completed in the postdividers.

Reorganization (Figs. 67-69, 71-74): Physiological regeneration largely resembles the development of the

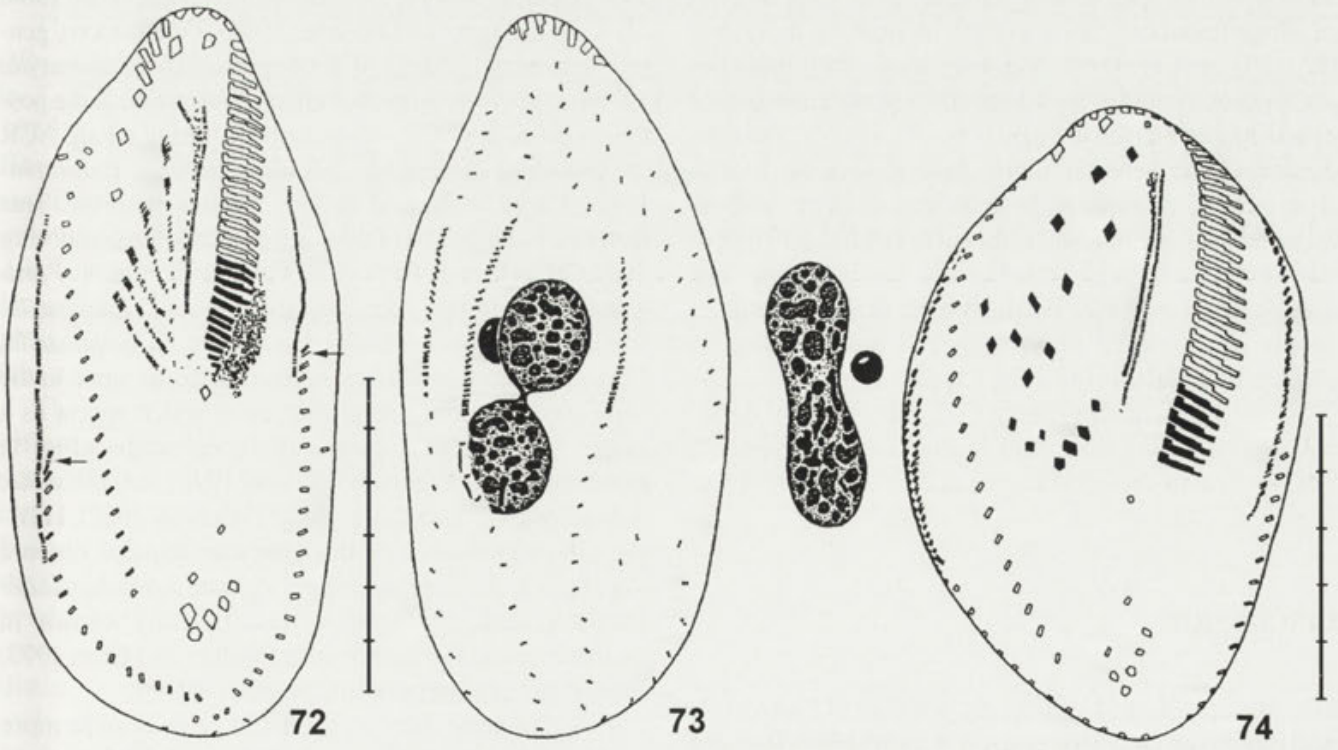

Figs. 72-74. Physiological regeneration of *Onychodromopsis flexilis*, protargol impregnation. 72, 73 - ventral and dorsal view of a middle reorganizer. The adoral zone is partially renewed. Arrows mark anlagen for inner right and outer left marginal row, respectively; 74 - late reorganizer. Scale bar division 10µm

proter. Very early reorganizers cannot be distinguished from early dividers because the oral primordium originates in a similar way. Reorganizers are distinguishable from dividers only after the first and second postoral cirrus IV/2 and V/4 have disintegrated and, in contrast to division, the third postoral cirrus V/3 has remained unchanged (Fig. 67). In one specimen however, cirrus V/3 probably proliferated some basal bodies (Figs. 67, 68).

Unlike in fission, cirri IV/2 and V/4 develop anlagen 5 and 6, respectively. As in division, frontal cirri IV/3 and III/2 produce anlagen 4 and 3, respectively. An inconspicuous streak of basal bodies extends anteriorly at the frontal end of the oral primordium. Later, this streak very likely contacts anlage 2 produced by the dedifferentiated buccal cirrus II/2 (Fig. 67).

The cirral streaks elongate by basal body proliferation, seemingly contacting the oral primordium (Figs. 68, 69). The paroral and endoral membrane lose integrity and are reorganized (Figs. 68, 69, 71). As in division, this process is accompanied by an evagination of the buccal cavity and the resorption of the buccal lip (Fig. 71).

Only few adoral membranelles differentiate at the anterior portion of the oral primordium. They become attached to the proximal end of the parental adoral zone where some membranelles have been resorbed (Figs. 68, 69, 71, 72). In spite of this resorption, the total number of adoral membranelles is slightly increased temporarily ($\bar{X}$ = 37.5, n = 11; Table 2). Subsequently, membranelles at the posterior end of the adoral zone disintegrate and the usual number is again attained (Figs. 71, 72, 74). The midportion of the parental adoral zone is very likely also reorganized, as indicated by shortened cilia, but without a special primordium; we could not determine whether or not the foremost membranelles are renewed (Fig. 71). The elongate posterior portion of the oral primordium, which is composed of unorganized basal bodies, is obviously resorbed (Figs. 69, 71, 72).

Cirral differentiation in the FVT, marginal and dorsal anlagen occurs as described in division (Figs. 68, 69, 72-74). The macro- and micronuclei fuse and redivide (Figs. 73, 74).

DISCUSSION

Morphogenesis and systematic position of *Lamtostyla* and improved characterization of amphisiellid genera

Eigner and Foissner (1994) redefined the Amphisiellidae emphasizing morphogenetic characters. According to their diagnosis, *L. edaphoni* undoubtedly belongs to this family. The pattern of ACR and transverse cirri formation even suggests transferring *L. edaphoni* to the genus *Amphisiella*, i.e. to liquidate *Lamtostyla*. However, the type of *Amphisiella*, *A. marioni* Gourret and Roeser, 1888, differs considerably in the origin of the oral primordium, which derives from, or at least develops in close contact with the ACR (Wicklow 1982). This applies also to most other genera assigned to the Amphisiellidae by Eigner and Foissner (1994). Only *Gastrostyla* develops the oral primordium apokinetally (Walker and Grim 1973) like *L. edaphoni* (Fig. 5), *L. hyalina* and *L. perisincirra* (Berger et al. 1984), and *L. australis* (Voss 1992). However, *Gastrostyla* is distinguished from *Lamtostyla* by having caudal cirri, at least one postperistomial cirrus and two dorsal kineties developing from right marginal cirri (Walker and Grim 1973, Eigner and Foissner 1994).

Thus, there are obviously two groups of amphisiellids, one developing the oral primordium in close contact with the ACR (*Amphisiella*, *Amphisiellides*, *Hemiamphisiella*, *Paragastrostyla*, *Paramphisiella*, *Pseudouroleptus*) and another forming it apokinetally near the left transverse cirrus, viz. *Gastrostyla* and *Lamtostyla* (Walker and Grim 1973, Hemberger 1982, Wicklow 1982, Berger et al. 1984, Voss 1992, Eigner and Foissner 1994). Furthermore, genera having a rather short ACR (*Amphisiellides*, *Lamtostyla*, *Paragastrostyla*) commence anlagen formation at the posterior end of the ACR, whereas those having a long ACR (*Amphisiella*, *Gastrostyla*, *Hemiamphisiella*, *Paramphisiella*, *Pseudouroleptus*) develop them within-row. This pattern is independent of the number of anlagen composing the ACR, which is formed by three primordia in *Paragastrostyla* and by two in *Amphisiellides* and *Lamtostyla*. In addition, *Hemiamphisiella*, *Lamtostyla*, *Paramphisiella*, *Pseudouroleptus* and *Amphisiellides atypicus* agree in the close contact of daughters' anlagen 1, which appear as a single primordium in certain divisional stages (Fig. 9; Hemberger 1982, Eigner and Foissner 1994); in *Amphisiella*, the anlagen are distinctly separate (Wicklow 1982). However, the significance of this character remains obscure since the anlagen 1 are also clearly separate in *Amphisiellides illuvialis*, and this detail is insufficiently known in *Gastrostyla* and *Paragastrostyla* (Walker and Grim 1973, Hemberger 1982, Eigner and Foissner 1994).

Based on these data, amphisiellid genera can be more precisely characterized using the following 10 characters: origin of oral primordium, site of anlagen formation in the ACR and origin of the new ACR, origin of dorsal

kineties, number of cirri left and right of ACR, arrangement and origin of transverse cirri, presence/absence of postperistomial and caudal cirri.

Genus *Amphisiella* Gourret and Roeser, 1888: The oral primordium originates in close contact with the ACR. The ACR commences anlagen formation within-row and originates from two rightmost anlagen. All dorsal kineties develop intrakinetally. More than one cirrus left of ACR. Transverse cirri obliquely arranged, originate from more than one anlage. Caudal cirri lacking.

This diagnosis does not match *Amphisiella terricola* Gellért, 1955, which develops the oral primordium apokinetally and the new ACR possibly from a single anlage within the parental ACR (Hemberger 1982). This pattern is quite similar to that of *Orthoamphisiella* Eigner and Foissner, 1991, which lacks, however, transverse cirri (Eigner and Foissner 1991, 1993). Thus, a proper classification of *A. terricola* must await more detailed investigations.

Genus *Lamtostyla* Buitkamp, 1977: The oral primordium originates apokinetally near the transverse cirri. The ACR commences anlagen formation at its posterior end and originates from two rightmost anlagen. All dorsal kineties develop intrakinetally. At least one cirrus left of ACR. Transverse cirri obliquely arranged, originate from more than one anlage. Caudal cirri lacking.

This pattern is also found in *Amphisiella australis* (Foissner 1988, Voss 1992), which is thus transferred to *Lamtostyla*: *L. australis* (Blatterer and Foissner, 1988) nov. comb. Likewise, *Tachysoma perisincirra* Hemberger, 1985, included in *Amphisiella* by Eigner and Foissner (1994), belongs to *Lamtostyla* as previously proposed by Berger and Foissner (1987). Other *Amphisiella* species might also belong to *Lamtostyla*. However, their proper classification must await morphogenetic investigations because interphasic characters are identical in both genera.

The ontogenesis of *L. australis* and *L. perisincirra* differs slightly from that of *L. edaphoni* in developing a sixth cirral streak which results in the higher number of cirri left of the ACR (Berger et al. 1984, Berger and Foissner 1987, Foissner 1988, Voss 1992); furthermore, the oral primordium of *L. australis* may originate either parakinetally from, or apokinetally close to the transverse cirri, and the proter's and opisthe's cirral anlagen are more distinctly connected (Voss 1992).

It should be mentioned that the morphogenesis of *L. lamottei*, type of *Lamtostyla*, is still unknown. However, the interphasic cirral pattern of *L. lamottei* is very similar to that of *L. perisincirra* whose morphogenesis nicely matches that described for *L. edaphoni*. Thus, *L. edaphoni*, *L. perisincirra* and *L. australis* are very likely congeneric with *L. lamottei*.

Genus *Amphisiellides* Foissner, 1988: The oral primordium originates in close contact with the ACR. The ACR commences anlagen formation at its posterior end and originates from two rightmost anlagen. One dorsal kinety develops from the right marginal row. More than one cirrus left of ACR. Usually two cirri right of ACR. Transverse cirri longitudinally arranged, usually originate from single anlage. Caudal cirri present.

Genus *Gastrostyla* Engelmann, 1862: The oral primordium originates apokinetally near the transverse cirri. The ACR commences anlagen formation within-row and originates from three rightmost anlagen. Two dorsal kineties develop from the right marginal row. One or two postperistomial cirri originating from third anlage from right. One cirrus left of ACR. Transverse cirri obliquely arranged, originate from more than two anlagen. Caudal cirri present.

Genus *Hemiamphisiella* Foissner, 1988: The oral primordium originates in close contact with the ACR. The ACR commences anlagen formation within-row and originates from three rightmost anlagen. All dorsal kineties develop intrakinetally. Usually one postperistomial cirrus developing from third anlage from right. One cirrus left of ACR. Transverse cirri longitudinally arranged, originate from single anlage. Caudal cirri present.

Genus *Paragastrostyla* Hemberger, 1985: The oral primordium originates in close contact with the ACR. The ACR commences anlagen formation at its posterior end and originates from three rightmost anlagen. All dorsal kineties develop intrakinetally. More than one cirrus left of ACR. Caudal cirri present, transverse cirri absent.

Genus *Paramphisiella* Foissner, 1988: The oral primordium originates in close contact with the ACR. The ACR commences anlagen formation within-row and originates from two rightmost anlagen. All dorsal kineties develop intrakinetally. One cirrus left of ACR. Transverse cirri longitudinally arranged, originate from single anlage. Caudal cirri present.

Genus *Pseudouroleptus* Hemberger, 1985: The oral primordium originates in close contact with the ACR. The ACR commences anlagen formation within-row and originates from three rightmost anlagen. All dorsal kineties develop intrakinetally. Usually one postperistomial cirrus developing from third anlage from right. One cirrus left of ACR. Transverse cirral row almost as long as body, parallels ACR, originates from single anlage. Caudal cirri present.

Key to amphisiellid genera using interphasic (non-morphogenetic) characters recognizable in protargol slides.

1 With (1 or 2) postperistomial cirri 2
- without postperistomial cirri 4
2 Few or no cirri right of ACR 3
- cirral row right of ACR, extending almost over entire body length ..... *Pseudouroleptus*
3 Posterior end broadly rounded, transverse cirri conspicuous and obliquely arranged ..... *Gastrostyla*
- posterior end pointed and/or elongate tail-like, transverse cirri inconspicuous and longitudinally arranged ..... *Hemiamphisiella*
4 With transverse cirri 5
- without transverse cirri ..... *Paragastrostyla*
5 With caudal cirri 6
- without caudal cirri ..... *Amphisiella*, *Lamtostyla*
6 Few cirri right of ACR ..... *Amphisiellides*
- without cirri right of ACR ..... *Paramphisiella*

Morphogenesis and systematic position of *Onychodromopsis*

The main characteristics of *Onychodromopsis* clearly match those of oxytrichid hypotrichs. The FVT-cirral pattern is identical with that of, e.g., *Oxytricha*, *Sterkiella* and *Stylonychia* (Foissner and Adam 1983, Berger et al. 1985, Wirnsberger et al. 1985a, 1986). Even the origin of the pattern is highly similar, particularly to *Oxytricha granulifera* Foissner and Adam, 1983 and *O. pseudosimilis* Hemberger, 1985, which also develop anlagen 5 and 6 of both, proter and opisthe, from cirri V/4 and V/3, respectively (Hemberger 1982, Foissner and Adam 1983). Most other oxytrichids produce proter's anlagen 5 and 6 de novo or either from cirrus IV/3 or V/4, and those of the opisthe either from cirrus V/4 or V/3 (Berger et al. 1985, Wirnsberger et al. 1985a, 1986, Voss 1991a,b, Voss and Foissner 1996).

However, interphasic specimens of *Onychodromopsis* are rather dissimilar to "typical" oxytrichids, for instance *Oxytricha* and *Stylonychia*, due to their doubled marginal rows. In this respect, *Onychodromopsis* resembles *Pleurotricha* Stein, 1859, which is most similar to *O. flexilis* not only in the ventral cirral pattern but also in the macronucleus, whose nodules, unlike in some other oxytrichids (Grimes 1973, Walker et al. 1975, Jareno 1984, Ricci et al. 1985), do not fuse in the resting cyst (see above; Jeffries 1956, Matsusaka 1976). Unfortunately, the morphogenesis of *Pleurotricha* is still unknown. However, it is distinguished from *Onychodromopsis* by the lack of caudal cirri, the rigidity of the body and the separation of the transverse cirri into two distinct groups (Kahl 1932, Jeffries and Mellott 1968, Martín-González et al. 1984). Thus, we do not follow Bütschli (1889), Borror (1972) and others, who synonymized *Onychodromopsis* with *Pleurotricha*.

Another genus matching the main characters of *Onychodromopsis* is *Parurosoma* Gelei, 1954, originally established as subgenus of *Holosticha*. However, its frontal cirri are arranged as in *Urosoma* (Foissner 1982) and the posterior body portion is narrowed tail-like. Thus, it might be a distinct genus within the oxytrichids; *Holosticha mononucleata* Gelei, 1954, which was found together with *Parurosoma dubium* Gelei, 1954, is very likely a reorganizer of *P. dubium*.

Allotricha Sterki, 1878 (single species *A. mollis*) has, like *Onychodromopsis*, doubled marginal rows and a metabolic body. Thus, *Onychodromopsis* could be a junior synonym of *Allotricha*. However, the description of *Allotricha* lacks any other details and also a figure. We thus suggest considering *A. mollis* as genus and species indeterminata.

Coniculostomum Njiné, 1979, usually also included in the Oxytrichidae, develops, unlike *Onychodromopsis*, only a single right marginal primordium and retains most of the parental marginal and some dorsal kineties (Kamra and Sapra 1990, Kamra et al. 1994). Based upon the mode of marginal row formation, Eigner (1995) transferred *Coniculostomum* to Kahliellidae.

Other genera very likely closely related to *Onychodromopsis* are *Laurentiella* Dragesco and Njiné, 1971 and *Onychodromus* Stein, 1859. The former is distinguished from *O. flexilis* by having only one right and left marginal row, an increased number of FVT-cirri and some dorsal kineties originating by multiple fragmentation of at least two primordia (Dragesco and Njiné 1971, Martin et al. 1983, Foissner et al. 1987). The latter differs from *Onychodromopsis* by having ventral cirral rows and dorsal kineties also formed by multiple fragmentation (Foissner et al. 1987, Kamra and Sapra 1993, Szabó and Wilbert 1995). Due to their peculiar marginal row development, *Laurentiella acuminata* and *Onychodromus quadricornutus* were recently also transferred to the Kahliellidae (Eigner 1995).

Several other genera, e.g. *Paraurostyla* Borror, 1972 and *Parakahliella* Berger et al., 1985, also have more than two marginal cirral rows and/or a few ventral cirral rows and are thus superficially rather similar to *Onychodromopsis*. However, they lack the typical oxytrichid FVT-cirral pattern and develop the ventral ciliature differently (Borror 1972, Grimes and L'Hernault 1978, Berger et al. 1985, Wirnsberger et al. 1985b, Berger and Foissner 1989, Eigner 1995).

Acknowledgments. Supported by Australian Antarctic Division, Kingston, Tasmania (Australia), Fonds zur Förderung der Wissenschaftlichen Forschung (Austria), project P10264-BIO, and Stiftungs- und Förderungsgesellschaft der Paris-Lodron-Universität Salzburg. Many thanks to Drs R. D. Seppelt and D. R. Melick (Australian Antarctic Division) and the 1993/94 crew of Casey Station for logistic support, to Dr A. Jackson (CSIRO, Hobart, Tasmania) for providing algal cultures and to Mag. E. Strobl for linguistic improvements.

REFERENCES

Berger H., Foissner W. (1987) Morphology and biometry of some soil hypotrichs (Protozoa: Ciliophora). *Zool. Jb. Syst.* **114:** 193-239

Berger H., Foissner W. (1988) Revision of *Lamtostyla* Buitkamp, 1977 and description of *Territricha* nov. gen. (Ciliophora: Hypotrichida). *Zool. Anz.* **220:** 113-134

Berger H., Foissner W. (1989) Morphology and morphogenesis of *Parakahliella haideri* nov. spec. (Ciliophora, Hypotrichida). *Bull. Br. Mus. nat. Hist. (Zool.)* **55:** 11-17

Berger H., Foissner W., Adam H. (1984) Taxonomie, Biometrie und Morphogenese einiger terricoler Ciliaten (Protozoa: Ciliophora). *Zool. Jb. Syst.* **111:** 339-367

Berger H., Foissner W., Adam H. (1985) Morphological variation and comparative analysis of morphogenesis in *Parakahliella macrostoma* (Foissner, 1982) nov. gen. and *Histriculus muscorum* (Kahl, 1932), (Ciliophora, Hypotrichida). *Protistologica* **21:** 295-311

Blatterer H., Foissner W. (1988) Beitrag zur terricolen Ciliatenfauna (Protozoa: Ciliophora) Australiens. *Stapfia* (Linz) **17:** 1-84

Borror A. C. (1972) Revision of the order Hypotrichida (Ciliophora, Protozoa). *J. Protozool.* **19:** 1-23

Borror A. C. (1979) Redefinition of the Urostylidae (Ciliophora, Hypotrichida) on the basis of morphogenetic characters. *J. Protozool.* **26:** 544-550

Buitkamp U. (1977) Die Ciliatenfauna der Savanne von Lamto (Elfenbeinküste). *Acta Protozool.* **16:** 249-276

Bütschli O. (1889) Protozoa. III. Abt.: Infusoria und System der Radiolaria. In: Klassen und Ordnungen des Thier-Reichs, (Ed. H. G. Bronn). Winter'sche Verlagshandlung, Leipzig, **I:** 1585-2035

Dragesco J., Njiné T. (1971) Compléments à la connaissance des Ciliés libres du Cameroun. *Annls Fac. Sci. Univ. féd. Cameroun* **7-8:** 97-140

Eigner P. (1995) Divisional morphogenesis in *Deviata abbrevescens* nov. gen., nov. spec., *Neogeneia hortualis* nov. gen., nov. spec., and *Kahliella simplex* (Horváth) Corliss and redefinition of the Kahliellidae (Ciliophora, Hypotrichida). *Europ. J. Protistol.* **31:** 341-366

Eigner P., Foissner W. (1991) *Orthoamphisiella stramenticola* nov. gen., nov. spec., a new hypotrichous ciliate (Ciliophora: Hypotrichida) occurring in walnut leaf litter. *Acta Protozool.* **30:** 129-133

Eigner P., Foissner W. (1993) Divisional morphogenesis in *Orthoamphisiella stramenticola* Eigner and Foissner, 1991 and *O. grelli* nov. spec. (Ciliophora, Hypotrichida). *Arch. Protistenk.* **143:** 337-345

Eigner P., Foissner W. (1994) Divisional morphogenesis in *Amphisiellides illuvialis* n. sp., *Paramphisiella caudata* (Hemberger) and *Hemiamphisiella terricola* Foissner, and redefinition of the Amphisiellidae (Ciliophora, Hypotrichida). *J. Euk. Microbiol.* **41:** 243-261

Engelmann T. W. (1862) Zur Naturgeschichte der Infusionsthiere. *Z. wiss. Zool.* **11:** 347-393

Finlay B. J. (1982) Procedures for the isolation, cultivation and identification of protozoa. In: Experimental Microbial Ecology, (Eds. R. G. Burns, J. H. Slater). Blackwell, Oxford, 44-65

Foissner W. (1982) Ökologie und Taxonomie der Hypotrichida (Protozoa: Ciliophora) einiger österreichischer Böden. *Arch. Protistenk.* **126:** 19-143

Foissner W. (1987) Soil protozoa: fundamental problems, ecological significance, adaptations in ciliates and testaceans, bioindicators, and guide to the literature. *Progr. Protistol.* **2:** 69-212

Foissner W. (1988) Gemeinsame Arten in der terricolen Ciliatenfauna (Protozoa: Ciliophora) von Australien und Afrika. *Stapfia* (Linz) **17:** 85-133

Foissner W. (1991) Basic light and scanning electron microscopic methods for taxonomic studies of ciliated protozoa. *Europ. J. Protistol.* **27:** 313-330

Foissner W. (1996) Terrestrial ciliates (Protozoa, Ciliophora) from two islands (Gough, Marion) in the Southern Ocean, with description of two new species, *Arcuospathidium cooperi* and *Oxytricha ottowi*. *Biol. Fertil. Soils* (in press)

Foissner W., Adam H. (1983) Morphologie und Morphogenese des Bodenciliaten *Oxytricha granulifera* sp. n. (Ciliophora, Oxytrichidae). *Zool. Scr.* **12:** 1-11

Foissner W., Schlegel M., Prescott D. M. (1987) Morphology and morphogenesis of *Onychodromus quadricornutus* n. sp. (Ciliophora, Hypotrichida), an extraordinarily large ciliate with dorsal horns. *J. Protozool.* **34:** 150-159

Foissner W., Blatterer H., Berger H., Kohmann F. (1991) Taxonomische und ökologische Revision der Ciliaten des Saprobiensystems. - Band I: Cyrtophorida, Oligotrichida, Hypotrichia, Colpodea. *Informationsberichte des Bayer. Landesamtes für Wasserwirtschaft* **1/91:** 1-478

Gelei J. (1954) Über die Lebensgemeinschaft einiger temporärer Tümpel auf einer Bergwiese im Börzsönygebirge (Oberungarn). III. Ciliaten. *Acta biol. hung.* **5:** 259-343

Gellért J. (1955) Die Ciliaten des sich unter der Flechte *Parmelia saxatilis* Mass. gebildeten Humus. *Acta biol. hung.* **6:** 77-111

Gellért J., Tamás G. (1958) Detritusz-turzások kovamoszatainak és csillósainak ökológiai vizsgálata a tihanyi-félsziget keleti partján. *Annls Inst. biol. Tihany* **25:** 217-240

Gourret P., Roeser P. (1888) Contribution á l'etude des protozoaires de la Corse. *Archs Biol., Paris* **8:** 139-204

Grimes G. W. (1973) Differentiation during encystment and excystment in *Oxytricha fallax*. *J. Protozool.* **20:** 92-104

Grimes G. W., L'Hernault S. W. (1978) The structure and morphogenesis of the ventral ciliature in *Paraurostyla hymenophora*. *J. Protozool.* **25:** 65-74

Hemberger H. (1982) Revision der Ordnung Hypotrichida Stein (Ciliophora, Protozoa) an Hand von Protargolpräparaten und Morphogenesedarstellungen. Diss. Math.-Naturwiss. Fak. Univ. Bonn

Hemberger H. (1985) Neue Gattungen und Arten hypotricher Ciliaten. *Arch. Protistenk.* **130:** 397-417

Jareno M. A. (1984) Macronuclear events and some morphogenetic details during the excystment of *Onychodromus acuminatus* (Ciliophora, Hypotrichida). *J. Protozool.* **31:** 489-492

Jeffries W. B. (1956) Studies on excystment in the hypotrichous ciliate *Pleurotricha lanceolata*. *J. Protozool.* **3:** 136-144

Jeffries W. B., Mellott J. L. (1968) New observations on the anatomy of *Pleurotricha lanceolata*. *J. Protozool.* **15:** 741-747

Kahl A. (1932) Urtiere oder Protozoa I: Wimpertiere oder Ciliata (Infusoria). 3. Spirotricha. *Tierwelt Dtl.* **25:** 399-650

Kamra K., Sapra G. R. (1990) Partial retention of parental ciliature during morphogenesis of the ciliate *Coniculostomum monilata* (Dragesco & Njiné, 1971) Njiné, 1978 (Oxytrichidae, Hypotrichida). *Europ. J. Protistol.* **25:**264-278

Kamra K., Sapra G. R. (1993) Morphometric and morphogenetic comparisons between *Onychodromus indica* n. sp. and *O. quadricornutus* Foissner, Schlegel et Prescott, 1987; phylogenetic note on *Onychodromus* and related genera. *Acta Protozool.* **32:** 107-121

Kamra K., Sapra G. R., Ammermann D. (1994) *Coniculostomum bimarginata* n. sp., a new hypotrich ciliate: description and systematic relationships. *Europ. J. Protistol.* **30:** 55-67

Lundin F. C., West L. S. (1963) The free-living protozoa of the Upper Peninsula of Michigan. Northern Michigan College Press, Marquette

Martin J., Fedriani C., Perez-Silva J. (1983) Morphogenetic pattern in *Laurentiella acuminata* (Ciliophora, Hypotrichida): its significance for the comprehension of ontogeny and phylogeny of hypotrichous ciliates. *J. Protozool.* **30:** 519-529

Martín-González A., Serrano S., Fernández-Galiano D. (1984) New aspects of the morphology of *Pleurotricha lanceolata* (Ciliophora, Hypotrichida): cirral and membranellar patterns and fibrillar systems. *J. Protozool.* **31:** 347-351

Matsusaka T. (1976) An ultrastructural study of excystment in the hypotrichous ciliate *Pleurotricha* sp. *Kumamoto J. Sci.* **13:** 13-26
Njiné T. (1979) Compléments a l'étude des Ciliés libres du Cameroun. *Protistologica* **15:** 343-354
Reuter J. (1961) Einige faunistische und ökologische Beobachtungen über Felsentümpel-Ziliaten. *Acta zool. fenn.* **99:** 4-42
Ricci N., Verni F., Rosati G. (1985) The cyst of *Oxytricha bifaria* (Ciliata: Hypotrichida). I. Morphology and significance. *Trans. Am. microsc. Soc.* **104:** 70-78
Sandon H., Cutler D. W. (1924) Some Protozoa from the soils collected by the 'Quest' expedition (1921-1922). *J. Linn. Soc.* **36:** 1-12
Small E. B., Lynn D. H. (1985) Phylum Ciliophora Doflein, 1901. In: An Illustrated Guide to the Protozoa, (Eds. J. J. Lee, S. H. Hutner, E. C. Bovee). Allen Press, Lawrence, Kansas, 393-575
Smith H. G. (1978) The distribution and ecology of terrestrial protozoa of sub-Antarctic and maritime Antarctic islands. *Br. Antarct. Surv. Sci. Rep.* **95:** 1-104
Šrámek-Hušek R. (1957) K poznáni nálevníkú ostravského kraje. *Věst. čsl. zool. Spol.* **21:** 1-24
Stein F. (1859) Wissenschaftliche Mittheilungen. Charakteristik neuer Infusorien-Gattungen. *Lotos* **9:** 2-5, 57-60
Sterki V. (1878) Beiträge zur Morphologie der Oxytrichinen. *Z. wiss. Zool.* **31:** 29-58
Stokes A. C. (1887) Some new hypotrichous infusoria from American fresh waters. *Ann. Mag. nat. Hist. (Serie 5)* **20:** 104-114
Stokes A. C. (1888) A preliminary contribution toward a history of the fresh-water infusoria of the United States. *J. Trenton nat. Hist. Soc.* **1:** 71-319
Szabó A., Wilbert N. (1995) A redescription of the morphology of *Onychodromus grandis* Stein 1859 and the systematic implications of its morphogenesis. *J. Euk. Microbiol.* **42:** 50-60
Thompson J. C., Jr. (1972) Ciliated protozoa of the Antarctic Peninsula. *Antarctic Res. Ser.* **20:** 261-288
Voss H.-J. (1991a) Die Morphogenese von *Cyrtohymena muscorum* (Kahl, 1932) Foissner, 1989 (Ciliophora, Oxytrichidae). *Arch. Protistenk.* **140:** 67-81
Voss H.-J. (1991b) Die Morphogenese von *Notohymena rubescens* Blatterer & Foissner, 1988 (Ciliophora, Oxytrichidae). *Arch. Protistenk.* **140:** 219-236
Voss H.-J. (1992) Morphogenesis in *Amphisiella australis* Blatterer and Foissner, 1988 (Ciliophora, Hypotrichida). *Europ. J. Protistol.* **28:** 405-414
Voss H.-J., Foissner W. (1995) Divisional morphogenesis in *Steinia sphagnicola* (Ciliophora, Hypotrichida): a comparative light and scanning electron microscopic study. *Europ. J. Protistol.* **32:** 31-46
Walker G. K., Grim J. N. (1973) Morphogenesis and polymorphism in *Gastrostyla steinii*. *J. Protozool.* **20:** 566-573
Walker G. K., Maugel T. K., Goode D. (1975) Some ultrastructural observations on encystment in *Stylonychia mytilus* (Ciliophora; Hypotrichida). *Trans. Am. microsc. Soc.* **94:** 147-154
Wallengren H. (1900) Zur Kenntnis der vergleichenden Morphologie der hypotrichen Infusorien. *Bih. K. svenska VetenskAkad. Handl.* **26:** 1-31
Wicklow B. J. (1982) The Discocephalina (n. subord.): ultrastructure, morphogenesis and evolutionary implications of a group of endemic marine interstitial hypotrichs (Ciliophora, Protozoa). *Protistologica* **18:** 299-330
Wilbert N. (1975) Eine verbesserte Technik der Protargolimprägnation für Ciliaten. *Mikrokosmos* **64:** 171-179
Wirnsberger E., Foissner W., Adam H. (1985a) Morphological, biometric, and morphogenetic comparison of two closely related species, *Stylonychia vorax* and *S. pustulata* (Ciliophora: Oxytrichidae). *J. Protozool.* **32:** 261-268
Wirnsberger E., Foissner W., Adam H. (1985b) Cortical pattern in non-dividers, dividers, and reorganizers of an Austrian population of *Paraurostyla weissei* (Ciliophora, Hypotrichida): a comparative morphological and biometrical study. *Zool. Scr.* **14:** 1-10
Wirnsberger E., Foissner W., Adam H. (1986) Biometric and morphogenetic comparison of the sibling species *Stylonychia mytilus* and *S. lemnae*, including a phylogenetic system for the oxytrichids (Ciliophora, Hypotrichida). *Arch. Protistenk.* **132:** 167-185

Received on 8th January, 1996; accepted on 1st March 1996

Acta Protozoologica (1996) 35: 281 - 285

ACTA
PROTOZOOLOGICA

Effects of Cadmium and Copper on *Astasia longa*: Metal Uptake and Glutathione Levels

Paola IRATO and Ester PICCINNI

Department of Biology, University of Padova, Padova, Italy

Summary. *Astasia longa* was grown in the presence of various doses of cadmium and copper, and the effects of these metals on growth, accumulation and glutathione levels are reported. Copper, an essential metal, is better tolerated and accumulated less than cadmium, which inhibits the growth rate even at very low doses. Neither metal induces synthesis of chelating proteins, but both induce an increase in total glutathione content according to dose and exposure time; the increase is more evident with cadmium. This datum is correlated with the greater toxicity of this non-essential metal. The effects of copper and cadmium on *Astasia* are discussed and compared with previous observations on the response of *Euglena gracilis*.

Key words: *Astasia*, cadmium, copper, glutathione.

INTRODUCTION

Heavy metals have toxic effects on organisms: the characteristics and intensity of damage depend on the nature and level of the metal, i.e., there are differences between the effects of essential and non-essential metals. The exposure of a variety of organisms, including Protists, to heavy metals induces the synthesis of low molecular weight, thiol-rich proteins such as metallothioneins (MTs) or chelatins. The various functions of these compounds span a wide range, and they play an important role in the regulation of essential metals (Kägi 1991, Roesijadi 1992).

In addition to these thiol-rich proteins, other sulphydryl-containing compounds such as non-protein thiols play an important role in protecting cells against heavy metals. Of these, glutathione is widespread in bacteria, plants and animals, and plays various roles in metabolic regulation (Meister and Anderson 1983). This tripeptide (γ-glutamyl-cysteinyl-glycine, GSH) has been reported to be the first line of defence against Cu, Cd and Hg toxicity in animals and Protists (Singhal et al. 1987, Freedman et al. 1989, Howe and Merchant 1992, Coppellotti and De Gabrieli 1995).

MTs or other chelating compounds have been reported to be induced by Cd and Cu in *Tetrahymena* and *Euglena* (Piccinni et al. 1985, 1990, 1994; Shaw et al. 1989). In particular, for *Euglena* it was demonstrated that Cd, but not Cu, also enhances glutathione levels (Coppellotti 1989).

The present study reports data on the effects of Cd and Cu on another euglenoid flagellate, the colourless *Astasia longa*. The induction of chelating molecules, metal accu-

Address for correspondence: Ester Piccinni, Department of Biology, University of Padova, Via Trieste 75, 35121 Padova, Italy; Fax: 049/8276300

mulation and glutathione levels were studied and the data compared with those reported for *Euglena*.

MATERIALS AND METHODS

Cell preparation

Astasia longa was grown axenically in *Euglena gracilis* medium (EGM) at 28°C. Cu and Cd were added as $CuSO_4 \cdot 5H_2O$ and $CdCl_2 \cdot 2.5 H_2O$, respectively, at various final concentrations (see Results).

Cell density was determined by counting the cells in a Bürker chamber.

Cells harvested by centrifugation on the second or fourth days of culture were rinsed in 10 mM Tris-HCl, pH 7.5, and then homogenized in the cold in the same buffer with 5 mM ascorbic acid added. The homogenate was centrifuged at 100,000 *g* for 1 h 30 min in a Kontron Centricon T-2060 centrifuge at 4°C. The final pellets were washed with the same buffer.

Isolation of proteins and estimation of metallothionein

The supernatant of treated cells with 0.5 µg Cd/ml was lyophilized and gel-filtered on a Bio-Gel P-60 (Bio-Rad) column, followed by anion-exchange chromatography on an HR 5/5 MonoQ (Pharmacia) column using a Pharmacia FPLC mod. LCC 500, as described previously (Piccinni et al. 1990).

MT contents in the supernatant treated with Cu and Cd was analysed by the silver saturation method (Scheuhammer and Cherian 1991).

Metal analysis

The supernatant was submitted to metal analysis (Cd, Cu and Zn) by atomic absorption spectroscopy with a Perkin-Elmer mod. 4000 spectrophotometer, without further processing. The metal contents of homogenate and sediment were measured after ashing in concentrated HNO_3 (AristaR grade 60%) in a teflon bomb. All measurements were corrected for background absorption using reagent blanks.

Total glutathione contents

Cells collected on the second and fourth days by centrifugation and rinsed in 10 mM Tris-HCl buffer, pH 7.5, were homogenized in the cold with 5% 5-sulfosalicylic acid. The homogenate was centrifuged at 22,000 *g* for 30 min at 4°C. The resulting supernatant was filtered with a Millex-HA 0.22 µm filter unit and analysed. Total glutathione (GSH+GSSG) was determined by DTNB-GSSG reductase assay, according to Anderson (1985). The amount of total glutathione was determined from a standard curve in which the GSH equivalents present (0.5, 0.75, 0.9 and 1) were plotted against the rate of change of absorbance at 412 nm, monitored for at least 5 min.

All samples and standards were assayed 5-6 times. Values are expressed as nmoles/g of dry weight; data are the means of three experiments.

Statistics

All results are reported as means ± SD. Results were submitted to one-way analysis of variance (ANOVA). The Student-Newman-Keuls test was used to assess which of the groups were significantly different ($p < 0.05$) from each other (shown by different superscript letters).

RESULTS

Growth curves and metal uptake

The duplication time of *Astasia longa* cells, cultured in EGM at 28°C, was about 16 h in the logarithmic phase. It increased up to 27, 61 and 45 h in the presence of 0.5 (4.4 µM) and 1 (8.9 µM) µg of Cd/ml and 20 µg of Cu/ml (0.31 mM) respectively, while it was the same as that of controls when the cells were treated with 10 µg of Cu/ml (0.157 mM). The higher dose of Cd is highly toxic (Fig. 1). Cd and Cu were accumulated to different extents by *Astasia* cells.

Values measured after 2 and 4 days are reported in Table 1. The amount of Cd accumulated after 4 days at a dose of 0.5 µg/ml was similar to the amount after 2 days of treatment (groups bc and b respectively); otherwise, the value obtained with 1 µg Cd/ml on day 4 was 23% higher than that with the same dose on day 2 (groups d and c respectively).

The value of Cu accumulating after 2 days of treatment with 20 µg Cu/ml was 32% higher than that obtained at a dose of 10 µg Cu/ml (111 and 83.8 µg/g dry wt respectively). After 4 days, unlike Cd, Cu showed a remarkable decrease at both doses.

Zn contents increased in both controls and metal-treated (Cu-Cd) cells from days 2 to 4; but a reduction in Zn was evident in treated cells compared with controls on both days 2 and 4, this is more evident for Cd treatment (Table 1).

In Cd-treated cells, the metal always accumulated mostly in the soluble fraction (Table 2). Cu was present mostly in the particulate fraction, in both controls and cells

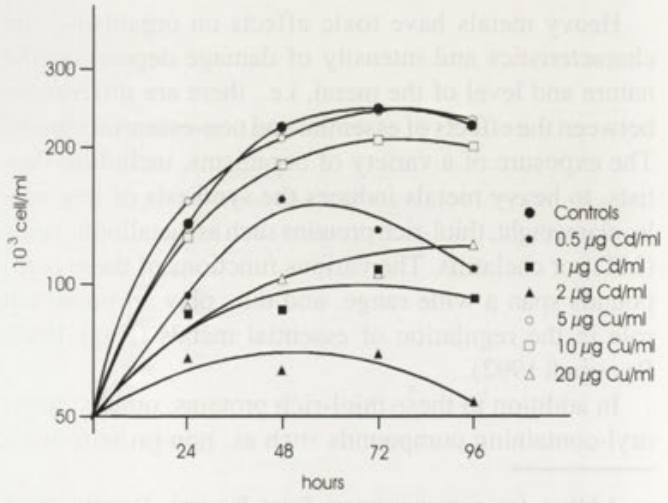

Fig. 1. Concentration-dependent effects of cadmium and copper on cell proliferation of *Astasia longa* up to day 4 of culture

Table 1. Metal contents (μg/g dry wt) in controls and treated cells of *Astasia longa* after 2 and 4 days of culture.

Treatment 2 days	Cadmium	Copper	Zinc
Controls	0 ± 0 a	24.6 ± 5.8 a	240.6 ± 46.4 a
0.5 μg Cd/ml	153.4 ± 8.0 b	16.1 ± 6.4 a	82.0 ± 2.7 b
1.0 μg Cd/ml	164.4 ± 15.3 c	17.0 ± 6.8 a	45.8 ± 15.3 c
10.0 μg Cu/ml	0 ± 0 a	83.8 ± 2.7 b	115.3 ± 0.8 d
20.0 μg Cu/ml	0 ± 0 a	111.0 ± 3.7 c	152.4 ± 2.4 e
Treatment 4 days			
Controls	0 ± 0 a	19.2 ± 5.0 a	322.5 ± 5.4 f
0.5 μg Cd/ml	156.4 ± 5.1 bc	3.8 ± 0.9 d	104.3 ± 2.7 bd
1.0 μg Cd/ml	202.7 ± 1.1 d	21.6 ± 0.4 a	119.3 ± 9.5 d
10.0 μg Cu/ml	0 ± 0 a	55.8 ± 5.0 e	150.8 ± 6.2 e
20.0 μg Cu/ml	0 ± 0 a	73.9 ± 6.2 f	209.2 ± 7.7 g

Means with different letters are significantly different at $p < 0.05$. Letters in each column refer to analyses of Cd, Cu or Zn contents. Data are means of 3 different experiments (see Materials and Methods)

Table 2. Percentage distribution of metals between supernatant and pellets in controls and threaded *Astasia longa* cells after 2 and 4 days of culture

Treatment 2 days	Cadmium		Copper		Zinc	
	Supernatant	Pellet	Supernatant	Pellet	Supernatant	Pellet
Controls	-	-	32	68	30	70
0.5 μg Cd/ml	79	21	40	60	54	46
1.0 μg Cd/ml	65	35	34	66	33	67
10.0 μg Cu/ml	-	-	21	79	58	42
20.0 μg Cu/ml	-	-	40	60	59	41
Treatment 4 days						
Controls	-	-	63	37	96	4
0.5 μg Cd/ml	67	33	50	50	82	18
1.0 μg Cd/ml	96	4	65	35	96	4
10.0 μg Cu/ml	-	-	55	45	88	12
20.0 μg Cu/ml	-	-	46	54	86	14

treated for 2 days, but after 4 days it was mostly found in the soluble fraction of controls and similarly distributed between both fractions in Cu-treated cells (Table 2).

Zn too was present mostly in the soluble fraction after 4 days, in both controls and treated cells (Table 2).

No specific Cd-binding proteins similar to metallothioneins and chelatins were isolated from supernatant submitted to gel- and anion exchange-chromatography.

These results confirm data (not shown) obtained using the silver saturation method, demonstrating the absence of MTs in cell-free extracts of Cu- and Cd-treated cultures.

Effects of metals exposure on total glutathione contents

Total glutathione levels are reported in Fig. 2, which clearly shows an increase in 4 days with respect to control

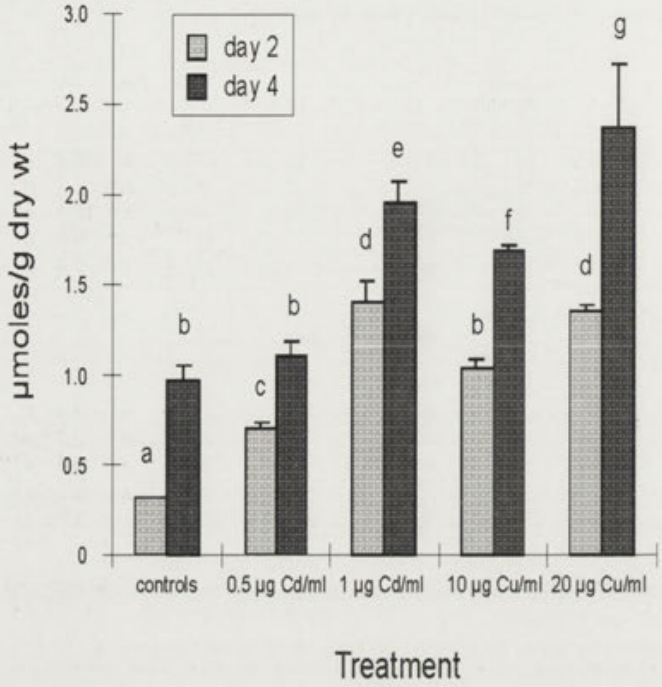

Fig. 2. Total glutathione (GSH + GSSG) levels (µmoles/g dry wt) in controls and treated cells of *Astasia longa*. Bars: means ± SD of 3 experiments. Bars not sharing a common superscript letter are significantly different ($p < 0.05$)

cells after 2 days. Both doses of Cd and Cu induce significant enhancement of glutathione in the cells, with the only exception of cells treated with 0.5 µg Cd/ml for 4 days, which show a level not statistically different from the corresponding control (group b). Glutathione contents induced by Cu were also statistically different, both as regards doses and length of treatment, but it should be noted that Cu doses were 20 times higher than those of Cd.

DISCUSSION

Astasia longa is sensitive to the toxic effects of heavy metals Cu and Cd.

As in many other organisms, including Protists, the essential metal Cu is better tolerated: the duplication time of cells treated with 5 µg Cu/ml is the same as that of controls, while a dose of Cd 10 times lower - 0.5 µg/ml - affects growth in the logarithmic phase, increasing the duplication rate to 27 h and producing a decrease after 48 h. This effect on growth rate may be related to the greater accumulation of Cd with respect to Cu. Furthermore, the Cu content in cells decreases from days 2 to 4 and growth continues more slowly, even at the more inhibiting dose of 20 µg/ml. The limited intracellular storage of Cu-treated cells and its decrease may be explained by assuming that the excess of metal is chelated soon after entering the cell and is later excreted to the external medium. This mechanism may also explain the Zn decrease in Cu-treated cells. This tolerance mechanism is similar to that described for *Euglena gracilis*, in which both Cu and Zn decrease (Albergoni et al. 1980).

Astasia is more sensitive to Cd when compared with other Protists such as the flagellates *Euglena gracilis* (Albergoni et al. 1980) and *Ochromonas danica* (Piccinni and Coppellotti 1982) and the ciliates *Uronema marinum* (Coppellotti 1994), *Tetrahymena thermophila*, *T. pigmentosa* and *T. pyriformis*; the latter can be cultured without damage in the presence of 7-10 µg Cd/ml (Piccinni 1995).

Cd-treated cells also show Zn depletion in contrast with the effects reported for *Tetrahymena* and *Oxytricha* in which an increase of 75% in Zn has been reported when the latter is treated with Cd. These co-accumulations may be related to the Cd-Zn linking proteins forming in both the above organisms (Piccinni et al. 1992, Piccinni 1995). Decreased Zn contents induced by Cd has been also reported in multicellular organisms and explained by assuming that Cd treatment causes Zn depletion due to exchange of this metal for Cd in Zn-containing proteins, which later release it in a biologically inactive form (Pool 1981). Zn depletion may therefore be explained by two different mechanisms according to the metal used - Cu or Cd.

Different compartmentalization is evident for the two metals. As reported in the Results, Cd is present in the soluble fraction on both days 2 and 4. Otherwise, Cu and Zn move to the soluble fraction after 4 days of treatment. This is in contrast with data reported for other Protist species, according to which metals move from the soluble to the particulate fraction after a few days of treatment, probably by linking to membrane and granules (Piccinni 1995, Piccinni and Albergoni 1996). In any case, the relation between metals and these two intracellular compartments is very complex.

It has been demonstrated that in some Protists, as in many multicellular organisms, Cd and Cu induce chelating molecules, which play a protective role. In particular, a Cd-Zn-thionein is isolated by *Tetrahymena* and other, different, chelating compounds are isolated by *Euglena* (Piccinni et al. 1985, 1990, 1994; Shaw et al. 1989). On the contrary, *Astasia* does not appear to have this specific intracellular detoxification mechanism. An increase in glutathione levels is detected after treatment with both metals, especially Cd, depending on dose and length of

exposure. In *Euglena gracilis*, only Cd enhances glutathione levels, whereas Cu does not affect the levels of this compound: this finding may be related to the biosynthesis of specific low molecular weight Cu-binding proteins (Piccinni et al. 1985, Coppellotti 1989).

The literature data on the role of glutathione may explain our findings. It is known that glutathione is capable of chelating and detoxifying metals soon after they enter the cell (Singhal et al. 1987) and that they may later be transferred to metallothioneins (Freedman et al. 1989). In *Astasia* cells, in which special chelating proteins are not induced, metal-induced enhancement of glutathione is the only detoxification mechanism found.

It may be concluded that the higher sensitivity to metals of *Astasia longa* with respect to *Euglena* is correlated to its inability to synthetise appropriate chelating proteins.

Acknowledgements. This research was supported by CNR 94.02837CT04 and MURST 40% 1993 grants.

REFERENCES

Albergoni V., Piccinni E., Coppellotti O. (1980) Response to heavy metals in organisms - I. Excretion and accumulation of physiological and non physiological metals in *Euglena gracilis*. *Comp. Biochem. Physiol.* **67C:** 121-127

Anderson M.E. (1985) Determination of glutathione and glutathione disulfide in biological samples. *Methods Enzymol.* **113:** 548-555

Coppellotti O. (1989) Glutathione, cysteine and acid-soluble thiol levels in *Euglena gracilis* cells exposed to copper and cadmium. *Comp. Biochem. Physiol.* **94C:** 35-40

Coppellotti O. (1994) Effects of cadmium on *Uronema marinum* (Ciliophora, Scuticociliatida) from Antarctica. *Acta Protozool.* **33:** 159-167

Coppellotti O., De Gabrieli R. (1995) Toxicity of copper in Ciliophora Hypotrichida. In: Heavy Metals in the Environment (Eds. R.D. Wilken, U. Förstner and A. Knöchel), CEP Consultants Ltd., Edinburgh, 281-284

Freedman J.H., Ciriolo M.R., Peisach J. (1989) The role of glutathione in copper metabolism and toxicity. *J. Biol. Chem.* **264:** 5598-5605

Howe G., Merchant S. (1992) Heavy metal-activated synthesis of peptides in *Chlamydomonas reinhardtii*. *Plant Physiol.* **98:** 127-136

Kägi J.H.R. (1991) Overview of metallothionein. *Methods Enzymol.* **205:** 613-626

Meister A., Anderson M.E. (1983) Glutathione. *A. Rev. Biochem.* **52:** 711-760

Piccinni E. (1995) Effects of cadmium on *Tetrahymena*. In: Actes de Colloques IFREMER "La biologie des protozoaires, invertébrés et poissons: modèles expérimentaux in vitro et applications" (Ed. IFREMER), Plouzané, **18:** 17-22

Piccinni E., Albergoni V. (1996) Cadmium detoxification in Protists. *Comp. Biochem. Physiol.* **113C:** 141-147

Piccinni E., Coppellotti O. (1982) Response to heavy metals in organisms - II. Effects of physiological and non physiological metals on *Ochromonas danica*. *Comp. Biochem. Physiol.* **71C:** 135-140

Piccinni E., Coppellotti O., Guidolin L. (1985) Chelatins in *Euglena gracilis* and *Ochromonas danica*. *Comp. Biochem. Physiol.* **82C:** 29-36

Piccinni E., Irato P., Guidolin L. (1990) Cadmium-thionein in *Tetrahymena thermophila* and *Tetrahymena pyriformis*. *Europ. J. Protistol.* **26:** 176-181

Piccinni E., Irato P., Cavallini L. and Ammermann D. (1992) Effects of cadmium in *Stylonychia lemnae*, *Stylonychia notophora* and *Oxytricha granulifera*: isolation of a cadmium-binding protein. *J. Protozool.* **39**: 589-593

Piccinni E., Staudenmann W., Albergoni V., De Gabrieli R., James P. (1994) Purification and primary structure of metallothioneins induced by cadmium in the protists *Tetrahymena pigmentosa* and *Tetrahymena pyriformis*. *Eur. J. Biochem.* **226:** 853-859

Pool M.L. (1981) Exposure and health effects of cadmium Part 3. Effects of cadmium on enzyme activities. *Toxic. Environ. Chem. Rev.* **4:** 179-203

Roesijadi G. (1992) Metallothioneins in metal regulation and toxicity in aquatic animals. *Aquat. Toxicol.* **22:** 81-114

Scheuhammer A.M., Cherian M.G. (1991) Quantification of metallothionein by silver saturation. *Methods Enzymol.* **205:** 78-83

Shaw III C.F., Petering D.H., Weber D.N., Gingrich D.J. (1989) Inorganic studies of the cadmium-binding peptides from *Euglena gracilis*. In: Metal Ion Homeostasis. Molecular Biology and Chemistry (Eds. D.H. Hamer and D.R. Winge), Alan R. Liss, Inc., New York, 313-324

Singhal R.K., Anderson M.E., Meister A. (1987) Glutathione, a first line of defense against cadmium toxicity. *FASEB J.* **1:** 220-223

Received on 6th May, 1996; accepted on 29th July, 1996

Acta Protozoologica (1996) 35: 287 - 295

ACTA
PROTOZOOLOGICA

Phototaxis and Gravitaxis in *Dunaliella bardawil*: Influence of UV Radiation

Carlos JIMÉNEZ[1], Félix L. FIGUEROA[1], José AGUILERA[1], Michael LEBERT[2] and Donat-P. HÄDER[2]

[1]Departamento de Ecología, Facultad de Ciencias, Universidad de Málaga, Málaga, Spain; [2] Institut für Botanik und Pharmazeutische Biologie, Friedrich-Alexander-Universität, Erlangen, Germany

Summary. The phototactic and gravitactic responses of the ß-carotene-accumulating halotolerant green alga *Dunaliella bardawil* has been investigated. It has been found that light-activated motile responses depend on (i) the irradiance, (ii) the light history of the cells, (iii) dark adaptation and iv) the quality of the actinic light. Low light-grown cells (low ß-carotene content) never showed positive phototaxis in the light range 1-1000 W m^{-2}, but rather a negative phototactic response at 350 - 500 W m^{-2} depending on prior dark adaptation (4 h). High light-grown cells (high ß-carotene content) showed a very different response depending on whether or not cells were dark adapted: not dark adapted cells presented negative phototaxis even at irradiances as low as 1 W m^{-2}; this behavior changed in dark adapted cells, which had positive responses to light of low irradiances (1 - 5 W m^{-2}) and negative ones only at ≥ 500 W m^{-2}. Intermediate irradiances in the range 10 - 100 W m^{-2} usually did not induce any phototactic response in *Dunaliella* and motility was reduced to 10 - 20 % of the cells. Blue light was shown to induce phototaxis in *D. bardawil*, whereas red light did not. Every phototactic response in *D. bardawil* was impaired after 10 h of exposure to UV-A or UV-B radiation; nevertheless, normal behavior was recovered after 24 h under the same UV treatment. In addition, *D. bardawil* showed negative gravitaxis, which was not affected by UV radiation.

Key words: *Dunaliella bardawil*, gravitaxis, light quality, phototaxis, UV radiation.

INTRODUCTION

Phytoplankton organisms are responsible for about half of the photosynthetic biomass production on our planet (Häder et al. 1995). In addition to diatoms, dinoflagellates and cyanobacteria, green algae are among the most important biomass producers. Any sizable reduction in the populations by, e.g., increased solar UV-B radiation is bound to have adverse effects on the whole ecosystem and the biomass production through all levels of the biological foodweb (El Sayed 1988).

Address for correspondence: Donat-P. Häder, Institut für Botanik und Pharmazeutische Biologie, Friedrich-Alexander-Universität, Staudtstr. 5, D-91058 Erlangen, Germany; Fax +49 9131 858215

Like many other motile microorganisms, the halophilic *Dunaliella bardawil* orients in its habitat using a number of external stimuli including light, thermal and chemical gradients and the earth's gravity vector (Nultsch and Häder 1988). Guided by these clues it moves to areas in its microenvironment with suitable conditions for growth and survival. Different species rely on different strategies for orientation. Some Cryptophyceae and a neuston-forming *Euglena* show exclusively positive phototaxis at all studied light intensities (Rhiel et al. 1988a, b; Gerber and Häder 1994). In contrast, other algae respond positive phototactically at low fluence rates and negative phototactically at higher fluence rates (Häder et al. 1987). A different group shows a pronounced diaphototaxis (orientation perpendicular to the light direction) at all studied

fluence rates (Rhiel et al. 1988a, b). In addition, gravitaxis plays a major role in many phytoplankton species (Häder 1987, Rhiel et al. 1988b).

Dunaliella salina and *D. viridis* have been found to show both positive and negative phototaxis depending on the irradiance (Posudin et al. 1991, 1992). The two species differ in their point of inversion between positive and negative phototaxis. In addition to phototaxis, these cells also show a clear-cut photokinesis (dependence of the swimming velocity on the absolute irradiance, Posudin et al. 1988, 1992). While the photoreceptor for the responses has not yet been identified, preliminary work indicates that a blue absorbing chromophore is involved; in addition, some activity in the UV has been observed (Posudin et al. 1990).

Solar radiation has been found to impair photoorientation and motility in a number of test systems studied so far (Häder and Häder 1988, 1989, 1990). DNA is an unlikely UV-B target for these inhibitions since the effects were visible within a few minutes and no photorepair mediated by a photolyase has been observed (Häder et al. 1986, Häder and Häder 1988). Other studies have indicated that the inhibition of phototaxis is caused by a specific destruction of the photoreceptor protein-pigment complex (Brodhun and Häder 1993).

The aim of this study is to demonstrate the sensitivity of *Dunaliella bardawil*, a ß-carotene accumulating species, to ultraviolet radiation and to analyze the effects of solar and artificial UV radiation on the photoorientation of the cells.

MATERIALS AND METHODS

Dunaliella bardawil Ben-Amotz and Avron was obtained from Prof. Uri Pick, Weizmann Institute of Science, Israel. It was grown in batch cultures in Johnson et al. (1968) medium at 1 M NaCl, 5 mM KNO_3, at 20° C, under continuous white light (WL) and under continuous orbital shaking. High (500 W m^{-2}) or low (20 W m^{-2}) irradiance were used in order to induce high and low ß-carotene cells, respectively (Ben-Amotz and Avron 1983).

Cells were collected in their exponential growth phase and used to estimate the phototactic response of this species. Cells were mounted on glass slides and placed under the microscope in infrared monitoring light (Schott RG740 cut-off filter). A CCD camera was coupled to the microscope and motility and orientation were estimated by means of an on-line image analysis system developed for this purpose (Häder and Vogel 1991). At least one thousand cell tracks were measured per histogram.

Most experiments were performed using white light but the phototactic response of *D. bardawil* was tested also under red and blue light. For this purpose, high light-grown cells, dark preadapted for 4 h, were selected, because under these conditions they had a clear positive phototaxis at low irradiance. Red light was obtained by placing either an Oriel filter 650FS40 (50 nm bandwidth) or two layers of red Plexiglas filters (Röhm and Haas, Darmstadt, Germany, PG502) in front of the light source; for blue light, an Oriel filter 450FS40 (50 nm bandwidth) or a combination of two blue Plexiglas filters Röhm PG627 and PG602 were used. Spectral irradiances were measured by means of a Licor 1800-UW spectroradiometer (Licor, Lincoln, Nebraska, USA); spectra of the halogen lamp and of the blue and red filters are shown in Fig. 1. The irradiances of photosynthetic active radiation (PAR, photosynthetic active radiation, 400 - 700 nm), UV-A and UV-B are summarized in Table 1. Gravitaxis was estimated in the same experimental set-up as described for phototaxis except that the microscope had been placed horizontally, so that the cells moved in a vertical cuvette.

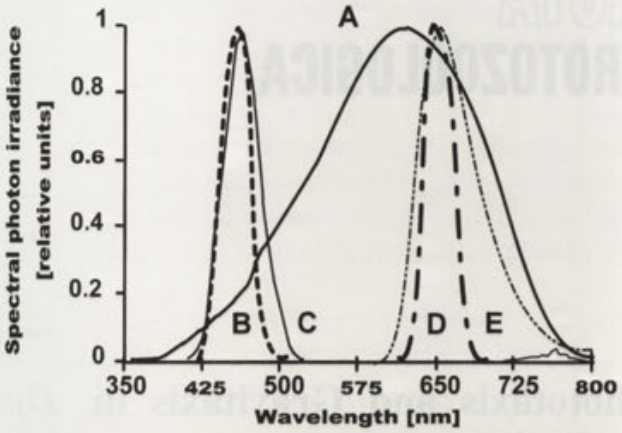

Fig. 1. Spectra of the light source (halogen lamp) used during the phototaxis experiments of *D. bardawil* (A), and of the same lamp with Oriel filter 450FS40 (B), Plexiglas filters Röhm PG627+PG602 (C), Oriel filter 650FS40 (D) and Plexiglas filter Röhm PG502 (E)

RESULTS

Phototaxis of low and high ß-carotene cells

Phototactic orientation of *D. bardawil* depended on the light history of the cells (low or high light-grown cells) and also on the application of a dark pretreatment (4 h)

Table 1. PAR, UV-A and UV-B radiation (W m^{-2}) in the mesocosms used for the estimation of the effects of UV radiation on phototaxis and gravitaxis in *D. bardawil*

	PAR	UV-A	UV-B	TOTAL
VISIBLE	25.29	1.28	0.27	27.97
VIS+UV-A	19.10	5.72	0.01	26.01
VIS+UV-A+UV-B	25.29	11.97	1.28	39.72

Table 2. Phototactic responses of low light-grown cells of *D. bardawil*, not dark preadapted, to increasing irradiances. (Θ- angle of preferred swimming; r- circular regression coefficient; % motil.- percentage of motile cells)

Light (W m^{-2})	Θ	r	% motil.	Phototaxis
Dark	267	0.106	81	no
1	301	0.059	55	no
5	119	0.037	58	no
10	178	0.038	51	no
25	168	0.045	55	no
50	239	0.020	49	no
100	175	0.046	55	no
350	206	0.066	76	no
500	192	0.576*	89	negative
700	192	0.531*	87	negative
1000	193	0.590*	91	negative

*Statistically significant non random orientation

Table 3. Phototactic responses of low light-grown cells of *D. bardawil*, dark preadapted, to increasing irradiances. (Θ- angle of preferred swimming; r- circular regression coefficient; % motil.- percentage of motile cells)

Light (W m^{-2})	Θ	r	% motil.	Phototaxis
Dark	341	0.029	76	no
1	166	0.065	40	no
5	174	0.076	11	no
10	130	0.086	29	no
25	274	0.044	29	no
50	226	0.025	7	no
100	126	0.052	34	no
350	179	0.464*	61	negative
500	180	0.435*	68	negative
700	187	0.487*	75	negative
1000	187	0.421*	69	negative

*Statistically significant non random orientation

Table 4. Phototactic responses of high light-grown cells of *D. bardawil*, not dark preadapted, to increasing irradiances. (Θ- angle of preferred swimming; r- circular regression coefficient; % motil.- percentage of motile cells)

Light (W m^{-2})	Θ	r	% motil.	Phototaxis
Dark	246	0.063	66	no
1	203	0.207*	84	negative
5	185	0.639*	68	negative
10	188	0.596*	62	negative
25	176	0.494*	69	negative
50	184	0.562*	56	negative
100	180	0.748*	70	negative
350	183	0.650*	72	negative
500	184	0.774*	69	negative
700	183	0.718*	64	negative
1000	185	0.584*	66	negative

*Statistically significant non random orientation

prior to the estimation of phototaxis. Cells grown under low light (LL, with low ß-carotene content) did not show any phototactic response at irradiances below 500 W m^{-2} (Table 2); higher irradiances (500 to 1000 W m^{-2}) clearly induced negative phototaxis in low light-acclimated cells of *D. bardawil*. After pretreatment of 4 h in the dark (Table 3), the phototactic response was mainly the same, but negative phototaxis appeared at lower irradiances (350 W m^{-2}). The proportion of active motile cells was clearly reduced in the irradiance range 1 - 100 W m^{-2} in both cases (only 10 - 50 % motile cells), increasing at higher irradiances and in the dark.

High light-grown cells (HL) presented a different behavior; not dark preadapted cells (Table 4) showed very clear negative phototaxis, even at very low irradiances, while they swam randomly in the dark, with high motility. Nevertheless, after 4 h in the dark this behavior changed, specially at low irradiances (Table 5). Cells showed random movement in the dark and positive phototactic responses at the lowest irradiances tested (1 - 5 W m^{-2}), with high motility (85 % active swimming cells). Higher irradiances, between 10 and 350 W m^{-2}, did not induce any phototactic response, and cells showed a totally random movement; in this range of irradiances a high proportion of cells stopped their movement, and only some 10 - 20 % showed active swimming, which was fully recovered at higher irradiances (500 - 1000 W m^{-2}), displaying clear negative phototaxis.

Influence of light quality on the phototactic response

Blue light of low irradiances induced clear positive phototaxis in *D. bardawil* in the range of 0.016-6.3 W m^{-2} (Table 6) with 20 - 90 % motile cells; higher irradiances (up to 63 W m^{-2}) induced the same response as white light: cells showed random movement and the percentage of actively moving cells was reduced to some 4 - 8 % of the total. Both Oriel and Plexiglas filters induced the same response. Nevertheless, red light of low irradiances never induced positive phototaxis in *D. bardawil*, either using Oriel or Plexiglas filters, in the range of 0.078 to 312 W m^{-2}.

Influence of UV irradiation on phototaxis and gravitaxis of *D. bardawil*

Cells were subjected to UV-A and UV-B treatments during 24 h. HL-grown cells, with high ß-carotene content, showed clear positive phototaxis at 1 W m^{-2} and negative at 1000 W m^{-2} (Table7). This response was maintained during the whole experi-

Table 5. Phototactic response of high light-grown cells of *D. bardawil*, dark preadapted, to increasing light intensity. (Θ- angle of preferred swimming; r- circular regression coefficient; % motil.- percentage of motile cells)

Light (W m^{-2})	Θ	r	% motil.	Phototaxis
Dark	66	0.017	83	no
1	353	0.745*	85	positive
5	354	0.885*	84	positive
10	345	0.029	34	no
25	34	0.071	6	no
50	177	0.027	16	no
100	310	0.022	20	no
350	205	0.028	14	no
500	188	0.201*	25	negative
700	188	0.378*	63	negative
1000	176	0.858*	84	negative

*Statistically significant non random orientation

Table 6. Induction of phototaxis by blue and red light in *D. bardawil*. Angle of preferred swimming of the cells (Θ) circular regression coefficient (r) and percentage of motile cells (% motil.) in high light cells dark preadapted

Light (W m^{-2})	Θ	r	% motil.	Phototaxis
Blue Oriel filter				
0.500	349	0.684*	91	positive
5.000	245	0.561*	33	positive
23.000	221	0.065	4	no
33.000	205	0.054	4	no
47.000	360	0.182	4	no
Red Oriel filter				
0.600	148	0.033	14	no
3.000	114	0.012	10	no
11.000	66	0.020	10	no
22.000	94	0.029	8	no
32.000	344	0.072	14	no
Blue Plexiglas filter				
0.016	22	0.294*	47	positive
0.063	358	0.578*	56	positive
0.630	356	0.703*	36	positive
6.300	359	0.749*	20	positive
63.000	3	0.179	8	no
Red Plexiglas filter				
0.078	308	0.048	52	no
0.312	288	0.031	87	no
3.120	125	0.014	34	no
31.200	154	0.145	17	no
312.000	126	0.105	20	no

*Statistically significant non random orientation

ments. Nevertheless, both UV-A- and UV-B-treated cells lost their phototactic response after 10 h of treatment. However, they recovered their normal phototactic behavior after 24 h. Therefore the effects of UV radiation on the phototactic response of *D. bardawil* were transient; moreover no significant variation of cell density among the three cultures was found (data not shown).

LL cells only showed clear phototactic responses at 1000 W m^{-2} (negative) at the beginning of the experiments. The behavior of UV-treated cells changed with time showing negative phototaxis at 100 W m^{-2} after 2 h (Table 8). However, after 10 h also LL cells lost every phototactic response, as shown for HL cells. The normal behavior was also recovered after 24 h, indicating that the effects of UV light were also transient in LL cells.

In the course of the UV experiments, gravitaxis of *D. bardawil* was also studied. It was found that this species displays negative gravitaxis, which is not affected by the UV treatment (Fig. 2).

DISCUSSION

Dunaliella bardawil shows different light-activated motile responses depending on (i) the irradiance, (ii) the light history of the cells, (iii) dark adaptation and (iv) the quality of the light. Several authors have found that *Dunaliella* presents a wide variety of phototactic, photophobic and photokinetic responses (Halldal 1958, Nultsch 1975, Wayne et al. 1991, Posudin et al. 1992).

Nevertheless, there is no agreement whether or not *Dunaliella* shows negative phototactic responses at high irradiances. Halldal (1958) and Posudin et al. (1992) clearly detected this negative phototaxis, while Wayne et al. (1991) did not find any negative phototactic response in *D. salina* at an irradiance as high as 1350 W m^{-2} at 490 nm. In the present work we find that the threshold of irradiance for negative phototaxis mainly depends on the light history of the cells. Cells of *D. bardawil* grown under low light of 20 W m^{-2} swim away from the light source at irradiances of 500 W m^{-2} and above; when the cells were dark preadapted during 4 h this negative threshold was found at 350 W m^{-2}. However, high light-grown cells (500 W m^{-2}) always show negative phototaxis, even at irradiances as low as 1 W m^{-2}. From our point of view, it is the high irradiance stress that induces this negative response, and under these conditions cells tend to escape from light whichever its irradiance. Nevertheless, after 4 h in dark, high ß-carotene cells show very significant positive phototactic responses at low irradiances (1 - 5 W m^{-2}) and negative ones only at ≥500 W m^{-2}.

It is important to point out that the percentage of active swimming cells of *D. bardawil* tends to be very small at irradiances of 5 to 100 W m^{-2} in LL cultures

Table 7. Angle of preferred swimming (Θ) of the cells of *D. bardawil*, circular regression coefficient (r) and percentage of motile cells (% motil.) in high light-grown cells and incubated during 24 h under visible light, visible+UV-A and visible+UV-A+UV-B. Irradiance to induce phototaxis was increased from 1 to 1000 W m^{-2}

		VISIBLE				VIS+UV-A				VIS+UV-A+UV-B			
	Light Wm^{-2}	Θ	r	% motil.	Phototaxis	Θ	r	% motil	Phototaxis	Θ	r	% motil.	Phototaxis
T=0	Dark	33	0.048	30	no	-	-	-	-	-	-	-	-
	1	5	0.385*	89	positive	-	-	-	-	-	-	-	-
	100	50	0.051	8	no	-	-	-	-	-	-	-	-
	1000	178	0.234*	81	negative	-	-	-	-	-	-	-	-
T=2 h	Dark	118	0.055	82	no	91	0.145	53	no	91	0.067	85	no
	1	1	0.564*	93	positive	356	0.392*	81	positive	0	0.416*	93	positive
	100	88	0.028	30	no	322	0.027	6	no	28	0.028	12	no
	1000	185	0.527*	65	negative	187	0.399*	14	negative	163	0.322*	38	negative
T=5 h	Dark	284	0.082	98	no	45	0.124	50	no	48	0.088	97	no
	1	13	0.540*	88	positive	356	0.274*	55	positive	357	0.619*	99	positive
	100	70	0.041	57	no	145	0.083	8	no	152	0.032	53	no
	1000	192	0.701*	83	negative	201	0.419*	29	negative	197	0.540*	84	negative
T=10 h	Dark	34	0.118	96	no	119	0.047	73	no	162	0.055	83	no
	1	1	0.714*	95	positive	57	0.029	55	no	134	0.013	83	no
	100	101	0.049	37	no	196	0.076	45	no	64	0.060	71	no
	1000	188	0.716*	84	negative	135	0.096	27	no	160	0.173	85	no
T=24 h	Dark	112	0.137	97	no	102	0.070	97	no	130	0.106	90	no
	1	14	0.442*	99	positive	1	0.694*	97	positive	1	0.841*	97	positive
	100	175	0.081	98	no	135	0.059	60	no	120	0.082	60	no
	1000	194	0.824*	94	negative	206	0.387*	82	negative	197	0.486*	76	negative

*Statistically significant non random orientation

Table 8. Angle of preferred swimming (Θ) of the cells of *D.bardawil*, circular regression coefficient (r) and percentage of motile cells (% motil.) in low light-grown cells and incubated during 24 h under visible light, visible+UV-A and visible+UV-A+UV-B. Light intensity of measurement of phototaxis was increased from 1 to 1000 W m^{-2}

		VISIBLE				VIS+UV-A				VIS+UV-A+UV-B			
	Light Wm^{-2}	Θ	r	% motil.	Phototaxis	Θ	r	% motil.	Phototaxis	Θ	r	% motil.	Phototaxis
T=0	Dark	310	0.155	97	no	-	-	-	no	-	-	-	-
	1	86	0.072	51	no	-	-	-	no	-	-	-	-
	100	129	0.096	31	no	-	-	-	no	-	-	-	-
	1000	189	0.480*	78	negative	-	-	-	no	-	-	-	-
T=2 h	Dark	93	0.086	31	no	6	0.083	99	no	61	0.110	98	no
	1	194	0.226*	10	positive	6	0.628*	100	positive	359	0.419*	98	positive
	100	145	0.040	12	no	191	0.482*	57	negative	177	0.291*	66	negative
	1000	192	0.473*	30	negative	193	0.748*	79	negative	193	0.534*	84	negative
T=5 h	Dark	126	0.027	55	no	159	0.0321	100	no	93	0.178	83	no
	1	162	0.090	56	no	0	0.801*	63	positive	1	0.799*	99	positive
	100	137	0.119	8	no	156	0.081	84	no	127	0.084	97	no
	1000	197	0.528*	29	negative	198	0.635*	50	negative	195	0.475*	99	negative
T=10 h	Dark	111	0.197	55	no	129	0.029	95	no	179	0.054	98	no
	1	176	0.095	48	no	148	0.143	94	no	86	0.026	88	no
	100	180	0.382*	77	negative	252	0.027	73	no	105	0.047	41	no
	1000	198	0.573*	58	negative	178	0.194	58	no	154	0.017	96	no
T=24 h	Dark	128	0.074	96	no	143	0.086	85	no	313	0.100	83	no
	1	56	0.160	58	no	157	0.084	90	no	14	0.067	84	no
	100	176	0.321*	53	negative	188	0.460*	60	negative	204	0.232*	71	negative
	1000	185	0.655*	92	negative	188	0.742*	97	negative	172	0.374*	77	negative

*Statistically significant non random orientation

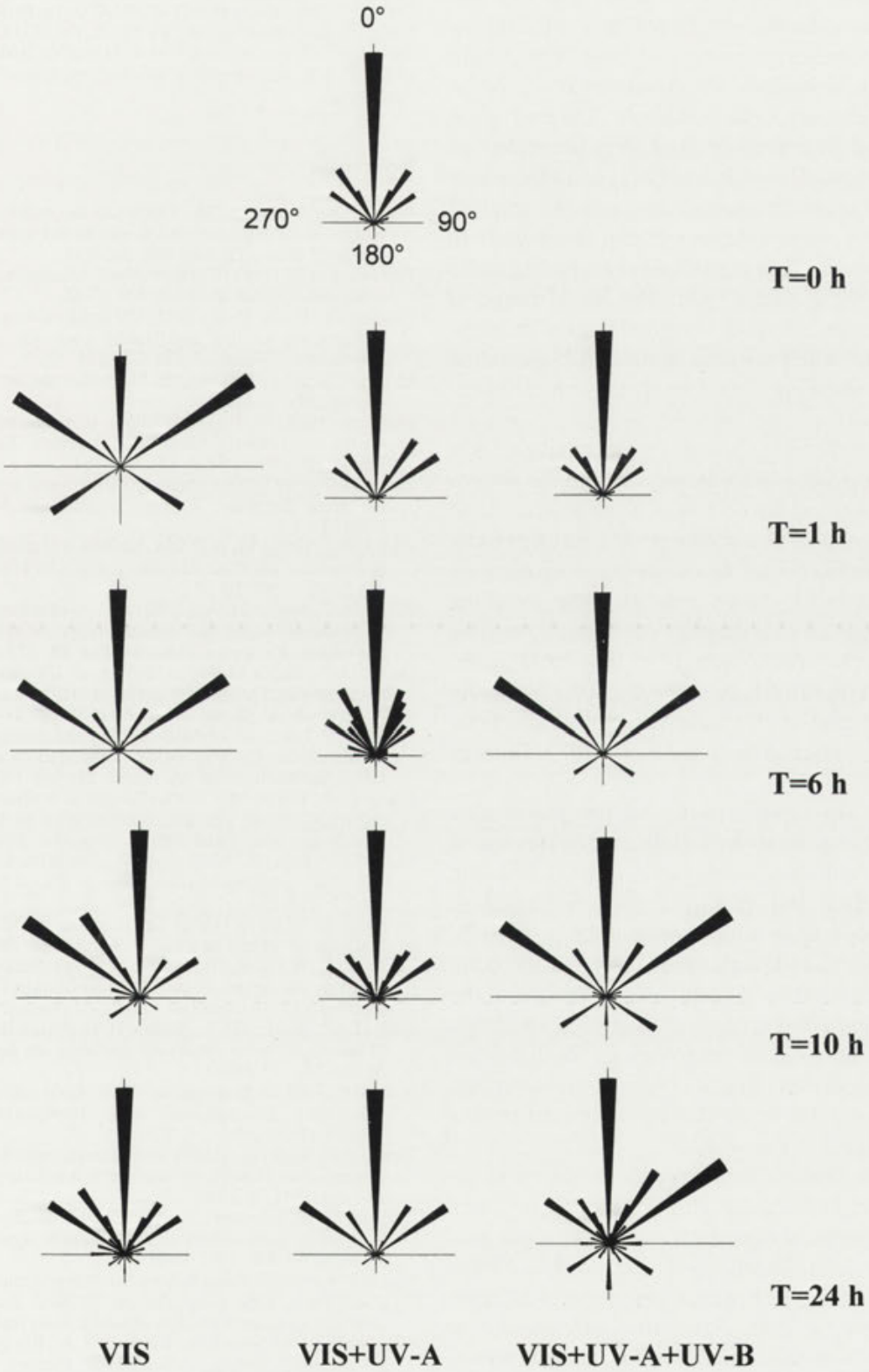

Fig. 2. Gravitactic response of high light-grown cells of *D. bardawil* after treatment under visible (VIS), visible + UV-A (VIS+UV-A) and visible + UV-A + UV-B (VIS+UV-A+UV-B) radiation during 24 h in a mesocosm system (see text for details)

(Table 3) and of 10 to 350 W m^{-2} in HL cultures (Table 5). Also under those light regimes cells did not show any preferred swimming direction. These light ranges seem to be optimal for growth of *D. bardawil* and no phototactic response was found. The ecological significance of these findings was already mentioned by Massjuk (1973), Borowitzka (1981) and Moulton et al. (1987); *Dunaliella* species are able to migrate vertically in the water column and can accumulate in the surface layers or near the sediment according to the irradiance of the incident light. The broad range of optimal irradiation allows *D. bardawil* to exist throughout most of the water column in natural hypersaline environments showing a very passive (nonmotile) behavior.

HL-grown cells of *D. bardawil* accumulate large amounts of ß-carotene in oil droplets within the chloroplast (Ben-Amotz and Avron 1983). It can be speculated that this pigment acts as a screen for the incident light, since higher irradiances are necessary to induce negative phototaxis than in LL-grown cells; also, the screening effect of those ß-carotene droplets could be responsible for the positive phototaxis found at 1 - 5 W m^{-2} in HL cells, which is not found in LL-grown cells. This screening effect of ß-carotene in *D. bardawil* is a well described phenomenon (see Ben-Amotz and Avron 1983, Jiménez and Pick 1993).

No studies on action spectra of the phototactic response of *D. bardawil* was conducted in this work. It has already been shown (Wayne et al. 1991, Posudin et al. 1992) that the spectrum for phototaxis in *Dunaliella* species has a maximum at 450 - 460 nm. The use of Oriel and Plexiglas blue filters with spectra centered at 450 nm (Fig. 1) confirms the results of the above mentioned authors; blue light significantly stimulates positive phototactic responses in *D. bardawil* which is not found in red light. These authors suggest that carotenoproteins or rhodopsins act as the photoreceptor pigments in *Dunaliella*.

UV radiation does not interfere with the natural negative gravitaxis of *D. bardawil*. This is in contrast to results in other phytoplankton organisms such as *Euglena gracilis* and several dinoflagellates (Häder and Liu 1990a, b; Tirlapur et al. 1993). However, phototaxis is affected in both HL and LL cells. After 10 h of exposure to UV-A and/or UV-B radiation *D. bardawil* lost its phototactic response, which is recovered after 24 h. Moreover, LL cells show negative phototaxis at 100 W m^{-2} after 2 h of UV treatment.

Acknowledgments. This work was financially supported by the European Community (EV5V-CT91-0026) to D.-P. H., by the Acción Integrada Hispano-Alemana No. 133-B, DAAD (322-AI-e-dr) and by the CICYT Projects No. AMB93-1211 and No. AMB94-0684-CO_2-O_2 to F. L. F. J. A. was supported by a doctoral fellowship of the Junta de Andalucía.

References

Ben-Amotz A., Avron M. (1983) On the factors which determine massive ß-carotene accumulation in the halotolerant alga *Dunaliella bardawil*. *Plant Physiol.* **83:** 593-597

Borowitzka L. J. (1981) The microflora. Adaptation to life in extremely saline lakes. *Hydrobiologia* **81:** 33-46

Brodhun B., Häder D.-P. (1993) UV-induced damage of photoreceptor proteins in the paraflagella body of *Euglena gracilis*. *Photochem. Photobiol.* **58:** 270-274

El Sayed S. Z. (1988) Fragile life under the ozone hole. *Natural History* **97:** 72-112

Gerber S., Häder D.-P. (1994) Effects of enhanced UV-B irradiation on the red coloured freshwater flagellate *Euglena sanguinea*. *FEMS Microbiol. Ecol.* **13:** 177-184

Häder D.-P. (1987) Polarotaxis, gravitaxis and vertical phototaxis in the green flagellate, *Euglena gracilis*. *Arch. Microbiol.* **147:** 179-183

Häder D.-P., Häder M. A. (1988) Inhibition of motility and phototaxis in the green flagellate, *Euglena gracilis*, by UV-B radiation. *Arch. Microbiol.* **150:** 20-25

Häder D.-P., Häder M. A. (1989) Effects of solar UV-B. irradiation on photomovement and motility in photosynthetic and colorless flagellates. *Environm. Experim. Bot.* **29:** 273-282

Häder D.-P., Häder M. (1990) Effects of UV radiation on motility, photo-orientation and pigmentation in a freshwater *Cryptomonas*. *J. Photochem. Photobiol. B: Biol.* **5:** 105-114

Häder D.-P., Liu S.-M. (1990a) Motility and gravitactic orientation of the flagellate, *Euglena gracilis*, impaired by artificial and solar UV-B radiation. *Curr. Microbiol.* **21:** 161-168

Häder D.-P., Liu S.-M. (1990b) Effects of artificial and solar UV-B radiation on the gravitactic orientation of the dinoflagellate, *Peridinium gatunense*. *FEMS Microbiol. Ecol.* **73:** 331-338

Häder D.-P., Rhiel E., Wehrmeyer W. (1987) Phototaxis in the marine flagellate *Cryptomonas maculata*. *J. Photochem. Photobiol. B: Biol.* **1:** 115-122

Häder D.-P., Vogel K. (1991) Simultaneous tracking of flagellates in real time by image analysis. *J. Math. Biol.* **30:** 63-72

Häder D.-P., Watanabe M., Furuya M.(1986) Inhibition of motility in the cyanobacterium, *Phormidium uncinatum*, by solar and monochromatic UV irradiation. *Plant Cell Physiol.* **27:** 887-894

Häder D.-P., Worrest R. C., Kumar H. D., Smith R. C. (1995) Effects of increased solar ultraviolet radiation on aquatic ecosystems. *Ambio* **24:** 174-180

Halldal P. (1958) Action spectra of phototaxis and related problems in volvocales, *Ulva*-gametes and dinophyceae. *Physiol.Plant.* **11:** 118-153

Jiménez C, Pick U. (1993) Differential reactivity of ß-carotene isomers *from Dunaliella bardawil* toward oxygen radicals. *Plant Physiol.* **101:** 385-390

Johnson M. K , Johnson E. J., MacElroy R. D., Speer H. L., Bruff B. S. (1968) Effects of salts on the halophilic alga *Dunaliella viridis*. *J. Bacteriol.* **95:** 1461-1468

Massjuk N. P. (1973) Morphology, taxonomy, ecology and geographic distribution of the genus *Dunaliella* Teod. and prospects for its potential utilization. Naukova Dumka, Kiev (in Ukrainian)

Moulton T. P., Sommer T. R., Burford M. A., Borowitzka L. J. (1987) Competition between *Dunaliella* species at high salinity. *Hydrobiologia* **151/152:** 107-116

Nultsch W. (1975) Phototaxis and photokinesis. In: Primitive Sensory and Communication Systems (Ed. M. J. Carlile), Academic Press., London, 29-90

Nultsch W., Häder D.-P. (1988) Photomovement in motile microorganisms - II. *Photochem. Photobiol.* **47:** 837-869

Posudin Y. I., Kononchuk V. R., Masyuk N. P., Lilitskaya G. G. (1991) On study of photoreception mechanisms of *Dunaliella salina* Teod. *Algologiya* **3:** 23-34

Posudin Y. I., Masyuk N. P., Lilitskaya G. G., Radchenko M. I. (1990) Phototopotaxis of two species of *Dunaliella* Teod. in the spectrum ultraviolet region. *Biofizika* **35:** 968-971

Posudin Y. I., Massjuk N. P., Lilitskaya G. G., Radchenko M. I. (1992) Photomovement of two species of *Dunaliella* Teod. (Chlorophyta). *Algologia* **2:** 37-48

Posudin Y. I., Massjuk N. P., Radchenko M. I., Lilitskaya G. G. (1988) Photokinetic reactions of two *Dunaliella* Teod. species. *Microbiologiya* **57:** 1001-1006

Rhiel E., Häder D.-P., Wehrmeyer W. (1988a) Diaphototaxis and gravitaxis in a freshwater *Cryptomonas*. *Plant Cell Physiol.* **29:** 755-760

Rhiel E., Häder D.-P., Wehrmeyer W. (1988b) Photo-orientation in a freshwater *Cryptomonas* species. *J. Photochem. Photobiol. B: Biol.* **2:** 123-132

Tirlapur U., Scheuerlein R., Häder D.-P. (1993) Motility and orientation of a dinoflagellate, *Gymnodinium*, impaired by solar and ultraviolet radiation. *FEMS Microbiol. Ecol.* **102:** 167-174

Wayne R., Kadota A., Watanabe M., Furuya M. (1991) Photomovement in *Dunaliella salina*: fluence rate-response curves and action spectra. *Planta* **184:** 515-524

Received on 13th December, 1995; accepted on 1st April, 1996

Acta Protozoologica (1996) 35: 297 - 308

ACTA
PROTOZOOLOGICA

Pattern of the Phosphorylated Structures in the Morphostatic Ciliate *Tetrahymena thermophila*: MPM-2 Immunogoldlabelling

Mauryla KIERSNOWSKA[1] and Krystyna GOLIŃSKA[2]

[1]Department of Cytophysiology, Warsaw University and [2]Nencki Institute of Experimental Biology, Warsaw, Poland

Summary. A monoclonal antibody (MPM-2) originally selected against a family of phosphorylated mitotic proteins and an antitubulin antibody were used to compare patterns of microtubules and phosphoproteins in the cytoskeleton of morphostatic *Tetrahymena*. It was shown, using the immunogold labelling technique that the MPM-2 antibody binds to: (1) - fuzzy linkers in proximal parts of the somatic cilia; (2) - amorphic material surrounding the proximal end of the basal bodies; (3) - kinetodesma; (4) - radiating filaments of the contractile vacuole pore; (5) - fine filamentous structures connecting, in the cortical folds, some microtubular systems with surface membranes and/or epiplasm; (6) - non-striated fine filamentous reticulum, localised at the bottom of the oral pouch (packing the oral lip and descending down along the deep fibres). Maximal MPM-2 binding was found on the latter structures. Comparison of the deployment of phosphoproteins with the sculpture of the oral cavity and somatic cortex, observed in scanning electron microscopy, strongly suggests that the cytoskeletal phosphoproteins are involved in the maintenance of the cell shape against distortions brought about by the local periodic activities (phagocytosis, the discharging of the contents of the contractile vacuoles and the contents expelled through the cytoproctal slit).

Key words: cytoskeleton, MPM-2 antibody, phosphoproteins, *Tetrahymena*.

INTRODUCTION

The monoclonal antibody MPM-2, originally selected against phosphoproteins of the mitotic apparatus of mammalian cells (Davis et al. 1983) also recognises the phosphoproteins within the interphase cells (reviewed by Davis and Rao 1987) and in distant organisms such as Paramecium (Keryer et al. 1987,1990; Kaczanowska et al. 1996) and *Tetrahymena* (Huelsmann et al. 1992, Gitz and Pennock 1995). Taagepera et al. (1994) showed that the MPM-2 antibody recognises phosphorylated epitopes on the threonine residue of the variable proteins.

Address for correspondence: Mauryla Kiersnowska, Department of Cytophysiology, Warsaw University, Krakowskie Przedmieście 26/28, 00-927 Warszawa, Poland

In the ciliate *Paramecium* some phosphoproteins associated with basal bodies were permanently stained with the MPM-2 antibody throughout the cell cycle, whereas other phosphoproteins appeared in various skeletal structures only at specific stages of the cell cycle (Keryer et al. 1987, 1990; Garreau de Loubresse et al. 1991; Sperling et al. 1991; Kaczanowska et al. 1996). Williams et al. (1986), Honts and Williams (1990), Dress et al. (1992), Jerka-Dziadosz et al. (1995) identified number of specific cytoskeletal components within the oral apparatus of *Tetrahymena*; among them, some tetrin (80 kDa) was also identified in the oral apparatus of *Paramecium* as a phosphoprotein recognised by the MPM-2 antibody (Keryer et al. 1990). This structure is also recognised by an anticentrosomal antibody CTR210 (Keryer et al. 1990). Huelsmann et al. (1992) observed a very dense binding of the MPM-2 antibody at the bottom

of the oral apparatus in *T. pyriforms*. These authors also identified a subset of phosphoproteins binding the MPM-2 antibody in the immunoblots from the cytoskeletal frameworks of these cells. During divisional morphogenesis the appearance of this labelling is correlated to the appearance of the deep fibre bundle at the bottom of the oral pouch in *Tetrahymena pyriforms* (Kiersnowska, unpublished observation, Kaczanowska et al. in prep.) and in *Paramecium* (Kaczanowska et al. 1996). However, the exact localisation of the MPM-2-binding sites has never been analysed at the ultrastructural level in the interphase cytoskeleton of *Tetrahymena*.

We focused our attention on the phosphorylation of materials possibly participating in the interaction between the microtubular elements of the cytoskeleton and the filamentous materials, functioning as the linkers among different skeletal elements. These elements and the general organisation of the cortical structures in the morphostatic *Tetrahymena* were described by Allen (1967), Frankel and Williams (1973), Allen and Wolf (1979). The details of the cytoskeleton of the oral apparatus were described by Forer et al. (1970) and by Williams and co-authors in a series of papers, notably Nilsson and Williams (1966), Williams and Luft (1968), Gavin (1977), Sattler and Staehelin (1979), Williams and Bakowska (1982), Williams (1986), Williams et al. (1986), Dress et al.(1992).

MATERIALS AND METHODS

Material. The ciliate *Tetrahymena thermophila* strain WU131 was grown in 10 ml tubes with 2% proteose peptone/yeast extract (Difco) according to Nelsen et al. (1981). Axenic stocks were maintained at room temperature in culture tubes and transferred twice a week. For experiments, cells were grown to a late logarithmic phase at 28° C then rinsed with Tris HCl buffer (pH 7.4). They were starved for 18 h prior to fixation to obtain a uniform population of the initiated cells (Bruns and Brussard 1974).

Antibodies. The monoclonal antibody MPM-2 was generously supplied by Dr P. Rao (University of Texas). To detect the microtubules, commercial monoclonal antibody against tubulin (clone TUB 1A2, Sigma) was used.

Indirect immunofluorescene. Starved cells were extracted for 3-5 min. in 0.5% Triton X-100 in PHEM buffer, pH 6,9 (Schliwa and Van Blerkom 1981) and then fixed for 30 min. with freshly prepared 2% paraformaldehyde. After 1h washing (4 x in PBS and thereafter 2 x in PBS containing 0.1% BSA), the cells were incubated overnight (4-5° C) in the primary antibody at dilution 1:250 in 1% BSA-PBS. The cells were washed (4 x, every 10 min.) in 0,1% BSA-PBS and then treated 1.5 h (30° C) with 1:100 diluted FITC-conjugated goat anti- mouse IgG in 1% BSA-PBS. After washing in PBS, the final pellet was mixed with PPD solution to slow the quenching of the fluorescent tag. The pattern of staining was observed with Carl-Zeiss Jena microscope equipped with epifluorescence illumination.

Immunogold localisation. The cells were permeabilized, fixed, washed and treated with MPM-2 antibody as for the indirect immunofluorescence. After washing the cell pellet was divided in two samples, one sample was prepared for indirect immunofluorescence, the other one was incubated (1.5 h, 30° C) in 1:5 dilution (in 1% BSA-PBS) of 5 nm gold-conjugated goat anti-mouse polyvalent immunoglobulins (G,A,M; Sigma). Cells were then washed and postfixed in 1:1 mixture of 6% glutaraldehyde and 2% OsO_4, freshly prepared with cacodylate buffer (pH 7.2, 0.05 M). The cell pellet was dehydrated and embedded in Epon. Thin sectioned cells were viewed with a JEOL 1200 EX transmission electron microscope.

Transmission electron microscope. Control, nonpermeabilized and nonlabelled cells were fixed in a mixture of glutaraldehyde and osmium tetraoxide, dehydrated and embedded as permeabilized, labelled cells. Sections of whole cells were stained with uranyl acetate and lead citrate.

Scanning electron microscope. Sampling, fixation and embedding followed the procedures described by Kiersnowska et al. (1993).

RESULTS

1. Indirect immunofluorescence staining

Figure 1 shows the immunodecoration of the ventral surface of *Tetrahymena thermophila* with the anti-tubulin antibody. This general cortical organisation is characterised by a regular pattern of longitudinal rows of basal bodies and by a subapically located oral apparatus.

The oral apparatus (OA) is bordered on its right edge by a single row of ciliated basal bodies of the undulating membrane (UM) paralleled by an internal row of unciliated basal bodies (the latter are seen only on some specimens, and not shown in Fig. 1). On the left dorsal wall of the buccal cavity there are three obliquely slanted membranelles (M_1, M_2 and M_3, Figs. 1 and 7) partly covered by the external rim of the oral aperture (Figs. 7-9). The cell surface is covered with 17-19 parallel meridional ciliary rows running within grooves; one to three postoral ciliary rows extend from the posterior edge of the OA to the posterior pole, whereas the other longitudinal rows of basal bodies run from the anterior to the posterior pole (Figs. 1, 3).

The indirect immunostaining of permeabilized *T. thermophila* with the MPM-2 antibody recognises phosphoproteins located within the OA and somatic structures (Figs. 2-6). The opening of the oral cavity is rimmed by the ridges of highly fluorescent material, with very weak labelling of the cilia of the membranelles (Fig. 2). The weak fluorescence of the basal bodies of the membranelles (the upper M_1 and intermediate M_2) is detected at the intermediate focus level of the OA (Fig. 4). The most intensive fluorescence (Figs. 4-6) is localised at

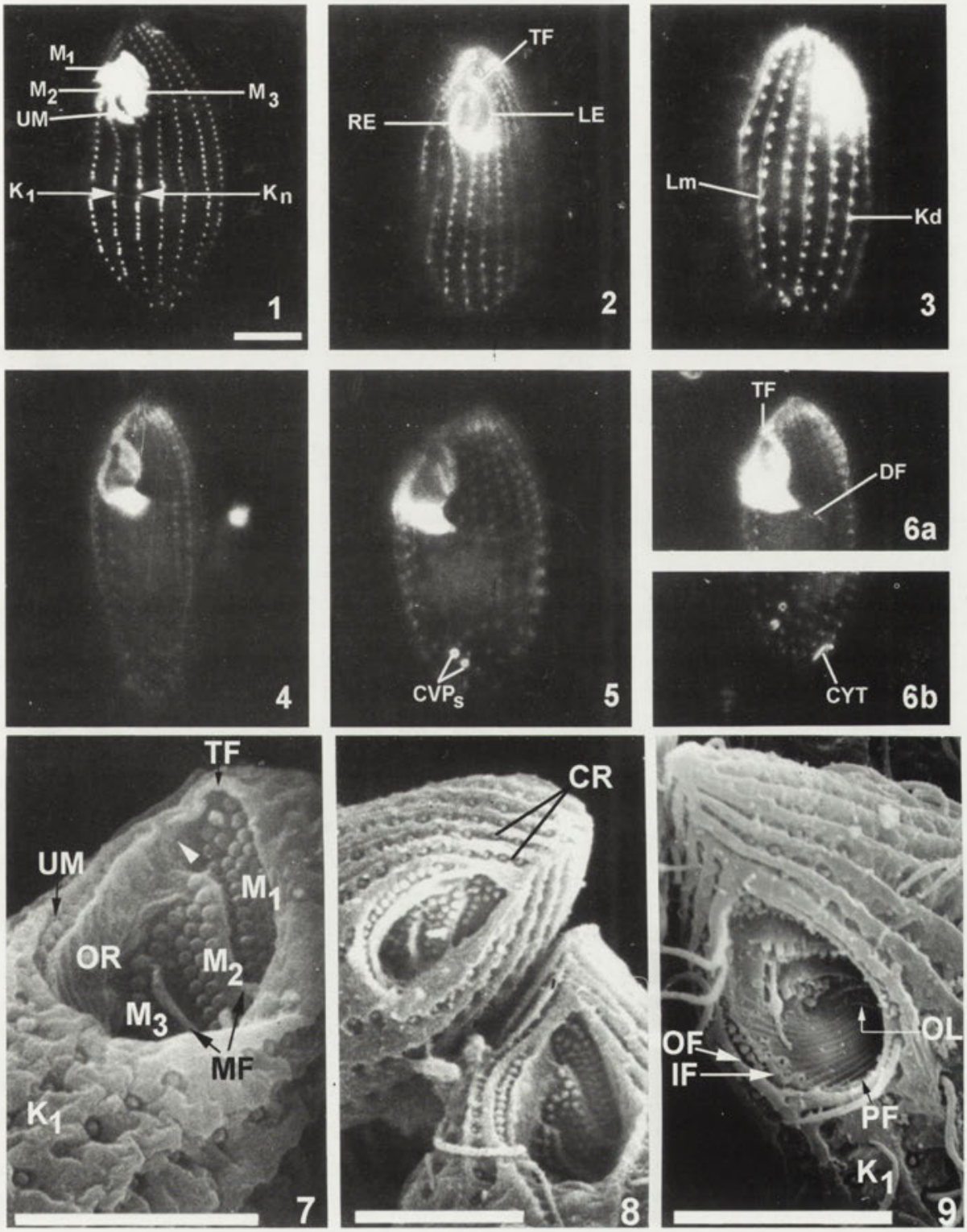

Figs. 1-6. Indirect immunoflourescence staining of the interphase cells of *T. thermophila*. 1 - immunostaining with the monoclonal anti-tubulin antibody. 2-6 - immunostaining with the MPM-2 antibody at different focuses; 2 - viewed from ventral side; 3 - viewed from laterodorsal side; 4, 5 and 6a - different optical sections of the oral apparatus; 6b - focused on contractile vacuole pores and the cytoproctal slit. CVPs - contractile vacuole pores; CYT - cytoproct; DF - deep fibre; Kd - kinetodesmal fibre; Lm - longitudinal microtubules; M_1, M_2, M_3 - membranelles; K_1 and K_n basal bodies rows number one and n; RE and LE - right and left edges of the buccal cavity; TF - top fold; UM - undulating membrane. Bar - 10 μm; Figs. 7-9. SEM micrographs of the apical region of *Tetrahymena*. CR - cortical ridge; K_1 - basal bodies rows number one; M_1, M_2, M_3 - membranelles; MF - membranellar fold; OF and IF - outer and inner folds of UM; OL - oral lip; OR - oral ribs; PF - posterior fold; TF - top fold; UM - undulating membrane. Bars - 10 μm

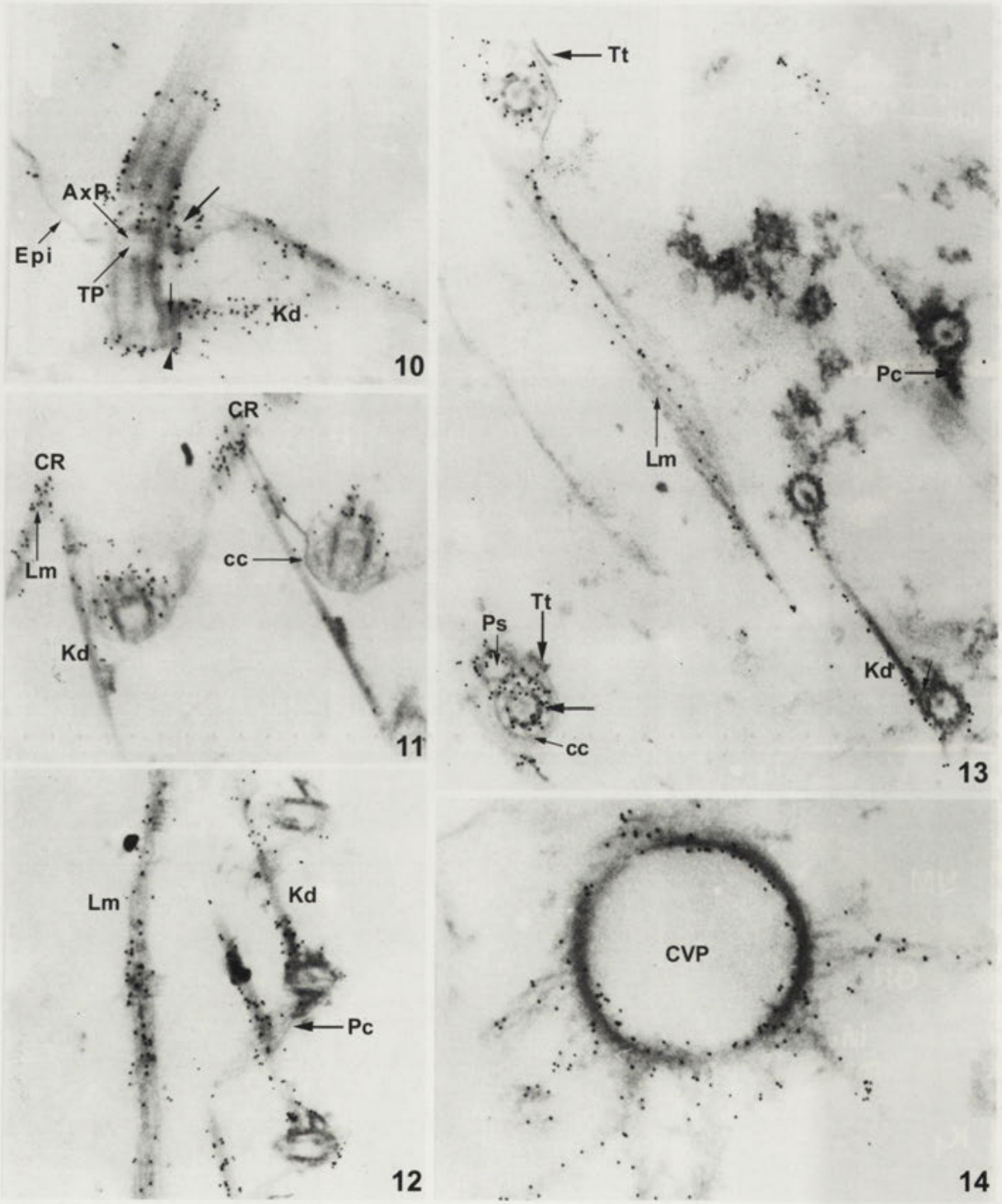

Figs. 10-14. The MPM-2 immunogold staining of cortical somatic structures of *Tetrahymena*. 10 - longitudinal section through cilium and basal bodies, X 45200; 11 - longitudinal section through cortical ridges, X 40500; 12 - oblique section at the level of the proximal part of basal bodies, X 32500; 13 - tangential section through somatic cortex, X 4500; 14 - tangential section through the contractile vacuole pore, X 41000. Arrowhead - linkers to the transversal microtubules; AxP and TP - axosomal and terminal plates; cc - circumciliary ring; CVP- contactile vacuole pore; Kd - kinetodesmal fibre; Epi - epiplasm; Pc-postciliary microtubules; Ps - parasomal sac; thick arrow - axosomal linkers; thin arrow - kinetodesmal linkers; Tt- transversal microtubules

the bottom of the oral cavity seen at the deepest plane of focus. A triangle-shaped structure appears in the left posterior part of the oral cavity and extends inwards to the left of the cell (Fig. 5). The lateral view of this structure (Figs. 5, 6) suggests that the MPM-2 antibody decorates the bottom of the oral cavity and some material along (or associated with) a deep fibre bundle directed toward the inner part of the cytoplasm.

The MPM-2 antibody labels individual basal bodies of the ciliary rows (Figs. 2-6). A single patch marking the basal body location has an anterior short extension which suggests phosphorylation of the kinetodesmal fibre. Along the ciliary rows longitudinal parallel lines of immunostained material are observed (Fig. 3, Lm). Their position suggests that this material is associated with the longitudinal bundles of microtubules underlying the cortical ridges (Figs. 8, 9). In the interphase cells, the MPM-2 antibody decorates the cytoproct (Fig. 6b) and the contractile vacuole pores (Figs. 3, 5, 6b).

Scanning photomicrographs of the oral apparatus of *Tetrahymena thermophila* (Figs. 7-9) are used to deduce the possible cytoarchitectural role of the oral MPM-2 immunostained structures seen in permeabilized cells.

2. The MPM-2-binding sites within the somatic cortex

Comparison of sections through fragments of cortex with extracted cytoskeletal frameworks shows that the outermost structures (plasma membrane and alveolar system) are removed leaving the fibrogranular sheet of the epiplasm as the outside layer. The ridges between ciliary rows are preserved on the sectioned frameworks (Fig. 11); on the right slope of the ridges, bundles of longitudinal microtubules run above the epiplasmic layer (Allen 1967). Allen (1967) showed that a fine fibrillar material surrounds and connects these longitudinal microtubules with the epiplasm. Distribution of the gold particles within the top of ridges (Figs. 11-13) suggests that the MPM-2 antibody labels this connective material, but not the microtubules themselves. From among the basal body associated structures, e.g., kinetodesma, transverse and postciliary microtubules, only the kinetodesma is labelled (Figs. 10-13, Kd, Pc and Tt respectively). Longitudinal sections through a single basal body and cilium (Fig. 10) clearly shows the specificity of the MPM-2 labelling. The intense and homogenous labelling of the cilium covers the region about 500 nm long, extending distally from the axosomal plate (AP), i.e., the dense plate just below the axosomal granule (Ax). The gold particles do not decorate the microtubular doublets, but they mark the fine fibrillar material outside of the doublets and the lateral branches of the extensions of the axosomal plate to the sites where the terminal plate (TP) joins the epiplasm (Figs. 10, 13). A cross section through this region at the level of the axosome, reveals the labelled axosomal linkers whereas the circumciliary ring supporting the terminal plate remains unlabelled (Fig. 13, Cc). The anterior side of the parasomal sac is also labelled (Fig. 13, Ps).

In the basal body, only its proximal end shows some labelling (Fig. 10). Some dense fibrogranular material (Allen 1967) forms a sleeve around the proximal 1/3 of the basal body, seen in a longitudinal section (Fig. 10) and as squares associated with the basal bodies at cross section (Allen 1967). The dense square condensation between the microtubular triplets of the basal body and the kinetodesmal fibre is not labelled (unlike the kinetodesmal fibre itself). However, the other square composed of fine filaments extending to the transverse microtubules is decorated (Fig. 10), whereas the transverse microtubules are free of gold particles (Fig. 13, Tt). The fibrogranular material extending between the transverse and postciliary (Pc) microtubules is also labelled. Thus, there is a very high specificity in the deployment of the phosphoproteins to particular components of the basal body-associated structures. Some sections of the cytoskeletal frameworks are made on the level of the contractile vacuole pores (Fig. 14). The filamentous material around the microtubular ring which forms the contractile vacuole pore is strongly decorated with the MPM-2 antibody. The labelling is also present in the network of fine filaments radiating from the rings toward the cytoplasm.

Diffused labelling is also detected within the macronucleus and within the filamentous material surrounding the micronuclear envelope (data not shown).

3. The MPM-2 binding sites within the oral apparatus

3.1. The structures framing the oral cavity

The three-dimensional image of the oral apparatus of *T. thermophila* (Figs. 7-9) shows that the UM is located between two folds: the outer fold is elevated in a continuity of the ridge located to the right of the ciliary row #1 and the inner fold is formed by the top of the oral ribs at the right edge of the OA. Both folds merge at the apical part of the oral aperture to create the top fold (TF on Figs. 7-9, 15, 16) which covers the apical part of the oral cavity.

At the base of the oral apparatus, the right ridge of the kinety #1 transforms into a very elevated posterior fold. This fold joins with the right ridge of the kinety #n which

Figs. 15-16. Distribution of the MPM-2 labelling in the oral structures. 15 - tangential section through the undulating membrane, the membranelles and the folds of the buccal cavity, X 20500; 16 - tangential section through the top fold, the left wall of the buccal cavity and membranellar fold between the membranelles number one and two, X 26000. M_1 -membranelle number one; mLW - microtubules of the left wall; MF - membranellar fold; OF and IF - outer and inner folds of UM; RF - right fold of the buccal cavity; TF - top fold; UM - undulating membrane; Fig. 17. Tangential section through the oral ribs (OR) of the nonpermeabilized cell, X 49000; Fig. 18. Section through the cytostom-cytopharyngeal region of the most deep part of oral cavity, non permeabilized cell, X 62500. Cy - cytostom; CYP - cytopharynx; mLW - microtubules of the left wall; mOR - microtubules of the oral ribs; nsFFR- nonstriated fine filamentous reticulum; OL oral lip, open arrow heads - groups of microtubules just beneath

is elevated to form the left border of the buccal cavity (Figs. 7, 8). The left ridge of the kinety # n merges into the top fold (Figs. 9, 16).

The outer fold of the UM, the top fold, the left and the posterior fold together create the collar-like structure framing the oral cavity of *Tetrahymena*. Labelling with the MPM-2 antibody detects the fine filamentous materials underlying these folds and associated to microtubules of the somatic ridges of the kineties #1 and # n-1 (Figs. 15, 16).

3.2. The right wall of the buccal cavity

The upper part of the right wall of the buccal cavity is smooth, whereas the lower part is ribbed (Figs. 7, 9). The organisation of the cortex of the ribbed wall has been previously described in detail (Sattler and Staechelin 1979, Smith and Buhse 1983).

There are 17 microtubular bundles that form the ribs. Each bundle represents a specific arrangement of microtubules in a "2 + 4 order". These bundles together with the alveolar sacs between them, bring about the specific sculpture of the oral ribs (OR) seen in SEM (Figs. 7-9) and in TEM sections (Fig. 17).

Beneath the OR complex extends a layer of ribosome free cytoplasm. Sattler and Staehelin (1979) distinguished two groups of fine filaments occurring within this layer: (1) the fine filaments that run parallel to the cell surface and which are regularly interspaced with dense bands and (2) the fine filaments that seem to anchor the microtubules and alveolar sacs to the previous system. Thus, the structurally organised part of the cytoplasm is designated here as the striated fine filamentous reticulum (sFFR on Figs. 19, 21, 25, 27; FFR in Sattler and Staehelin 1979 and in Williams and Bakowska 1982) in contrast to the non-striated filamentous layer (nsFFR, Figs. 18, 21, 22, 27) occurring within the oral lip and around the deep fibres (see section 3.3). Sattler and Staehelin (1979) also noted that the groups of microtubules and the alveolar sacs are linked among themselves and to the plasma membrane by fine filaments.

The MPM-2 antibody marks only the fine material running along the oral ribs microtubules. Probably this fine material links the microtubules to the plasma membrane and to the alveolar sacs membranes. The MPM-2 antibody does not bind to the filaments of the sFFR (Figs. 19, 25).

The smooth, upper part of the right wall is marked with MPM-2 antibody merely beneath the plasma membrane, whereas the more deeply located filamentous layer remains unlabelled (Fig. 15, note the labelled RF in continuity with the unlabelled lower parts sectioned at a deeper level).

The UM is composed of an outer, ciliated and an inner, unciliated row of basal bodies (Figs. 15, 19). The proximal parts of the cilia and their basal bodies are decorated by the gold granules as it is observed in somatic cilia and basal bodies (Figs. 19, 20 versus Fig. 10). The unciliated basal bodies of UM have some phosphorylated epitopes only under the terminal plate (Figs. 19, 25).

Both rows of basal bodies are connected by the filamentous network designated as the UMN (Nilsson and Williams 1966, Williams 1986) that forms a curtain-like structure (Fig. 19). The filaments of the bottom of the UMN join to the cables of the microtubules and probably accompany them (Figs. 25-27). These cables run parallel to the course of the UM and subsequently split into some branches extending from their anterior and posterior ends. Then, the anterior-left branches connect with the microtubular cables issued from the membranellar bases (Williams and Bakowska 1982) and with membranellar folds (Fig. 26). The posterior branches curve towards the cytostomal-cytopharyngeal region and then merge with nsFFR (Fig. 27). A little scarce MPM-2 labelling is associated with the UMN but the cables remains unlabelled (Fig. 25).

In conclusion it is suggested that the strong luminescence of the right border of the oral apparatus (Figs. 2, 4, 5) results from the MPM-2-immunofluorescence of the phosphorylated epitopes of: (1) - the filamentous material of the edge of the right ridge of the kinety #1, (2) - the UM cilia and basal bodies, (3) - the UMN and (4) - the filamentous material along the microtubules of OR.

3.3. The left wall of the buccal cavity

The organisation, the final spatial arrangement and morphology of the adoral zone of the membranelles sculptured within the left part of the buccal cavity have been extensively characterised (Frankel et al. 1984). Between upper M_1 and middle M_2, between M_2 and M_3 and finally posterior to M_3 the three additional folds occur that run parallel to these membranelles (Figs. 7-9, 15). The filaments of the network connecting the basal bodies of membranelles become ordered alongside the walls of these folds (Fig. 16). Within the edge of the folds this fibrillar material is more condensed and it intrudes into the part of the left wall of the buccal cavity free-of-

the cell membrane; Fig. 19. Distribution of the MPM-2 labelling in the oral structures localised on the right side of the oral apparatus, X 29000. mOR-microtubules of the oral ribs; OF and IF - outer and inner folds of UM; sFFR - striated fine filamentous reticulum; UMN - undulating membrane network

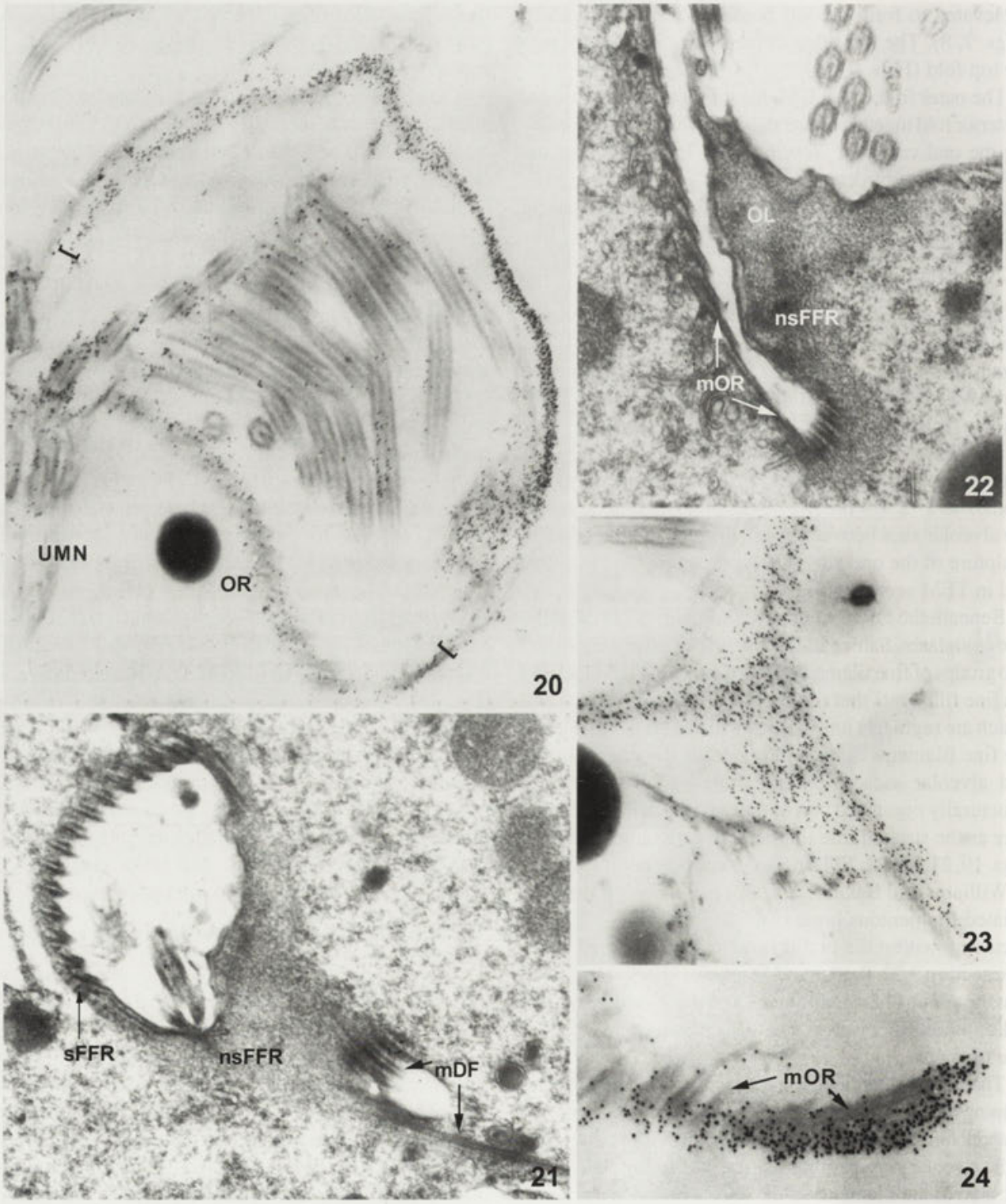

Fig. 20. Distribution of the MPM-2 labelling in the oral lip. Section through the edge of lip (bracket), X 26700.OR - oral ribs; UMN - undulating membrane network; Fig. 21. Oblique section through the cytopharyngeal region of nonpermeabilized cell, X 23500. mDF - microtubules of the deep fibre; nsFFR and sFFr - nonstriated and striated fine filamentous reticulum; Fig. 22. Longitudinal section through the oral lip of the nonpermeabilized cell, X 23900. mOR - microtubules of the oral ribs; nsFFR - nonstriated fine filamenous reticulum; OL - oral lip; Figs. 23-24. Distribution of the MPM-2 labelling in the oral lip and in the distal part of the deep fibre, X 29500 and X45750, respectively. mOR - microtubules of the oral ribs

membranelles (Fig. 15). The left wall is also strengthened by the row of the microtubules (Figs. 15, 16) located beneath the alveolar sacs (Fig. 18).

The MPM-2 antibody marks the filamentous material between the basal bodies of the membranelles (Figs. 15, 16), the upper part of the folds and the filaments around the microtubules of the left wall (Figs. 15, 16). Particularly dense labelling occurs at the edge of the pleat located anterior to the M_2 (data not shown). The basal bodies and cilia of the membranelles are labelled in a pattern corresponding to that observed in the somatic cilia and in the UM (not shown, except cross sections in Figs. 15, 16).

3.4. Cytostome-cytopharyngeal pocket within the oral cavity

The buccal cavity of *Tetrahymena* is directed to the left. This cavity is divided into two compartments due to the similar crescent valve elevated from the left wall and descending to the inner side of the posterior fold (Fig. 9). This valve partly separates the outer (membranellar) part from the inner part designated as the cytostome-cytopharyngeal pocket where food vacuoles are formed. The distal part of the valve forms the oral lip (Fig. 18). The oral lip is strengthened by groups of four microtubules located superficially to the alveoli and with the layer of the epiplasm. The row of microtubules that are located beneath the alveolar sacs of the left wall is absent in the oral lip. The dense epiplasmic layer of the oral lip meets with the fine filamentous material associated with microtubules of the oral ribs extending to the upper side of the cytopharynx. The epiplasm of the oral lip also remains in intimate contact with the fibro-granular matrix packed inside the oral lip (Fig. 18). This matrix corresponds to the specialised cytoplasm observed by Nilsson and Williams (1966). On oblique sections of the oral lip, the fine filaments run parallel to each other, whereas in the other sections this matrix shows a granulo-reticular structure (Figs. 27, 21, 22; respectively). This material is described as the non-striated fine filamentous reticulum (nsFFR). The nsFFR layer surrounds the cytopharyngeal pocket and wraps the microtubules in the form of a funnel which is not closed on its ventral side (Fig. 22). It seems that at least some cables of the UMN and striated fine filamentous reticulum (sFFR) directly merge with the nsFFR (Figs. 21, 27). This nsFFR represents the structure maximally binding the MPM-2 antibody (Figs. 20, 23, 24). Distribution of the phosphorylated structures within the oral apparatus of a non-dividing *Tetrahymena thermophila* is shown on the scheme (Fig. 28) summarising data all presented above.

DISCUSSION

Skeletal phosphoproteins recognised by the MPM-2 antibody in non-dividing *Tetrahymena thermophila* are detected mainly in the filamentous material associated with some specific sets of microtubules as well as in specialised non-microtubular structures like the subsurface filamentous meshwork, kinetodesmal fibres or in the fibrogranular matrix within the cytopharyngeal region.

It may be speculated that the MPM-2 antibody labelling reflects the activation of structures involved in very different functions like: (1) - the reception of the external signals; (2) - the control of the activity of cellular MTOCs; (3) - the control of the periodically functioning organellar systems, such as food vacuole formation, the discharge of the contractile vacuole and the emptying of undigested remnants of food vacuoles, and; (4) - the maintenance of the specific sculpturing of *Tetrahymena*'s surface against the tension of the internal cytosol and against mechanical distortions caused by the above listed local periodical activities.

The phosphorylated epitopes within the cilia and the basal body, recognised by the MPM-2 antibody are recorded by many authors (Keryer et al. 1987, Harper et al. 1993, Gitz and Pennock 1995). In the present study, it was impossible to determine the exact role of the fuzzy linkers observed in the cilia. However, it is reasonable to admit, that a non-random distribution of the MPM-2 labelling within the cilia at the level above the axosomal plate reflects the structural and functional differentiations relevant for the reception of signals controlling the activity of cilia and an imput of Ca^{2+} signal (Plattner 1975).

The amorphic, peribasal body's material represents the microtubules organising centres- the ciliate MTOCs. Thus the labelling within the proximal regions of the basal bodies of *Tetrahymena* corresponds to the previous data about the phosphorylation of MTOCs (Vandre et al. 1984). Keryer et al. (1987) pointed out that the basal bodies in Paramecium are phosphorylated throughout cell cycle. Such phosphorylation, marked by faintly MPM-2 antibody labelling, is also observed in non-proliferating basal bodies of *Tetrahymena*. However, the basal bodies of, either the anarchic field area, or the organising membranelles in the dividing *Tetrahymena* are transiently very strongly labelled with the same antibody (our nonpublished observations and Kaczanowska et al., in prep.). It suggests, that some proteins of the peribasal material, at least in the OA of *Tetrahymena* are the subject of the cell cycle dependent phosphorylation. Similarly, Messinger and Albertini (1991) showed in the mouse oocyte two discrete populations of

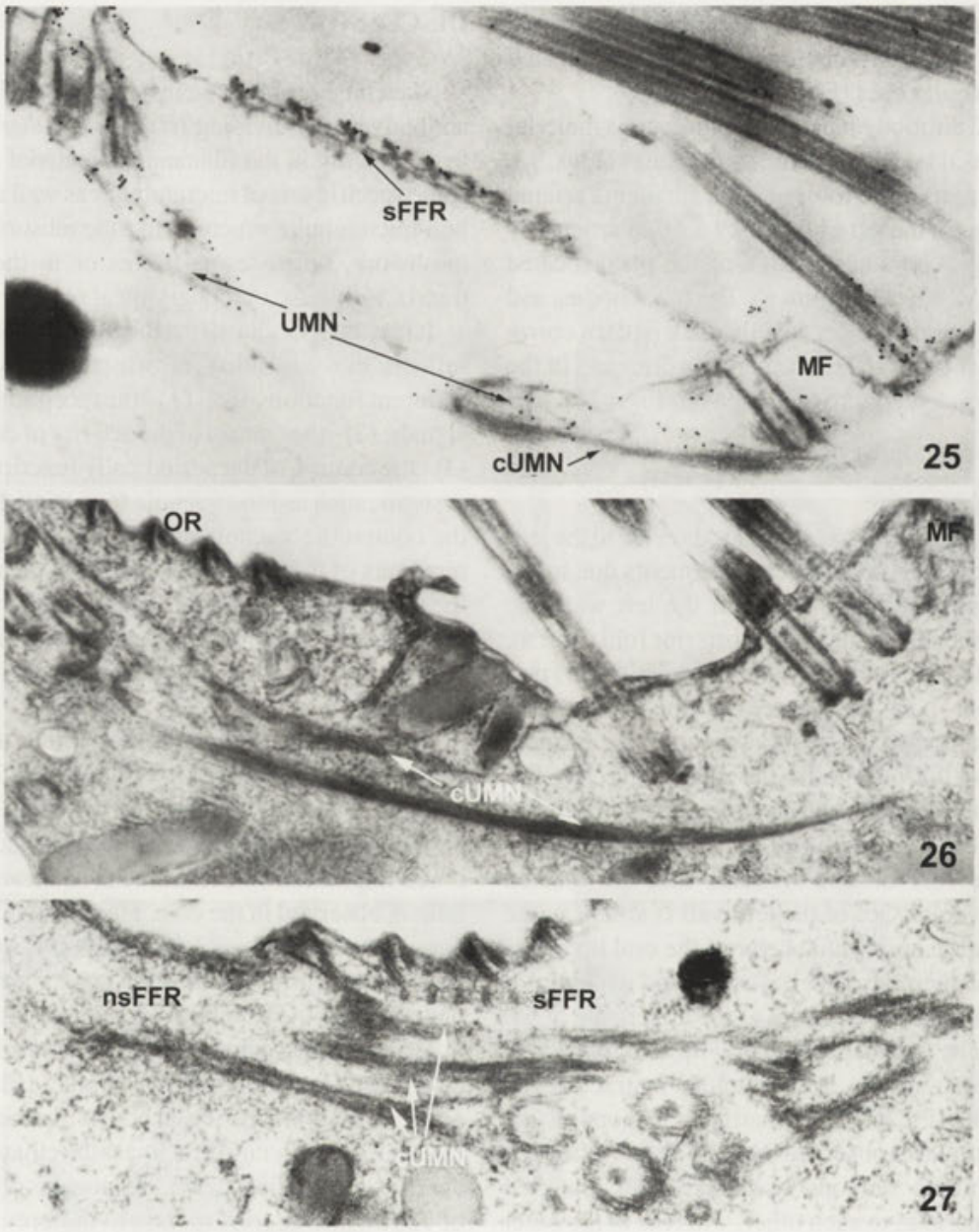

Fig. 25. Distribution of the MPM-2 labelling in the undulating membrane network , X 28000. cUMN - microtubular cables of the undulating membrane network; MF - membranellar fold; sFFR - striated fine filamentous reticulum; UMN - undulating membrane network; Figs. 26-27. Sections through deepest parts of the membrane undulating network of the nonpermeabilized cells, X 31600 and X41250, respectively.cUMN - microtubular cables of the undulating membrane; MF - membranellar fold; nsFFR and sFFR - nonstriated and striated fine filamentous reticulum; OR - oral ribs; UMN - undulating membrane network

centrosomes different in their nucleation capacity and phosphorylation. We suggest that some phosphoproteins are involved in the connection of the microtubular ribbons to the microtubular triplets of the kinetosome and they are phosphorylated throughout cell cycle.

The deeper parts of the oral apparatus, the contractile vacuole discharging system and the opening of the cytoproctal slit are involved in periodic activities. All of them are accompanied by structures labelled by the MPM-2 antibody.

The phosphorylated state of the non-ordered filamentous material (nsFFR) localised in the oral lip, cytopharyngeal pocket and along the deep fibre may be related to its ability to form the food vacuoles. It has been proposed (Williams and Bakowska 1982, Smith-

Sommerville and Bushe 1984) that the striated filamentous material underlying the oral ribs (sFFR) is a calcium regulated system and participates in forming a sealed food vacuole. Nevertheless, the sFFR is not recognised by the MPM-2 antibody. However, it might be that the sFFR is a structure only holding the oral ribs, and is not active in the motile activities. Instead, some phosphorylated proteins of the non-striated FFR packing the oral lip and descending down along the deep fibres could be involved in either the opening and closing movements of the lip, pinching off the food vacuole, or pushing it inwards along the deep fibre. It is consistent with the description of the functioning of the calmyonemin within the oral apparatus of some Entodiniomorpha (Vigues and David 1995). The other intriguing question concerns the functioning of actins in such periodically activated systems (Cohen and Beisson 1988).

It is striking that some microtubular structures of the oral and somatic cortex are associated with the fine filamentous material labelled with the MPM-2 antibody, whereas the other microtubular bundles are completely free of the label. As a rule the structures, either microtubular (Pc, Tt, UMNc) or filamentous (UMN,sFFR) which anchored the somatic cilia, membranelles or oral ribs within the cytoplasm (Allen 1967, Sattler and Staehelin 1979, Williams and Bakowska 1982) are not, or only slightly (UMN), phosphorylated. From the fibre appendices associated with the basal bodies an exception concerns the kinetodesma which are labelled by the MPM-2 antibody. The immunogold staining of *Tetrahymena* presented here, does not allow us to distinguish whether the filaments constructing the kinetodesma or the fine material surrounding them (as in Paramecium, Keryer et al. 1987) are phosphorylated. Numerous contacts between the striated rootlets and the cytoskeletal components such as the actin (Tamm and Tamm 1987, Chailley et al. 1989) or the intermediate filaments (Lemullois et al. 1987) have been documented in other systems. Some connections between the distal parts of the kinetodesma and the fibrogranular material either of the circumciliary ring or the somatic ridges were observed in *Tetrahymena* (Allen 1967, Collins et al. 1980. According to our observations, the dense labelling in the top of the somatic ridges concern not only the phosphoproteins linking lm to the epiplasm layer and/or to the alveolar membrane but also the phosphoproteins of the fine linkers presumably holding down the kinetodesma to the cell surface.

The set of phosphoproteins are localised within all cortical folding creating the specific sculpturing of the cortex of the *Tetrahymena* seen on the SEM pictures: (1)

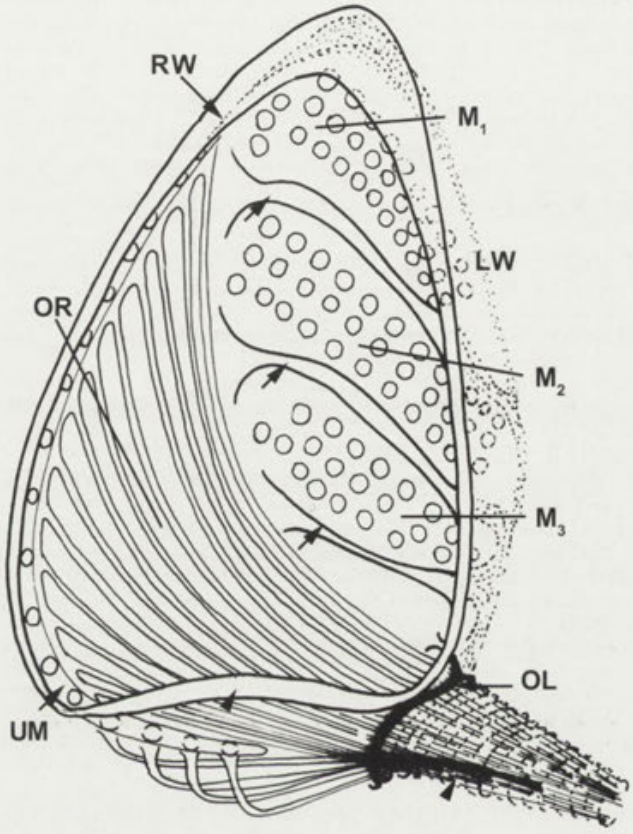

Fig. 28. Scheme of the distribution of the phosphorylated structures within the oral apparatus of a non-dividing *T. thermophila*. Arrows - membranellar folds; filled arrowhead - funnel surrounding a deep fiber; M_1, M_2, M_3 - oral membranelles; OL - oral lip; open arrowhead - collar framing the buccal cavity; OR - oral ribs; RW and LW - right and left walls of the buccal cavity; UM - undulating membrane

- around the longitudinal microtubules in the somatic ridges; (2) - accompanying the microtubules of the oral ribs; (3) - accompanying microtubules of the collar framing the buccal cavity; (4) - in the filamentous material packed in the right hand side of the UM ridge; (5) - in the membranellar folds; (6) - in the oral lip, and; (7) - in the linkers between the parasomal sacs and the epiplasm. Finally, the material accompanying the microtubules of the deep fibre related to the maintenance of the buccal cavity is also labelled with the MPM-2 antibody (the oral apparatus is flattened when this structure transiently disappears during cell division, or conjugation, Kiersnowska et al. 1993, Kaczanowska pers. inf.).

This correlation of the deployment of phosphoproteins with the sculpture of the oral cavity and somatic cell surface observed in SEM suggests that these phosphoproteins may display an important role in maintaining the unmodified cell shape against distortions brought about by the local periodic activities.

Acknowledgements. The authors thank Drs Potu Rao, Jian Kuang and Cheryl Ashorn (University of Texas) for the gift of the MPM-2 antibody. Thanks are also due to Drs Janina Kaczanowska (Warsaw University), Joseph Frankel and Norman Williams (Iowa University) for the critical reading of the manuscript. This work was supported by grants from Polish Science Committee # 6P203060 to Dr Andrzej Kaczanowski and from Warsaw University # B.W. 1203/51 to M.K.

REFERENCES

Allen R.D. (1967) Fine structure, reconstruction and possible functions of components of the cortex of *Tetrahymena pyriforms J. Protozool.* **14:** 553- 572

Allen R.D., Wolf R.W.(1979) Membrane recycling at the cytoproct of *Tetrahymena. J. Cell Sci.* **35:** 217-227

Bruns P., Brussard T.B. (1974) Pair formation in *Tetrahymena pyriforms*, an inducible developmental system. *J. Exp. Zool.* **188:** 337-344

Chailley B., Nicolas G., Laine M-C. (1989) Organisation of actin microfilaments in the apical border of oviduct ciliated cells. *Biol. Cell.* **67:** 81-90

Cohen J., Beisson J. (1988) Cytoskeleton. In: *Paramecium*, (Ed. H.-D. Görtz). Springer - Verlag, Berlin, 363 - 392

Collins T., Baker R.L., Wilhelm J-M., and Olmsted J-B. (1980) A cortical scaffold in the Ciliate *Tetrahymena. J. Ultrastr. Res.* **70:** 92-103

Davis F.M., Rao P.N. (1987) Antibodies to mitosis-specific phosphoproteins. In: Molecular Regulation of Nuclear Events in Mitosis and Meiosis, (Eds. R.A. Schlegel, M.S. Halleck and P.N. Rao). N.Y. Academic, 259-293

Davis F.M., Tsao T.Y., Fowler S.K., Rao P.N. (1983) Monoclonal antibodies to mitotic cells. *Proc. Natl. Acad. Sci.* USA, **80:** 2926-2930

Dress V.M., Yi H., Musal M.R., Williams N.E. (1992) Tetrin polypeptides are colocalized in the cortex of *Tetrahymena. J. Structural Biol.* **108:** 187-194

Forer A., Nilsson J.R., Zeuthen E. (1970) Studies on the oral apparatus of *Tetrahymena pyriforms* GL.*C. R. Trav.Lab.* Carlsberg **38:** 67-86

Frankel J., Williams N.E. (1973) Cortical development in *Tetrahymena*. In: Biology of *Tetrahymena* (Ed. A.M. Elliot). Dowden Hutchinson & Ross Inc. Stroudsbourg, 375-409

Frankel J., Jenkins L.M., Bakowska J., Nelsen E.M. (1984) Mutational analysis of patterning of oral structures in *Tetrahymena*. I. Effects on increased size on organisation. *J. Embryol. Exp. Morphol.* **82:** 41-66

Garreau de Loubresse N., Klotz C., Vigues B., Rutin J., Beisson J. (1991) Ca^{2+} binding proteins and contractility of the infraciliary lattice in *Paramecium. Biol.Cell.* **71:** 217-225

Gavin R. H. (1977) The oral apparatus of *Tetrahymena pyriforms*, strain WH-6.IV. Observation on the organisation of microtubules and filaments in the isolated oral apparatus and the differential effect of potassium chloride on the stability of oral apparatus microtubules. *J.Morphol.* **151:** 239-258

Gitz D-L., Pennock D-G. (1995) Deciliation induces phosphorylation of a 90-kDa cortical protein in *Tetrahymena thermophila. J. Euk. Microbiol.* **42:** 742-748

Harper J.D.I., Sandres M.A., Salisbury J.L. (1993) Phosphorylation of nuclear and flagllar basal apparatus proteins during flagellar regeneration in *Chlamydomonas reinhardii. J. Cell. Biol.* **122:** 877-886

Honts J.E., Williams NE. (1990) Tetrins: polypeptides that form bundled filaments in *Tetrahymena. J. Cell Sci.* **96:** 293-302

Huelsman D.A., Gitz D.L., Pennock D.G (1992) Protein phosphorylation and the regulation of basal body microtubular organising centres in *Tetrahymena. Cytobios* **71:** 37-50

Jerka-Dziadosz M., Jenkins L.M., Nelsen E.M. Williams N.E., Jaeckel-Williams R., Frankel J. (1995) Cellular polarity in ciliates: persistence of global polarity in a disorganized mutant of *Tetrahymena thermophila* that disrupts cytoskeletal organisation. *Dev. Biol.* **169:** 644-662

Kaczanowska J., Iftode F., Coffe G., Prajer M., Kosciuszko H., Adoutte A. (1996) The protein kinase inhibitor 6-dimetylaminopurine does not inhibit micronuclear mitosis, but impair the rearrengement of cytoplasmic MTOCs and execution of cytokinesis in the ciliate *Paramecium* during transmission to interphase. *Europ. J. Protistol.* **32:** 2-17

Keryer G., Davis F.M.,. Pao P.N., Beisson J. (1987) Protein phosphorylation and dynamics of cytoskeletal structures associated with basal bodies in *Paramecium. Cell Motil. and Cytosk.* **8:** 44-54

Keryer G., Iftode F., Bornens M. (1990) Identification of proteins associated with microtubule organising centres and filaments in the oral apparatus of the ciliate *Paramecium tetraurelia. J. Cell Sci.* **97:** 553-563

Kiersnowska M., Kaczanowski A., de Haller G. (1993) Inhibition of oral morphogenesis during conjugation of *Tetrahymena thermophila* and its resumption after cell separation. *Europ. J. Protistol.* **29:** 359-369

Lemullois M., Gounon P., Sandoz D. (1987) Relationships between cytokeratin filaments and centriolar derivatives during ciligenesis in the quail oviduct. *Biol. Cell.* **61:** 39-49

Messinger M.S., Albertini D.F. (1991) Centrosome and microtubule dynamics during meiotic progression in the mouse oocyte. *J. Cell Sci.* **100:** 289-298

Nelsen E.M., Frankel J., Martel E. (1981) Development of ciliature of *Tetrahymena thermophila.*Temporal coordination with oral development.*Dev.Biol.*.**88:**27-38

Nilsson J.R., Williams N.E. (1966) An electron microscopy study of the oral apparatus of *Tetrahymena pyriforms. C. R. Trav. Lab.* Carlsberg **35:** 119-141

Plattner H. (1975) Ciliary granule plaques: membrane-intercalated particle aggregates associated with Ca^{2+} -binding sites in *Paramecium. J. Cell. Sci.* **18:** 257-269

Sattler C.A., Staehelin L.A. (1979) Oral cavity of *Tetrahymena pyriforms. J. Ultrastructure Res.* **66:** 132-150

Schliwa M., Van Blerkom J. (1981) Structural interaction of cytoskeletal components. *J. Cell. Biol.* **90:** 222-235

Smith H.E., Bushe Jr. H.E. (1983) On the of origin of the deep fibre in *Tetrahymena. Trans. Am. Microsc. Soc.* **102:** 264-271

Smith-Somerville H.E., Bushe Jr. H. (1984) Changes in oral apparatus structure accompanying vacuolar formation in the macrostomal form of *Tetrahymena vorax*. A model for the formation of food vacuoles in *Tetrahymena. J. Protozool.* **31:** 373-380

Sperling L., Keryer G., Ruiz F., Beisson J. (1991) Cortical morphogenesis in *Paramecium*: a transcellular wave of protein phosphorylation involved in ciliary rootlet disassembly. *Dev. Biol.* **148:** 205-218

Taagepera S., Dent P., Her J.H., Sturgill T.W., Gorbsky GJ. (1994) The MPM-2 antibody inhibits mitogen-activated protein kinase activity by binding to an epitope containing phosphothreonine-183. *Molec. Biol. Cell.* **5:** 1243-1251

Tamm S.L., Tamm S. (1987) Massive actin bundle couples macrocilia to muscles in the Ctenophore *Beroe. Cell Motil. Cytoskel.* **7:** 116-128

Vandre D.D., Centozone V.E., Peloquin J., Tombes R.M., Borisy G.G. (1984) Proteins of the mammalian mitotic spindle: phosphorylation /dephosphorylation of MAP-4 during mitosis. *J. Cell Sci.* **98:** 577-588

Vigues B., David C. (1995) Calmyonemin: A centrin analog in entodiniomorphid ciliates. In: Protistological Actualities.(Eds. Brugerolle G., Mignot J-P.). Clermont-Ferrand, 138-139

Williams N.E. (1986) The nature and organisation of the filaments in oral apparatus of *Tetrahymena. J. Protozool.* **33:** 352-358

Williams N.E., Bakowska J. (1982) Scanning electron microscopy of cytoskeletal elements in oral apparatus of *Tetrahymena. J. Protozool.* **29:** 382-389

Williams N.E., Luft J.H. (1968) Use of a nitrogen mustard derivative in fixation for electron microscopy and observation on the ultrastructure of *Tetrahymena. J. Ultrastructure Res.* **25:** 271-292

Williams N.E., Honts J.E., Greff R.W. (1986) Oral filament proteins and their regulation in *Tetrahymena pyriforms. Exp. Cell Res.* **164:** 295-310

Received on 9th October, 1995; accepted on 19th July, 1996

Acta Protozoologica (1996) 35: 309 - 315

ACTA
PROTOZOOLOGICA

The Fine Structure of Cell Surface and Hair-like Projections of *Filipodium ozakii* Hukui 1939 Gamonts

Kazumi HOSHIDE[1] and Kenneth S. TODD, Jr.[2]

[1]Biological Institute, Faculty of Education Yamaguchi University Yamaguchi, Japan; [2]Department of Veterinary Pathobiology, College of Veterinary Medicine, Universityof Illinois, Urbana, Illinois, USA

Summary. The ultrastructure of the cell surface and the hair-like projections of *Filipodium ozakii* gamonts was studied by TEM and SEM. The surface of the entire body of *F. ozakii* was covered with the regular longitudinal folds along the body axis and hair-like projections. The deep and shallow grooves alternately separated the folds and the hair-like projections which originated at the bottom of every 2nd or 4th groove. The inner and outer membranes at the cell periphery and longitudinal microtubules under the inner membrane were observed. The structures of the cell surface were similar to those of *Selenidium fallax* which have been previously described. The appearance of projections resembled cilia or flagella but their ultrastructure was completely different and characteristic not having the typical arrangements of 9 + 2 microtubules inside the projections.

Key words: *Filipodium ozakii,* fold, gregarine, hair-like projection, microtubule.

INTRODUCTION

Filipodium ozakii Hukui 1939 (phylum Apicomplexa, class Sporozoea, order Eugregarinida, suborder Aseptatina) was described from Japanese Sipunculoidea, *Siphonosoma cumanense*. Sixteen species of gregarines belonging to 7 genera are reported from Sipunculoidea until now (Levine 1977). Among them, *Filipodium* is very characteristic appearance. It was covered with numerous hair-like projections on it's surface, resembling a ciliate. The hair-like projections are rare in Apicomplexa. Their ultrastructure was not shown yet. The structures of cell surface, folds and microtubles were studied in comparison with those of other gregarines.

Address for correspondence: Kazumi Hoshide, Faculty of Education, Yamaguchi University, Yamaguchi 753 Japan; Fax: 839-25-2152; E-mail: khoshide @inf.edu.yamaguchi-u.ac.jp

MATERIALS AND METHODS

Specimens of *Siphonosoma cumanense* (Keferstein)1865 were collected at the muddy beach of Aio, Seto Inland Sea, Japan. The gamonts *of Filipodium ozakii* Hukui 1939 were obtained from the intestine of *S. cumanense*. During the summer, 10-15% *S. cumanense* were infected with *F. ozakii*. The intestines were carefully removed, placed in sea water, and dissected. The intestines were usually filled with fine sand which was washed away with sea water using a pipette; this removed the mature gamonts, but the young gamonts remained attached to the intestinal wall. The digestive tracts with young gamonts and the liberated matured gamonts were fixed with 5% glutaraldehyde in cacodylate buffer (pH 7.2) for 2 h. Following this, they were rinsed twice with cacodylate buffer and transferred to 1% OsO_4 solution for further fixation for 2 h. After fixation, the samples were dehydrated with an ethanol series and propylene oxide and embedded in araldite. Thin sections were obtained with a LKB ultramicrotome with a diamond knife. The sections were collected on monohole grids with supporting membrane. The grids were stained with uranyl acetate and lead citrate (Reynolds 1963). Transmission electron micro-

graphs were obtained with a JEOL-1200 EX electron microscope. The samples for SEM were fixed and dehydrated by the same methods as those for TEM. After dehydration with ethanol, they were placed in isoamyl acetate. They were then treated by the critical points method using CO_2 as the transition liquid. The samples were placed on an aluminium stubs, sputter coated with gold and examined with a JEOL T-300 scanning electron microscope.

RESULTS

The morphology of the gamont of *F. ozakii* differed during the stage of maturation. The young gamont was slender and cylindrical but the mature gamont decreased in length, increased in width and flattened (Fig. 12). The surface of both young and mature gamonts were covered with numerous long hair-like projections and longitudinal folds along the body axis (Figs. 1-3). The hair-like projections were 130-160 nm in diameter, about 10 μm long and almost the same diameter from the base to the tip. They consisted of 2 elements, electron-dense tubules and outer membranes (Figs. 7,8). The electron-dense tubule, about 100 nm in diameter was at the centre of each projection. The outer membrane covered the electron-dense tubule. There was no other structure inside the projection (Fig. 13). The hair-like projections were in a line along the grooves at almost regular intervals and they emerged from the bottom of the grooves between the folds (Figs. 2,3). In cross section of gamonts the projections emerged from every 2 or 4 grooves (Figs. 4,5).

The entire body was covered with straight longitudinal folds (Figs. 2,3). The cross sections of the folds of young gamonts were different from those of mature gamonts. The cross sections of the folds of young gamonts were mound-shaped with broad basement (Fig.4) and those of mature gamont were U-shaped with a decrease in the width of the basement (Fig. 5). Mature gamonts had two-size grooves, deep and shallow ones. The two size grooves appeared alternately (Fig. 5). They were about 300-400 nm high and 300 nm wide. The pellicle was covered with outer and inner membranes, each of which was about 10 nm thick and was separated by about 20-40 nm-thick clear space. Inside the inner membrane, numerous microtubules lie parallel to the folds (Fig. 6). In some sections, the arrangement of the microtubules appeared like a reed screen (Fig. 11).

Siphonosoma cumanense possessed numerous cilia on the inner surface of the intestinal wall. In the section of the intestine to which *F. ozakii* attached, the hair-like projections and cilia of the host were mixed up around the *F. ozakii* (Figs. 10,11).

DISCUSSION

The surface of the entire body of *F. ozakii* was covered with numerous hair-like projections which are unusual among the Apicomplexa. The appearance of the hair-like projections resembled cilia or flagella, but the ultrastructure of the hair-like structure was completely different in that there was no 9 + 2 configuration of microtubules inside the projections. Instead a single, comparatively large electron-dense tubule was present centrally along the entire length. The diameter of hair-like projections was about half compared with the cilia of the host intestine (Fig. 7). The fundamental structure of the hair-like projections was the same as that of the surface of the fold. The outer membranes of the fold continued to the outer membranes of hair-like projection and the electrondense tubule continued to the inner membrane of the fold. Based on this arrangement it is the hair-like projections that may arise from the extension of the cell surface.

The projections of the gregarine *Rhynchocystis pilosa* from *Lumbricus terrestris* were named cytopilia (Warner 1968). The diameter of the cytopilia were three times larger than that of the projections found in the present study and the length of the former are 2 to 4 times longer than that of the latter. The former had a characteristic fibrillar system but the latter had none.

Projections of *Diplauxis hatti* from *Perinereis cultrifera* were described and named microvillosites (Vivier and Petitprez 1968). The diameter of the microvillosites was 400-600 nm and they were about three to four times larger than that of the hair-like projections found in the present study. There was some constriction at the base of the microvillosites but no constriction was observed in the projections found in the present study. The microvillosites consisted of three membrane systems while the filamentous projections were composed of outer membrane and electron-dense tubule. The appearance of the microvillosites and the hair-like projections were similar and the structure of both projections have some features in common. There were no distinguishing structures for the microtubule or fibrillar system, except the one electron-dense tubule at the centre of both projections. The membranous system of both projections contin-

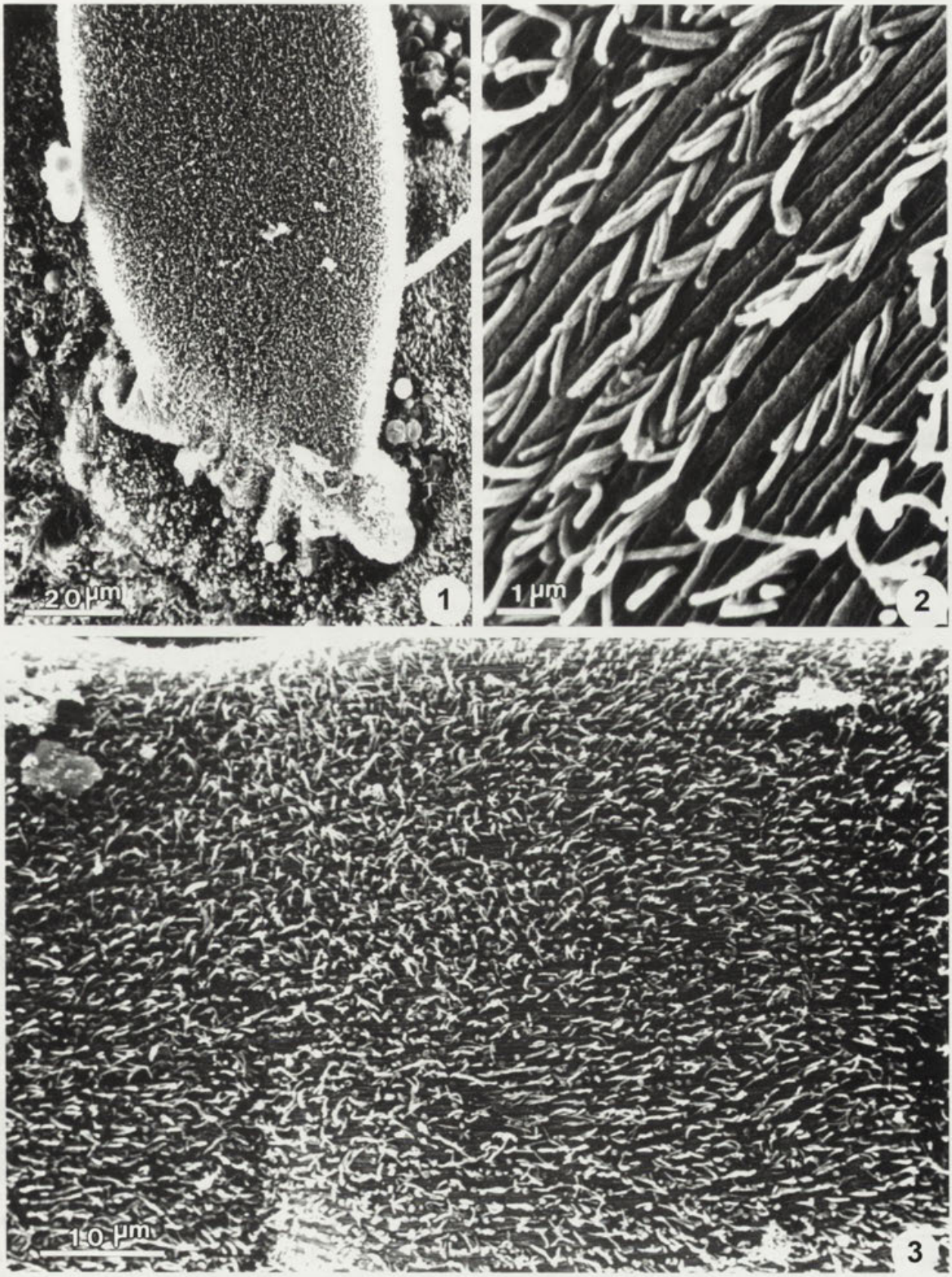

Figs. 1-3. *Filipodium ozakii* - scanning electron micrographs. 1 - *F. ozakii* attached to the wall of the host intestine. 2 - surface of *F. ozakii* with the hair-like projection protruding from every two or four grooves. 3 - hair-like projections on the body surface

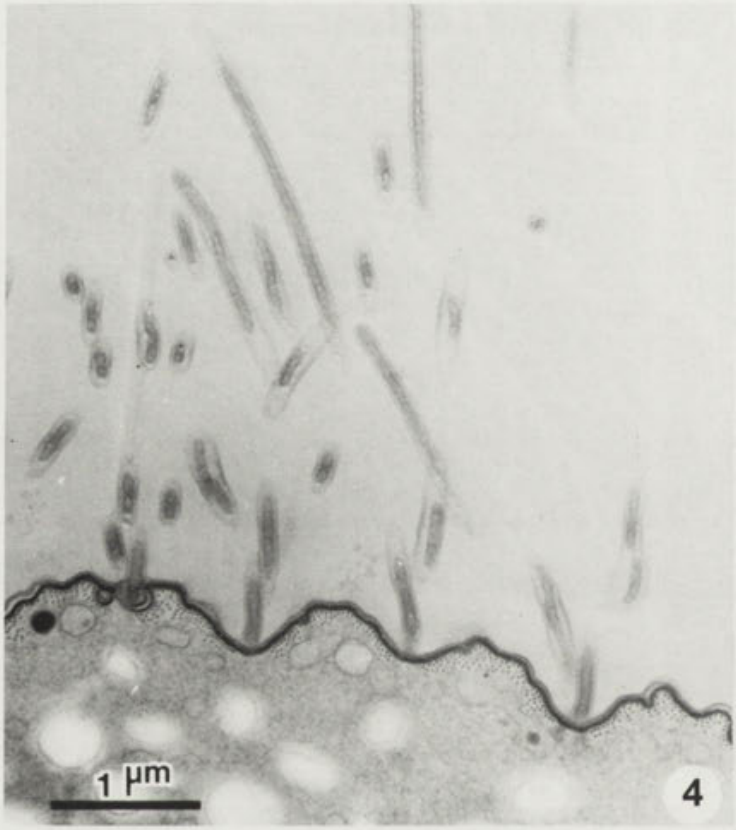

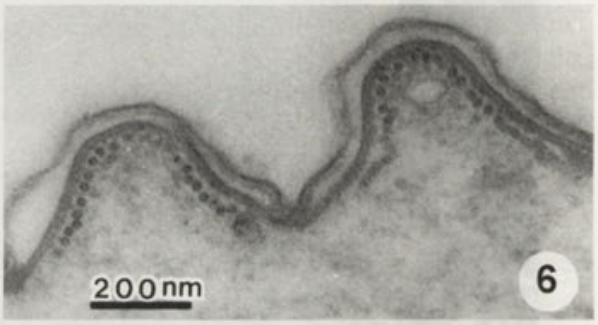

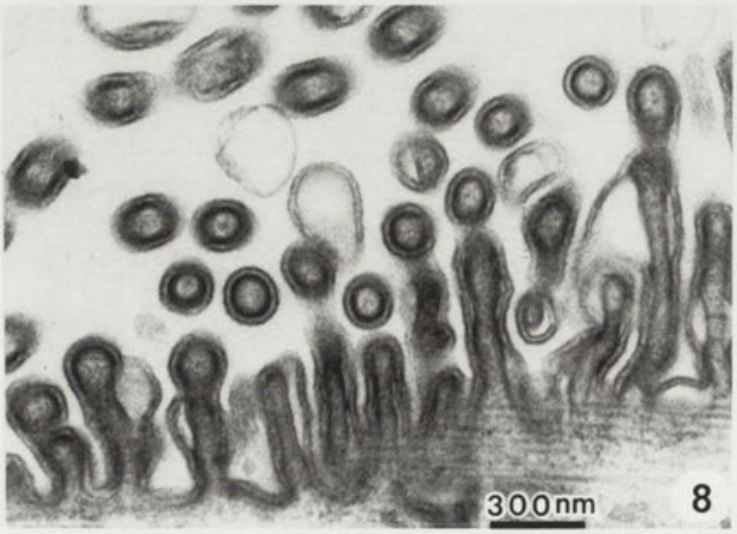

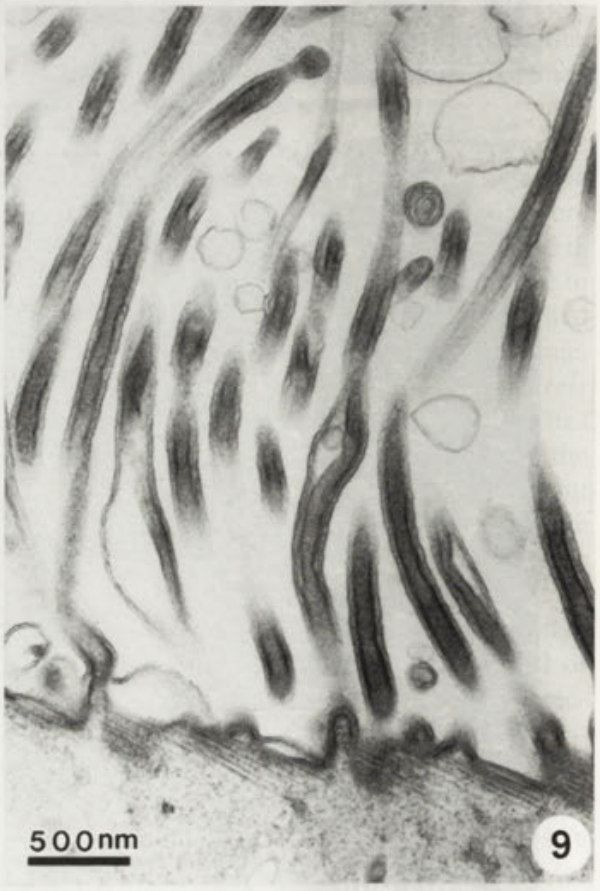

Figs. 4-9. *Filipodium ozakii* - transmission electron micrographs. 4 - cross section of periphery and hair-like projection of young *F. ozakii* three grooves are shallow but every four grooves deep and big. 5 - cross section of periphery and hair-like projection of matured *F. ozakii*. 6 - periphery folds and microtubules. 7 - cross section of filamentous projection and cilia of host intestine. 8 - longitudinal section of the basement of the filamentous projections. 9 - longitudinal section of filamentous projections

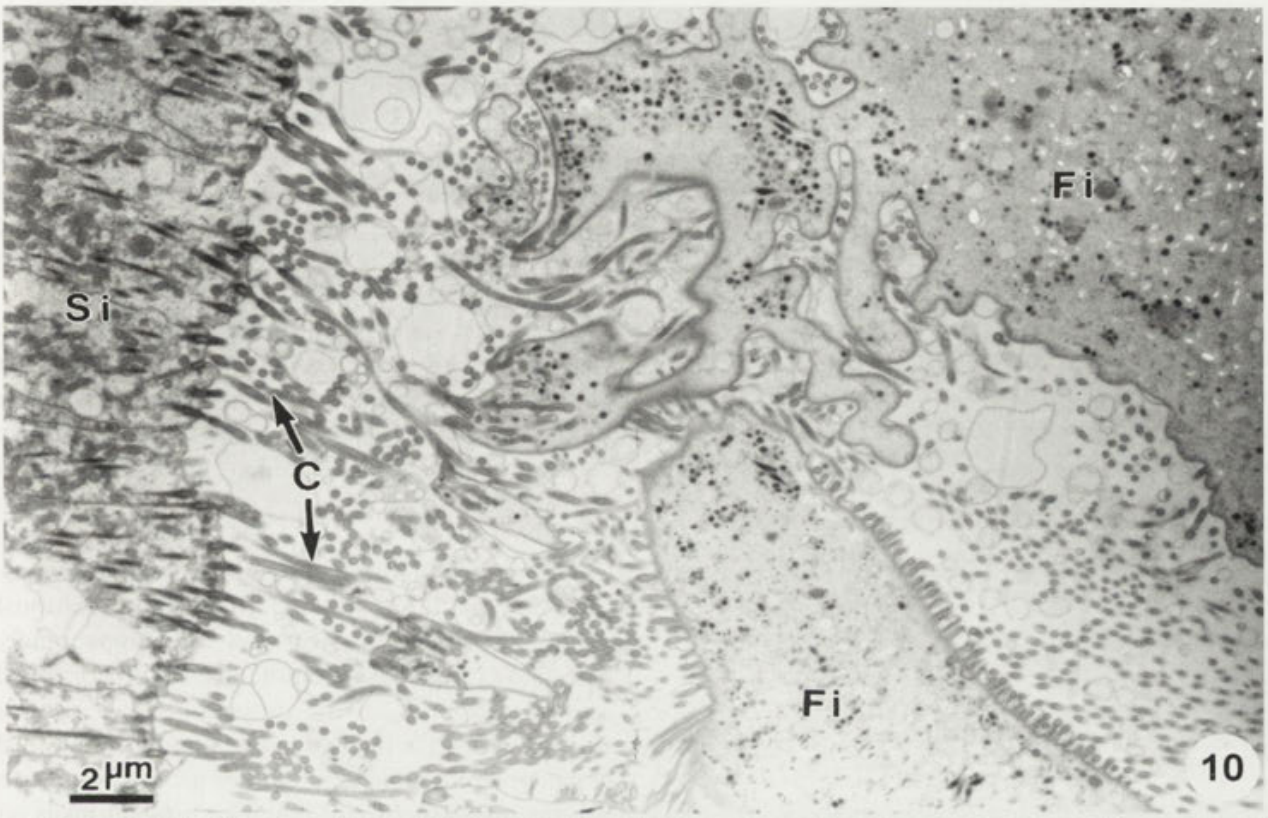

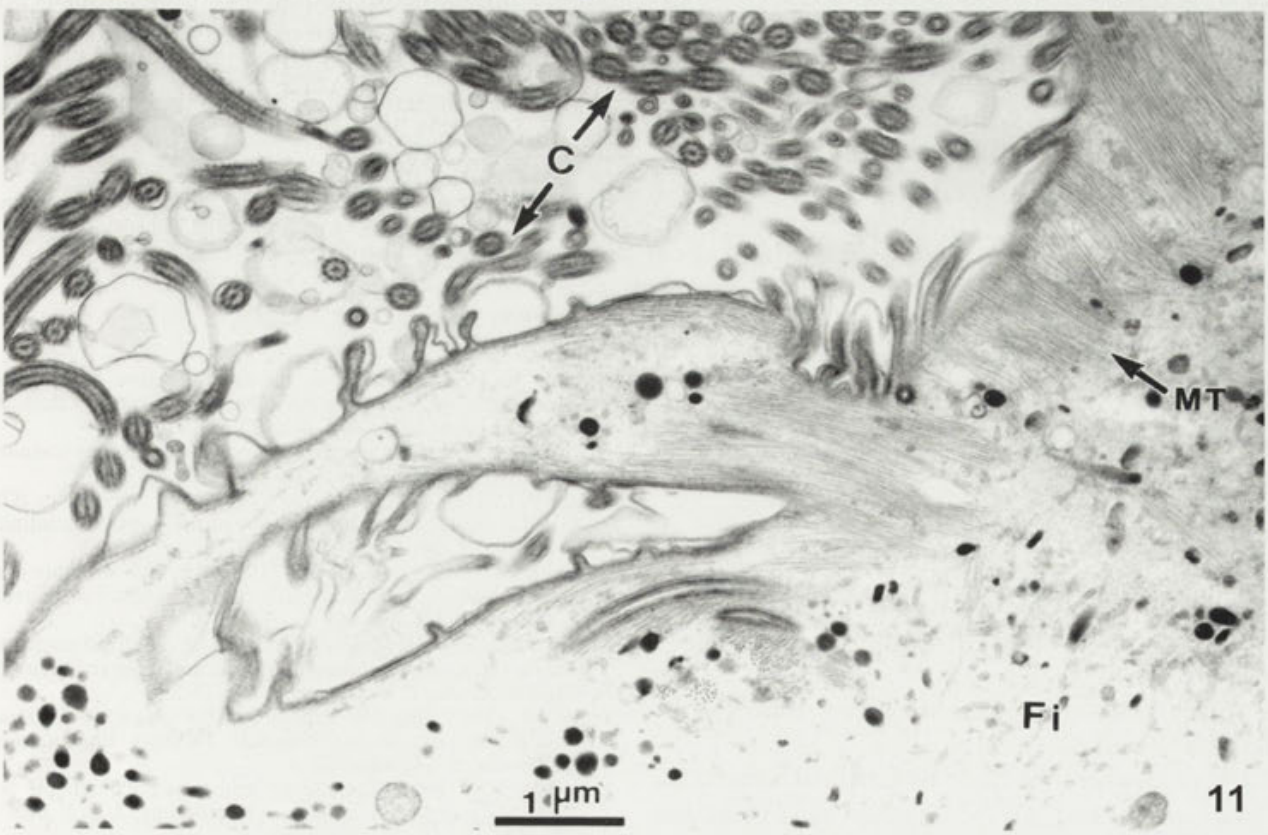

Figs. 10-11. *Filipodium ozakii* - transmission electron micrographs. 10 - section of intestine of *S. cumanense* with *F. ozakii*; 11 - enlargement of a part of *F. ozakii*. C - cilia of *S. cumanense*, Fi - *F. ozakii*, MT- microtubule, Si - *S. cumanense*

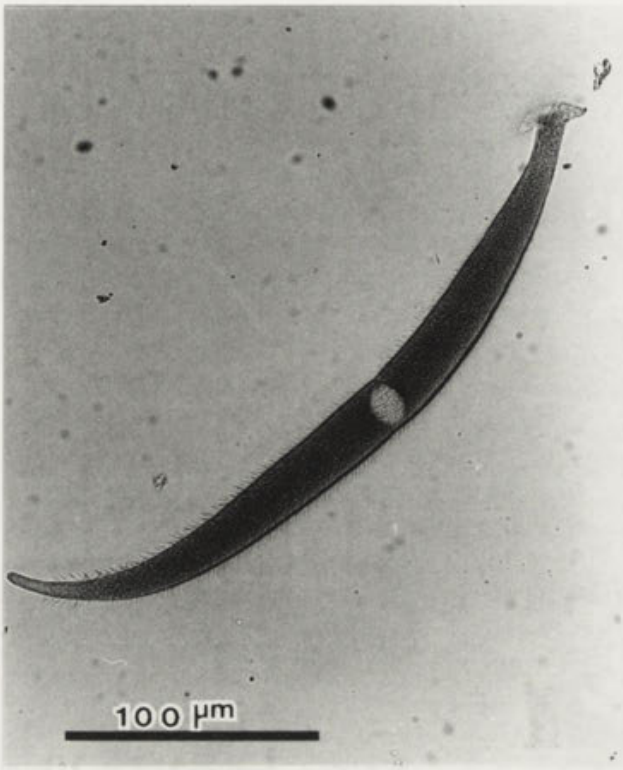

Fig. 12. Young gamont of *F. ozakii*. Light microscopy

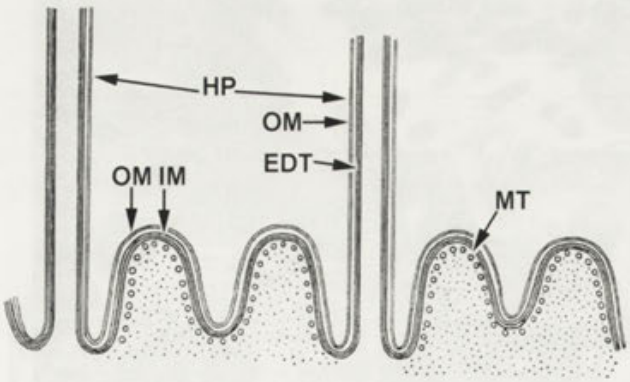

Fig. 13. Scheme of surface of *F. ozakii*; EDT - electron dense tubule, HP - hair-like projection, IM - inner membrane, MT - microtubule, OM - outer membrane

ued to the cell surface and they may form by the extension of the cell surface.

Most of the gregarines have longitudinal folds on the surface along the body axis (Macgregor and Thomasson 1965, Reger 1967, Hoshide 1973, Ormiéres 1979, Walker et al. 1979). Warner reported that *Selenidium fallax* had two types of grooves, a primary deep one and a secondary shallow one (Warner 1968). They appeared alternately and two folds appeared to be a single unit. *Filipodium ozakii* also had two kinds of grooves, deep and shallow one appeared alternately like *Selenidium fallax* but every 2 or 4 groove, the filamentous projections emerged. The resemblance of peripheral structures of *Filipodium* and *Selenidium* may demonstrate an affinity of the two genera.

Generally speaking, protozoa is a very difficult group to determine phylogenetic relationships, because of their size and lack of fossil records except very limited groups. The apicomplexa is especially difficult because it is a highly adapted group to parasitism; the simplification of structure by retrograde development and complicated life cycle. The comparison of the ultrastructure of organelles among some groups of protozoa is one of the keys to find the relationship among the group of protozoa. The appearance of hair-like projections resemble that of cilia or flagella. The ultrastructure of the projections of *F. ozakii* is studied with great interest to elucidate the relationship between Apicomplexa and other groups of protozoa. But the ultrastructure of hair-like projections is completely different from that of cilia or flagella. This time the structure of projections gives us no clue to the phylogenetic relationships among the other groups of the protozoa.

Acknowledgement. This work was supported in part by grant-in-aid 06640905 For Scientific Research from the Ministry of Education, Science and Culture of Japan.

REFERENCES

Hoshide K. (1973) Studies on the fine structure of gregarines. Observation on *Ferraria cornucephala iwamusi*. *Bull. Fac. Educ. Yamaguchi Univ.*, Japan. **23:** 87-91

Hukui T. (1939) On the gregarines from *Siphonosoma cumanense* (Keferstein). *J. Sci. Hiroshima Univ.*, **7:** 1-23

Levine N.D. (1977) Revision and Checklist of the species (Other than Lecudina) of the aseptate gregarine family Lecudinidae. *J. Protozool.* **24:** 41-52

Macgregor H.C., Thomasson P.A. (1965) The fine structure of two Archigregarines, *Selenidium fallax* and *Ditrypanocystis cirratuli*. *J. Protozool.* **12:** 438-443

Ormiéres, R. (1979) *Selenidium cantoui* n.sp., Archigrégarine parasite de *Physcosoma granulatum* (Leuckart), Sipunculien Etude ultrastructurale. *Z. Parasitenkd.* **61:** 13-20

Reger J.F. (1967) The fine structure of the gregarine *Pyxinoides balani* parasitic in the barnacle *Balanus tintinnabulum*. *J. Protozool.* **14:** 488-497

Reynolds, E.S. (1963) The use of lead citrate at high pH as an electron-opaque stain in electron microscopy. *J. Cell. Biol.* **17:** 208-212

Vivier M. E., Petitprez A. (1968) Les ultrastructures superficielles et leur évolution au niveau de la jonction chez les couples de

Diplauxis hatti, grégarine parasite de *Perinereis cultrifera*. *C.R. Acad. Sc.* Paris, **266(D):** 491-493, Pl. 2

Walker M.H., Mackenzie C., Bainbridge S.P., Orme C. (1979) A study of the structure and gliding movement of *Gregarina garnhami*. *J. Protozool.* **26:** 566-574

Warner F. D. (1968) The fine structure *of Rhynchocystis pilosa* (Sporozoa, Eugregarinida) *J. Protozool.* **15:** 59-73

Received on 3rd November, 1995; accepted on 19th June, 1996

Acta Protozoologica (1996) 35: 317 - 320

ACTA
PROTOZOOLOGICA

An European Population of *Bryometopus hawaiiensis* Foissner, 1994 (Protozoa: Ciliophora)

José L. OLMO and Carmen TÉLLEZ

Departamento de Microbiología III, Facultad de Ciencias Biológicas, UCM, Madrid, Spain

Summary. *Bryometopus hawaiiensis* Foissner, 1994 was found in moss samples from emergent stones collected in the Guadarrama river (Central Spain). Study of cell morphology and infraciliature is based on observations of living and silver carbonate impregnated specimens. This population show some variations when compared with type species from Hawaii consisting on differences in number of kinetids per kinety and the presence of more than one micronucleus. The differences observed in size of cells and macronucleus are caused by the different methods used. New data on habitat and cyst formation are provided.

Key words: *Bryometopus hawaiiensis*, ciliates, cyst, infraciliature.

INTRODUCTION

The genus *Bryometopus* Kahl, 1932 includes 9 reliable species described by Kahl (1932) and Foissner (1993) that can be distinguished by various features (Table 1). *B. hawaiiensis* has been recently described by Foissner (1994) and differs from other *Bryometopus* species in the presence of very conspicuous mucocysts and in the organization of the infraciliature of the paroral membrane. Although Foissner considers this species as been rare and probably endemic of the Hawaiian Archipielago, we found in Central Spain populations that can be recognized as to be *B. hawaiiensis*.

Address for correspondence: José L. Olmo, Departamento de Microbiología III, Facultad de Ciencias Biológicas, UCM, 28040 Madrid, Spain; Fax: 394 49 64; E-mail: risquez@eucmax.sim.ucm.es

MATERIALS AND METHODS

Bryometopuus hawaiiensis was collected from moss samples of emergent stones at the bank of the river Guadarrama in Spain (4° 3' W, 40° 45' N). This site is 1188 m above sea-level.

In the laboratory the moss was saturated with distilled water as in the non-flooded Petri dish method described by Foissner (1992) to recover the ciliates. Final pH was 6.0.

Cells were studied *in vivo* using bright field and phase contrast microscopy. To demonstrate the infraciliature the pyridinated silver carbonate method (Fernández-Galiano 1994) was used.

Attempts to establish pure cultures with usual methods failed. Measures were taken on 16 fixed and impregnated specimens. Standard deviation and coefficient of variation were calculated.

RESULTS

Morphology and infraciliature

Living cells of *B. hawaiiensis* are ellipsoid in shape. Main morphometric data are shown in Table 2.

Table 1. Diagnostic features of *Bryometopus* species [1]

Species	Shape	Size[2] (μm) Length	Size[2] (μm) Width	n	AO	mi
B. atypicus Foissner, 1980	Ovoid	50-85	30-40	17-30	17-23	1
B. balantoidioides Foissner, 1993	Reniform	50-70	25-35	15-16	25-26	1
B. chlorelligerus Foissner, 1980	Elliptical	75-95	-	40	25	2
B. edaphonus Foissner, 1980	Elliptical	40-60	-	16-20	-	1
B. hawaiiensis Foissner, 1994	Elliptical	50-70	35-45	25-30	31-42	1-4
B. pseudochilodon Kahl, 1932	Variable	40-80	-	20-42	15-30	2-9
B. sphagni (Penard, 1922) Kahl, 1932	Variable	77-130	-	40-65	40-54	1-4
B. triquetrus Foissner, 1993	Triangular	45-55	25-35	16-20	16-27	1
B. viridis Foissner, 1980	Ovoid	70-115	37-70	70-80	45-60	1

[1] Data from Foissner (1993, 1994). [2] Measurements *in vivo*. AO - number of adoral organelles, mi - number of micronucleus, n - number of somatic kineties

Table 2. Morphometric characterization of *Bryometopus hawaiiensis*. European population, 1st line; all data based on silver carbonate impregnated specimens. Type population (Foissner 1994), 2nd line; body and macronucleus size data based on cells after protargol impregnation; other characters measured on silver carbonate impregnated specimens. All measurements in μm

Character	x	M	SD	CV	Min	Max	n
Body, length	68.7	70.0	5.0	7.4	60	75	16
	51.6	52.0	4.4	8.5	45	63	21
Body, width	37.7	38.0	2.7	7.3	30	42	16
	30.1	30.0	2.6	8.6	27	37	21
Macronucleus, length	21.6	21.5	2.1	9.6	18	26	16
	11.4	11.0	1.6	14.0	8	11	21
Macronucleus, width	21.0	21.0	2.0	9.5	18	25	16
	9.6	9.0	1.3	13.4	8	11	21
Somatic kineties, number	27.4	27.0	1.4	5.2	25	30	16
	27.3	27.5	1.9	7.1	25	30	10
Adoral organelles, number	36.5	36.0	2.3	6.3	33	40	16
	35.1	35.0	2.9	8.3	31	42	11
Paroral dikinetids, number	38.4	40.0	3.8	9.9	30	42	16
	29.2	28.8	3.5	11.8	24	36	11
Macronucleus segments, number	1.0	1.0	0	0	1	1	16
	1.0	1.0	0	0	1	1	11
Micronucleus, number	2.2	2.0	0.9	44.0	1	4	14
	1.0	1.0	0	0	1	1	11

CV - coefficient of variation in %, M - median, Max - maximum, Min - minimum, n - size of sample, SD - standard deviation, x - arithmetic mean

The somatic infraciliature consists of 25-30 kineties of which the right and the dorsal ones are longer having 25-33 dikinetids (Figs. 1, 2). The buccal cavity lies at the anterior left quadrant of the cell and is limited at the left side by an adoral zone of organelles (aO) constituted by 33-40 organelles which form a sigmoid line. Each organelle is composed of three kineties: the upper one is shorter, with 4-6 basal bodies and two longer ones with 8-10 basal bodies (Fig. 3). The cytopharynx is short and tubular and it is invaded by about 10 adoral organelles. The paroral membrane (pM) is very long and forms a sigmoid line of approximately 40 dikinetids that runs from

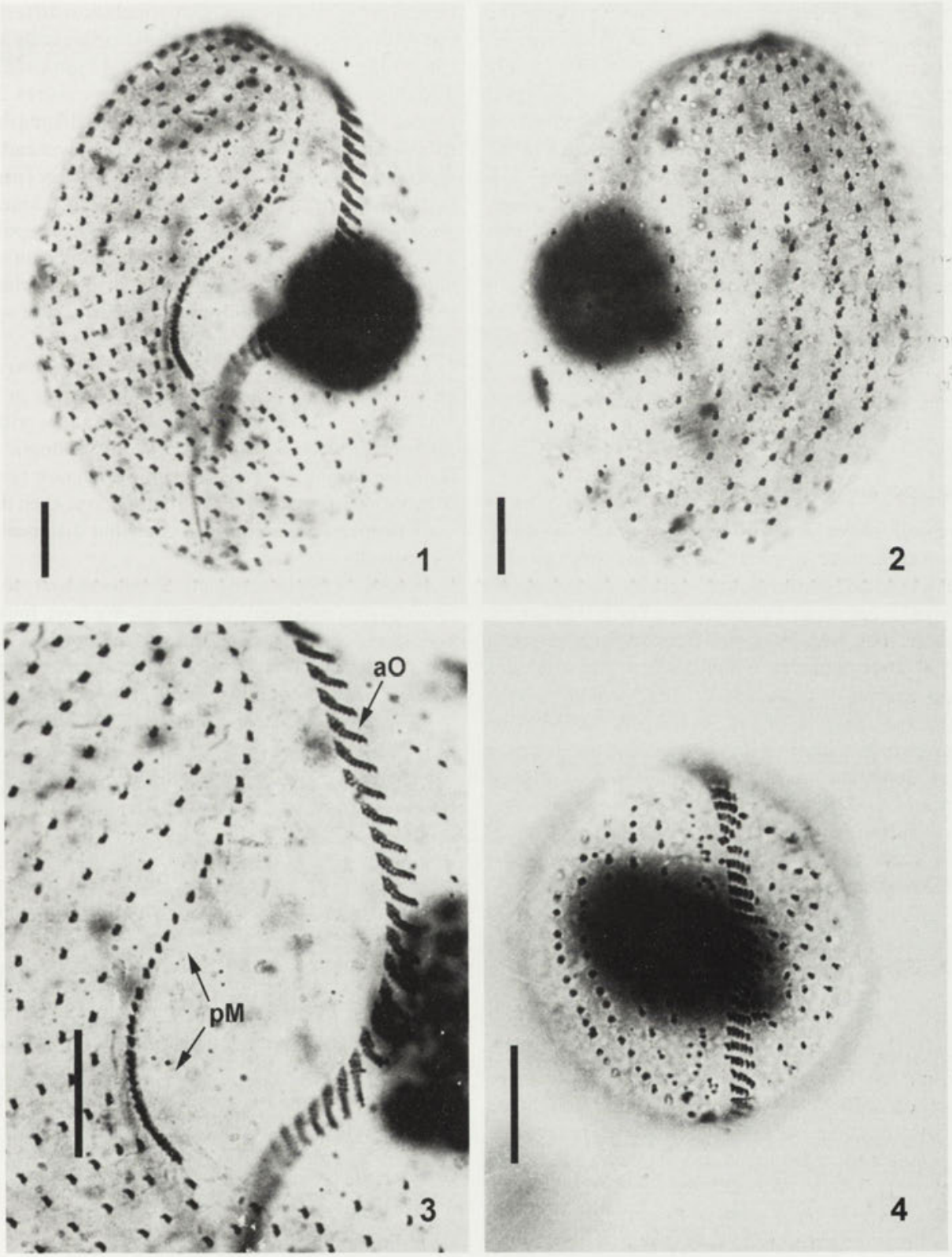

Figs. 1-4. *Bryometopus hawaiiensis* after silver carbonate impregnation. 1,2 - somatic and oral infraciliature in right lateral (ventral) and left lateral views; 3 - detail of adoral zone of organelles and paroral membrane; 4 - cyst in excystment stage showing the primordia of the oral structures. aO - adoral zone of organelles, pM - paroral membrane. Bars - 10 μm

the anterior pole of the cell towards the oral aperture. The organization of the paroral dikinetid is the most conspicuous feature: the anterior 12-20 dikinetids are loosely spaced (as in somatic kineties) while in the posterior part the last 15-20 dikinetids are closely packed together. The contractile vacuole has a single excretory pore in the posterior third of the cell in the postoral zone. It is surrounded by small collecting vesicles during diastole. Cytoplasm is colorless and the cortex has conspicuous extrusomes. The nuclear apparatus is formed by an spherical macronucleus and one to four (usually two) spherical micronuclei, adjacent to the macronucleus. The position of the macronucleus is very conservative, it lies at the left side of the cell in an area delimited by the proximal portion of the adoral zone of organelles, the excretory pore of the contractile vacuole and the left body margin.

Occurrence and ecology

The cells move rather quickly in liquid medium by rotation around the longitudinal axis and they can also creep over soil particles and debris. *Bryometopus hawaiiensis* occurs in mosses, and it feeds on bacteria and algae. This organism can form resting spherical cysts, 30 μm in diameter. Within the cyst, oral structures dissorganize and reorganize prior to excystment with the primordia of the adoral organelles in a row parallel to the right kineties and scattered kinetosomes that will form the paroral membrane at its right (Fig. 4). As a typical inhabitant of edaphic biotopes, this species was found in association with other ciliates as *Phacodinium metchnicoffi, Epispathidium regium, Spathidium muscicola, Platyophrya vorax* and *Kreyella minuta.*

DISCUSSION

The population of *B. hawaiiensis* studied here was formerly described as a new species, *B. muscicola* by us (Olmo et Téllez, 1995), unaware of the prior description of *B. hawaiiensis* by Foissner (1994). Due mainly to the organization of the paroral membrane, very peculiar for a *Bryometopus* species and similar in both populations. We identify the species found in Spain with *B. hawaiiensis* Foissner, 1994. We consider that the paroral infraciliature and its disposition should be considered the most important diagnostic feature of this species. Our population differs from the type species on the size of the cells; cells longer (60-75 μm vs. 45-63) and wider (30-42 μm vs. 27-37). The macronucleus is also longer, it measures 21 μm instead of 11 μm. However, it must be considered that our measurements may be larger in flattened silver carbonate specimens compared to those taken in protargol preparations. The number of dikinetids in the dorsal kineties is also an important feature: 25-33 in the Spanish population, 12-19 in the Hawaiian specimens. The number of micronuclei is also a distinguishing feature of this population, it varies from 1 to 4 usually two, while the type species presents only one micronucleus.

Foissner (1994) considers that *B. hawaiiensis* must be a rare species, since he did not found it in about 1000 other soil and moss samples collected worldwide. Therefore, he assumed it was probably endemic to the Hawaiian Archipelago. However, we can now consider *B. hawaiiensis* as a comospolitan species, even though our European population is somewhat different morphologically.

Foissner (1994) considers *B. hawaiiensis* to be a limnetic or a moss and soil species. We have found our population of *B. hawiiensis* in soil and mosses. Therefore, this species is probably a real moss inhabitant if we also consider that it always appear associated to other moss species like *Phacodinium metchnicoffi.*

Acknowledgments. We wish to thank Professor Wilhelm Foissner for his recommendations and advice. This work has been supported by a grant from the DGICYT within the project PB91-0384.

REFERENCES

Fernández-Galiano D. (1994) The ammoniacal silver carbonate method as a general procedure in the study of protozoa from sewage (and others) waters. *Wat. Res.* **28:** 495-496

Foissner W. (1992) Estimating the species richness of soil protozoa using the "non-flooded petri dish method". In: Protocols in Protozoology (Eds. J. J. Lee and A. T. Soldo). Society of Protozoologists, Allen Press, Lawrence, Kansas, B-10.1 to B-10.2

Foissner W. (1993) Colpodea (Ciliophora). G. Fischer, Stuttgart, Jena, New York

Foissner W. (1994) *Bryometopus hawaiiensis* sp. n., a new colpodid ciliate from a terrestrial biotope of the Hawaiian Archipelago. *Annls. Naturhist. Mus. Wien.* **96 B:** 19-27

Kahl A. (1932) Urtiere oder Protozoa I: Wimpertiere oder Ciliata (Infusoria). Spirotricha.- Tierwelt Dtl., **25:** 399-650

Olmo J. L., Téllez C. (1995) A new colpodid ciliate from mosses, *Bryometopus muscicola* nov. sp. (Ciliophora, Colpodea). *Europ. J. Protistol.* **31:** 170 A

Received on 4th March, 1996; accepted on 20th June, 1996

Acta Protozoologica (1996) 35: 321 - 330

ACTA
PROTOZOOLOGICA

Description of *Metabakuella bimarginata* sp. n., and Key to the Ciliate Subfamily Bakuellinae Jankowski, 1979

Carmen FRANCO[1], Genoveva F. ESTEBAN[2] and Carmen TÉLLEZ[3]

[1]Estación Biogeológica de "El Ventorrillo", Museo Nacional de Ciencias Naturales, CSIC, Madrid, Spain; [2]Institute of Freshwater Ecology, Windermere Laboratory, England; [3]Departamento de Microbiología III, Facultad de Ciencias Biológicas, UCM, Madrid, Spain

Summary. The stichotrich ciliate *Metabakuella bimarginata* sp. n. was isolated from the sandy sediment of Manzanares stream in Guadarrama, near Madrid (Spain). Its morphology and infraciliature were studied *in vivo* and in silver carbonate and protargol impregnated specimens. The organism measures about 225 x 85 µm and has 4-6 enlarged frontal cirri, one row of 5-8 buccal cirri, 2 frontoterminal cirri, 13-18 pairs of midventral cirri at the anterior part of the cell, 2 marginal rows at each side, 8-11 transverse cirri, 3 dorsal kineties, more than 100 macronuclear fragments, and 4-12 micronuclei. The anterior part of the midventral cirri is a single row of 3 cirri that curves to the left. This single row together with the frontal cirri forms a double crown. The midventral cirri in the posterior part of the cell form 4-7 obliquely arranged rows. Some macronuclear fragments in wild forms of *M. bimarginata* sp. n. bear endonuclear bacteria of unknown identity. The obliquely arranged rows of midventral cirri in the posterior half of the cell, the number of marginal rows, and the double crown formed by the frontal cirri, are the typical characteristics of the genus *Metabakuella*. We include this genus in the subfamily Bakuellinae Jankowski, 1979, within the family Holostichidae Fauré-Fremiet, 1961. A comparison of the genera included in the subfamily Bakuellinae along with a key for the genera are presented here.

Key words: ciliates, Holostichidae, infraciliature, *Metabakuella*, Stichotrichida.

INTRODUCTION

Alekperov (1989) established the genus *Metabakuella* for the stichotrich ciliate *Metabakuella perbella*, originally described as *Keronella perbella* Alekperov and Musayev, 1988. The genus *Metabakuella* is characterized by the following characters (Alekperov 1989): frontal cirri that form a crown with the anterior part of the midventral cirri; a row of frontoterminal cirri; numerous buccal cirri and transverse cirri; several oblique ventral rows in the posterior half of the cell; one or more right marginal rows and two or more left marginal rows. According to Alekperov (1989, 1992) this genus includes two species: *M. perbella* Alekperov 1989, and *M. variabilis* Alekperov, 1992, formerly described as *Bakuella variabilis* (Borror and Wicklow 1983).

Metabakuella bimarginata sp. n. was found during an investigation of benthic ciliates inhabiting the sediment of freshwater streams. We have included the genus *Metabakuella* in the subfamily Bakuellinae, Jankowski, 1979. Diverse studies on ciliates of this subfamily have been published in the last few years (Alekperov 1992, Song et al. 1992). However, their independent simulta-

Address for correspondence: Carmen Franco, Departamento de Microbiología III, Facultad de Ciencias Biológicas, UCM, 28040 Madrid, Spain.

neous publication resulted in some contradictions regarding the revision of the genera investigated. Eigner (1994) recently revised and redescribed the subfamily Bakuellinae. He redefined it as "Holostichidae with a midventral row composed of pairs of cirri or several short oblique midventral rows in the anterior part of the cell and several obliquely arranged midventral rows of cirri in the posterior part". Eigner (1994) also included four genera in this subfamily: *Bakuella* Agamaliev and Alekperov, 1976, *Keronella* Wiąckowski, 1985, *Holostichides* Foissner, 1987, and *Eschaneustyla* Stokes, 1886. Considering the morphological similarities between these genera and *Metabakuella* we include the latter within the same subfamily. A key with the characters of the five genera is included in this study.

MATERIALS AND METHODS

Metabakuella bimarginata sp. n. was found in the sediment of Manzanares stream in Guadarrama Mountains (Madrid, Spain). The sediment of the sample site was predominantly composed of medium-coarse sand - 35% - (average grain size: 400µm) and fine-coarse sand - 32% - (average grain size: 200 µm).

The cells were isolated from the original sample and transferred to Petri dishes containing mineral water and crushed wheat grains. *Glaucoma chattoni*, *Cyclidium glaucoma*, and an unidentified colourless flagellate from the same sample were extra sources of food. The cultures were maintained at 4°C and were transferred to fresh medium every 15 days.

The ciliates were silver stained using the pyridinated silver carbonate method (Fernández-Galiano 1994) and protargol (Wilbert 1975). Cell measurements were made on living specimens. The data of infraciliature, and other cellular features; number, length and width of macronuclei and micronuclei, were based on impregnated cells (Table 1). The terminology used throughout this article follows Borror (1972).

The endonuclear bacteria of *M. bimarginata* sp. n. were studied on silver carbonate impregnated ciliates. We calculated the volume of the ciliates and the volume fraction of bacteria inside each ciliate. Ciliate cell volume was calculated as the product of a photographed image area and the cell thickness, calculated using the calibrated focusing wheel on the microscope. The number of bacteria were counted in each cell; two or more photographs were sometimes taken at different planes of the ciliate to record all the bacteria inside it. To measure the bacterial volume, we assumed the bacteria as a geometrical figure. The length, the width and the thickness of at least 15 bacteria per ciliate were manually measured and the average value was calculated. The total bacterial volume was calculated by multiplying the mean value by the total number of bacteria inside the ciliate.

RESULTS

Metabakuella bimarginata sp. n. (Figs. 1-12, Table 1)

Diagnosis: *in vivo* 225 x 85 µm. Two rows of cirri running along each margin of the ventral surface of the cell. More than 100 ellipsoid macronuclear fragments.

Table 1. *Metabakuella bimarginata* sp. n. morphometric characterization

	Min	Max	Mean	SD	SE	n
Body, length[1]	150	300	227	38.2	4.8	63
Body, width[1]	50	115	82.9	30.5	4.5	46
Body, length	150	280	215.8	31.9	5.24	37
Body, width	50	100	70.3	11.07	1.82	37
No. of membranelles[2]	40	50	46	3.6	1.3	7
No. of buccal cirri[2]	5	8	7	1.08	0.29	13
No. of frontal cirri[2]	4	6	4.8	1.08	0.29	10
No. of midventral pairs of cirri[2]	13	18	16.2	2.21	0.83	7
No. of midventral rows	4	7	5.3	1.23	0.35	9
No. of cirri (1st RMR)	40	55	47.4	6.04	2.01	9
No. of cirri (2nd RMR)	40	68	53.6	8.33	2.77	9
No. of cirri (1st LMR)	37	64	52.2	7.71	1.99	15
No. of cirri (2nd LMR)	32	62	49.4	10.54	2.92	13
No. of transverse cirri	8	11	9.8	0.93	0.27	12
No. of macronuclei	110	263	184.9	39.3	7.44	28
Macronuclei length	8.3	14.4	11.3	1.8	0.4	19
Macronuclei width	2.7	6	4.06	0.92	0.21	19
No. of micronuclei	4	12	8.8	2.21	0.49	20
Micronuclei length	8.9	13.3	10.3	1.44	0.49	12
Micronuclei width	4	7	4.88	0.89	0.25	12
No. of dorsal kineties[2]	3	3	3	0	0	10

All data based on measurements on cells after Fernández-Galiano silver impregnation except [1] that were living cells, and [2] that are based on cells after protargol. All measurements in µm, LMR - left marginal row, Max - maximum, Min - minimum, n - number of organisms measured, RMR - right marginal row, SD -standard deviation, SE - standard error

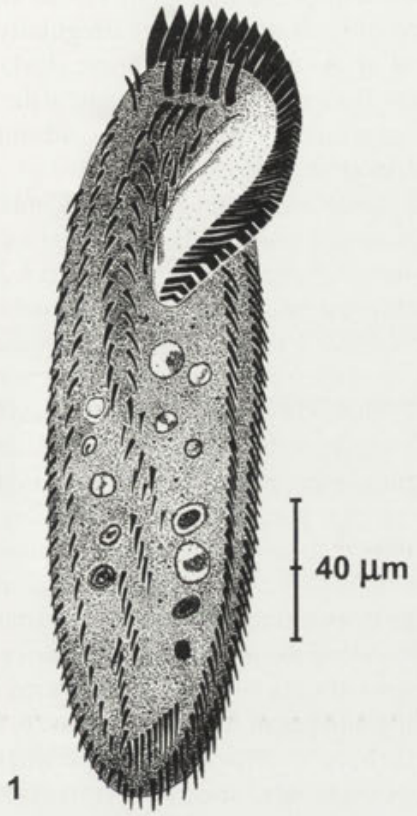

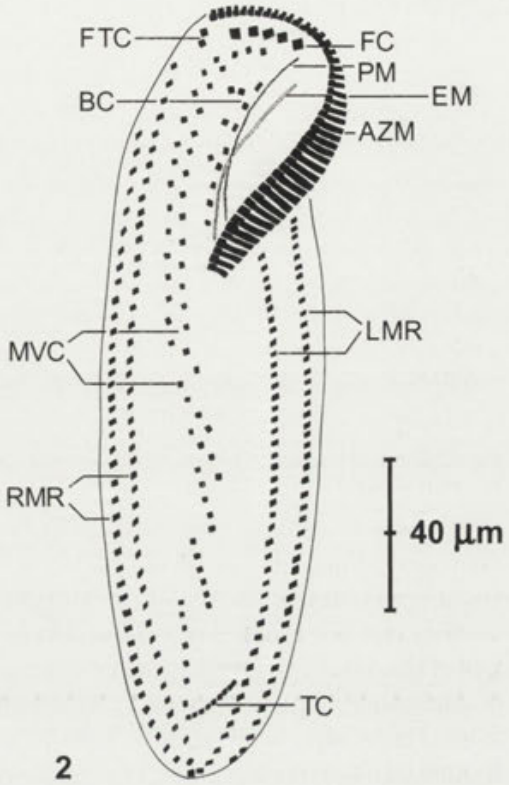

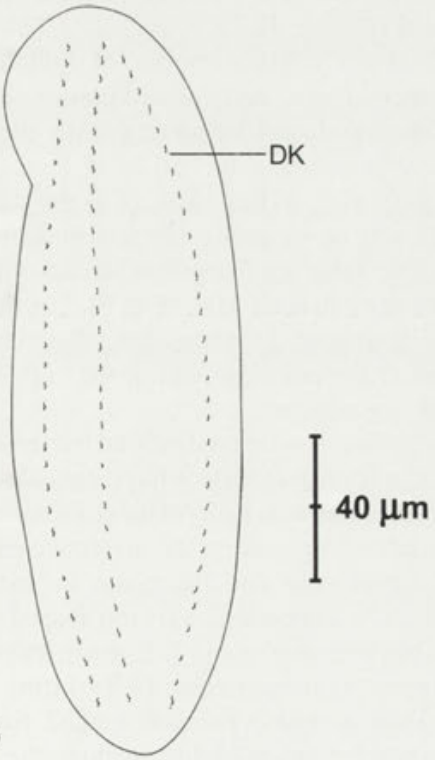

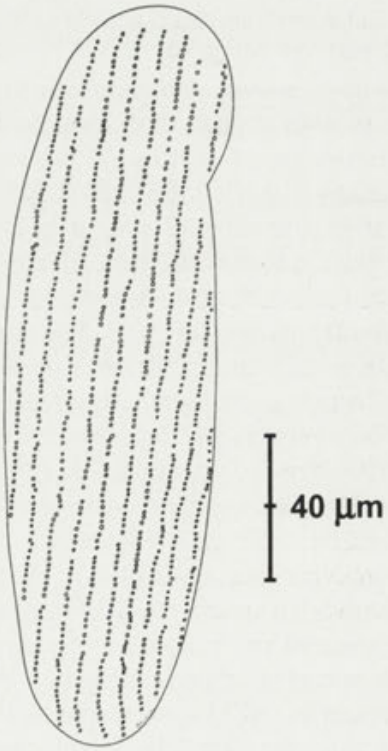

Figs. 1-4. Morphology of *Metabakuella bimarginata* sp. n. (1, 4 - *in vivo*; 2, 3 - after protargol impregnation). 1, 2 - ventral view; 3 - dorsal view; 4 - cortical granules arrangement. AZM - adoral zone of membranelles, BC - buccal cirri, DK - dorsal kineties, EM - endoral membrane, FC - frontal cirri, FTC - frontoterminal cirri, LMR - left marginal row, MVC - midventral cirri, PM - paroral membrane, RMR - right marginal row, TC - transverse cirri

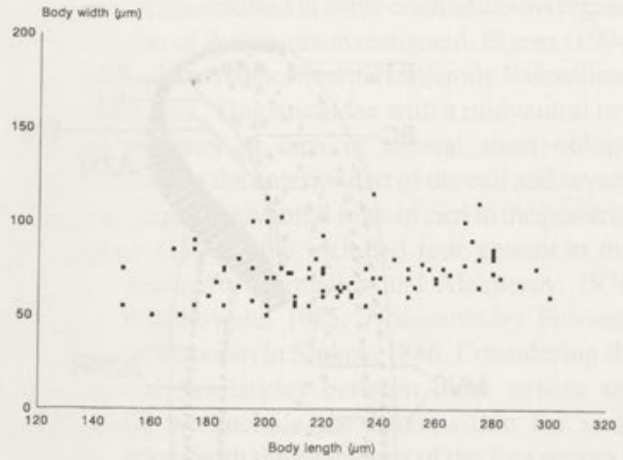

Fig. 5. Measured lengths and widths of living specimens of *Metabakuella bimarginata* sp. n.

One row of buccal cirri. Four to six frontal cirri, 2 frontoterminal cirri, 13-18 pairs of midventral cirri in the anterior part of the cell. Midventral cirri in the posterior half of the cell as rows with a gradually increasing number of cirri towards the rear of the cell. Cytoplasm with distinct rows of greenish cortical granules. Transverse cirri present. Caudal cirri absent.

Type location: benthos of a freshwater stream (Manzanares stream) at Guadarrama Mountains (Madrid, Spain), 40° 45' N; 3° 54' W.

Derivatio nominis: *bimarginata* to indicate the two marginal rows of cirri on each side of the cell.

Description: *Metabakuella bimarginata* sp. n. is a stichotrich ciliate. It is elliptical shaped, flexible, dorsoventrally flattened with a slightly concave dorsal surface. Both margins of the cell are almost parallel, slightly narrowed at the posterior end. Both cell ends are broadly rounded (Fig. 1). The contractile vacuole is at the level of the cytostome, on the left side of the cell. The living ciliates measure 150-300 µm in length, and 50-115 µm in width (Table 1, Fig. 5). They have over 100 ellipsoid macronuclear fragments (110-260) about 11 x 4 µm, regularly distributed in the cytoplasm, and usually 4-12 micronuclei (10 x 4 µm) near the macronuclear fragments (Table 1). The cells present small greenish spherical cortical granules distributed along the cell and visible *in vivo* (Fig. 4).

The buccal ciliature is formed by the adoral zone of membranelles (AZM) and two parallel undulating membranes along the right side of the peristome, the endoral membrane, and the paroral membrane (Figs. 2, 7). The AZM occupies 1/3 of the body length and is composed of 40-50 membranelles. Both undulating membranes consist of a double row of kinetosomes (Fig. 7). The kinetosomes of the paroral membrane (PM) are irregularly arranged, while those of the endoral membrane (EM) form two parallel lines. Both membranes terminate at the same level near the proximal portion of the adoral zone of membranelles (Fig. 6).

The 4-6 frontal cirri (FC) are slightly enlarged compared to the rest of somatic cirri and form a curved row parallel to the anterior part of the AZM (Figs. 2, 7). There are 5-8 buccal cirri (BC) parallel to the paroral membrane. There are usually 2 or 3 cirri in one row between the buccal cirri and the left midventral cirri, and 2 frontoterminal cirri (FTC). The 13-18 pairs of midventral cirri (MVC) are arranged in zigzag at the anterior part of the cell (Fig. 7). The midventral pairs end in mid-body as Figure 6 indicates. The anterior part of the midventral cirri is a single row of 3 cirri that curves to the left. This single row together with the frontal cirri forms a double crown (Fig. 7). The midventral cirri (MVC) are arranged in 4-7 oblique rows along the posterior half of the cell (Figs. 6, 8). These rows always bear more than 2 cirri each, with an increasing number of 3 to 7 cirri (Figs. 6, 8); the last row being the longest which is oriented parallel to the main axis of the cell and ends close to the transverse cirri (Figs. 6, 9). The transverse cirri (TC) form a curved row of 8-11 cirri (Figs. 6, 9).

The somatic ciliature consists of right marginal cirri, left marginal cirri, and dorsal kineties. The marginal rows are numbered beginning with the inner row, closest to the centre of the cell. In *M. bimarginata* sp. n. there are two parallel rows of right marginal cirri (RMR) and two parallel left marginal rows (LMR) (Figs. 6, 9, Table 1). The posterior end of the marginal rows do not join each other (Fig. 9). The dorsal surface of the ciliate bears 3 kineties (DK) that extend from the anterior to the posterior end of the cell (Figs. 3, 10). Caudal cirri absent.

The presence of long rod-shaped bacteria of unknown identity in the macronuclear fragments was observed in wild cells, as well as in many of the ciliates in culture. They were confined to some of the macronuclear fragments, usually with only one bacterium in each fragment, (Figs. 11, 12). The bacteria were rod-shaped with rounded ends. They measured about 3-25 µm in length, and about 1 µm in width (average value 10.9 x 1 µm). The number of bacteria observed per cell ranged from 7 to 52. Unfortunately, we could not conclude the study of the relationship between these endonuclear bacteria and the life cycle of the host as the former disappeared after some generations of the latter.

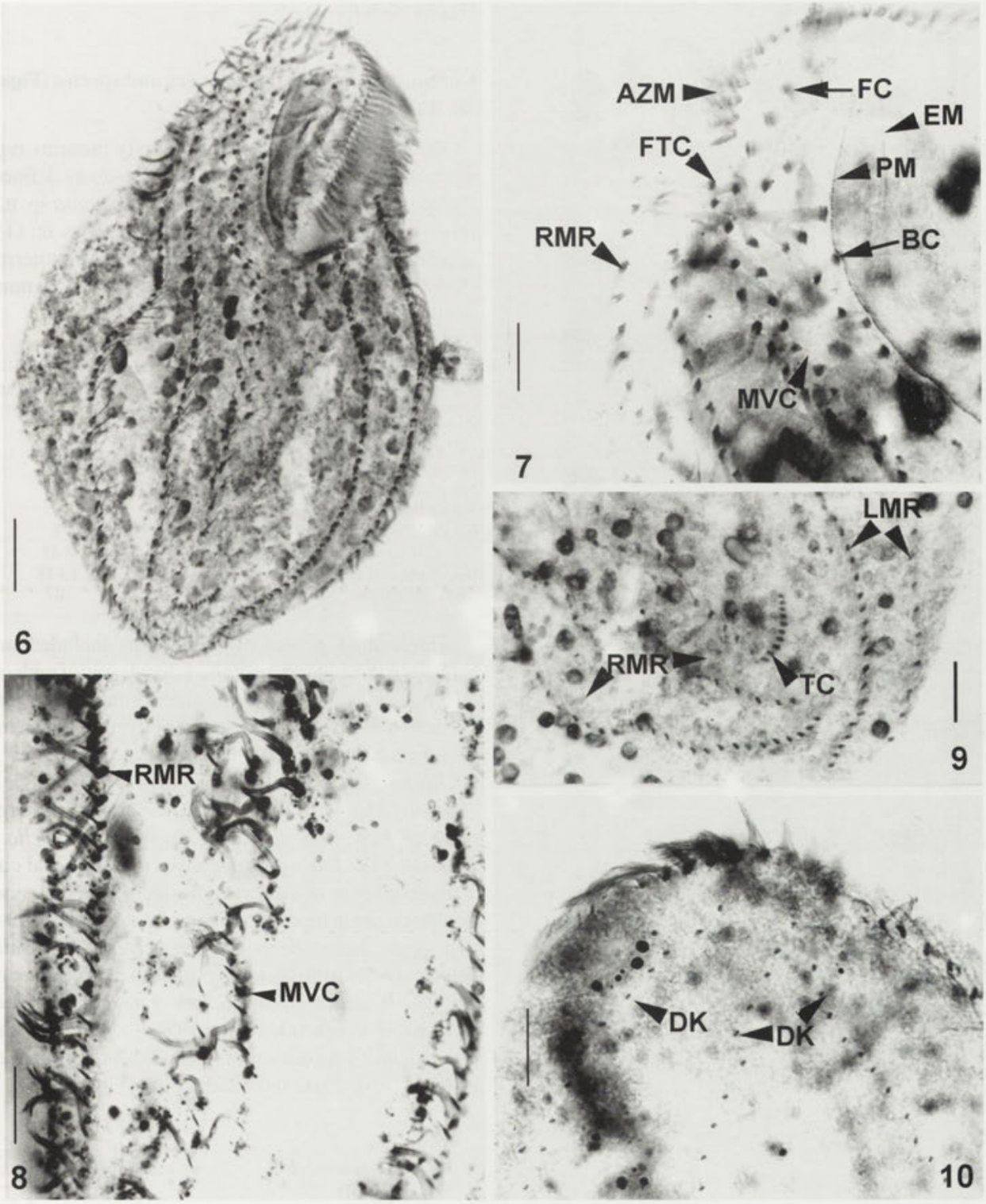

Figs. 6-10. *Metabakuella bimarginata* sp. n., somatic and oral infraciliature after silver carbonate impregnation (8, 9) and after protargol impregnation (6, 7, 10). 6 - ventral view. Bar - 25 µm. 7 - anterior part of the ventral side showing the frontal cirri (FC), the buccal cirri (BC), the frontoterminal cirri (FTC), the midventral cirri (MVC) and the right marginal rows (RMR). AZM - adoral zone of membranelles, EM - endoral membrane, PM - paroral membrane. Bar - 10 µm. 8 - midventral cirri (MVC) in the posterior part of the cell. RMR - right marginal row of cirri. Note obliquely arranged rows of cirri. Bar - 20 µm. 9 - posterior part of the ventral surface showing the transverse cirri (TC) and the right and left marginal rows of cirri (RMR and LMR). Bar - 10 µm. 10 - dorsal view showing the dorsal kineties (DK). Bar - 10 µm

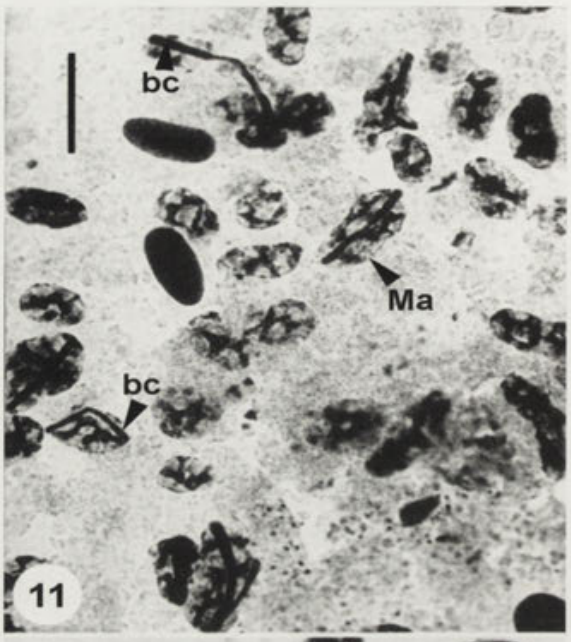

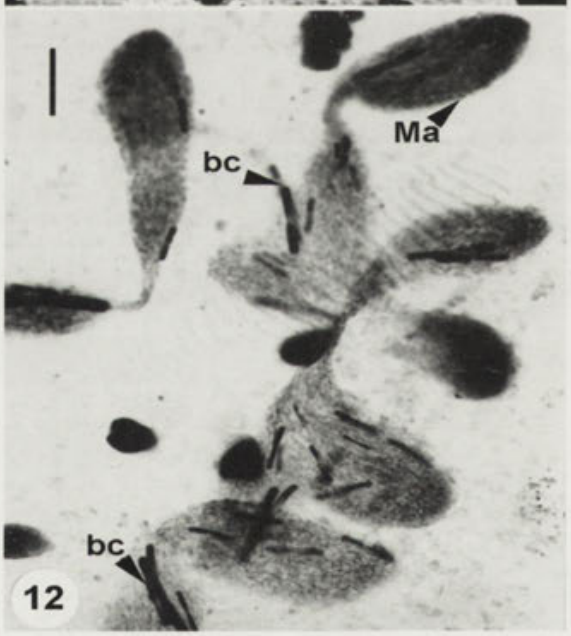

Figs. 11, 12. Micrographs of the macronuclear fragments after silver carbonate impregnation. 11 - bacteria inside the macronuclear fragments. bc - bacteria, Ma - macronuclei. Bar - 10μm. 12 - bacteria inside the macronuclei during the division of *Metabakuella bimarginata* sp. n. bc - bacteria. Ma - macronuclei. Bar - 10 μm

DISCUSSION

Comparison with related genera and species (Figs. 13-28, Tables 2, 3)

The species described in this study presents typical characteristics of the genus *Metabakuella* as defined by Alekperov (1989). *Metabakuella bimarginata* sp. n. differs from other previously described species in: (1) the number of frontal cirri; (2) the number of frontoterminal cirri; (3) the pairs of midventral cirri, and (4) the number of right marginal rows (Table 2).

Table 2. Morphological comparison of *Metabakuella* species

	M. perbella	*M. bimarginata* sp. n.
Body, length (μm)	90	227
No. of buccal cirri	7	5-8
No. of frontal cirri	12	4-6
No. of frontoterminal cirri	12	2
No. of right marginal rows	3	2
No. of left marginal rows	2-3	2
No. of transverse cirri	9	8-11
No. of pairs of midventral cirri	8	13-18
Midventral rows	7	4-7

Three other genera of stichotrichs included in the subfamily Bakuellinae have also a double row of midventral cirri in a zigzag pattern in the anterior part of the ventral surface, and obliquely arranged midventral rows in the posterior part of the cell: *Bakuella* Agamaliev and Alekperov, 1976, *Keronella* Wiackowski, 1985, and *Holostichides* Foissner, 1987. The number of marginal rows of cirri separates the genera *Metabakuella* and *Bakuella*. The latter presents more than 1 buccal cirrus, 1 marginal row of cirri at each side of the cell, and no double crown at the anterior part of the cell (Figs. 13-20). Our species cannot be included in the genus *Keronella* as the one species in this genus has more than 2 frontoterminal cirri, caudal cirri, and only one row of marginal cirri at each side of the ventral surface (Fig. 21). The genus *Holostichides* presents more than 2 frontoterminal cirri, no transverse cirri, and caudal cirri (Figs. 22-25). The

Table 3. Characters of the genera included in the subfamily Bakuellinae

	Bakuella	*Keronella*	*Holostichides*	*Eschaneustyla*	*Metabakuella*
No. of buccal cirri	more than 1	1	0-1	1	5-8
No. of frontal cirri	3-5	7-9	3	1	4-6
Presence of double crown	no	yes	no	no	yes
No. of frontoterminal cirri	2 or more	more than 2	more than 2	many	2
Transverse cirri	with	with	without	without	with
Caudal cirri	without	with	with	with	without
No. of right marginal rows	1	1	1	2 or more	2
No. of left marginal rows	1	1	1	2 or more	2

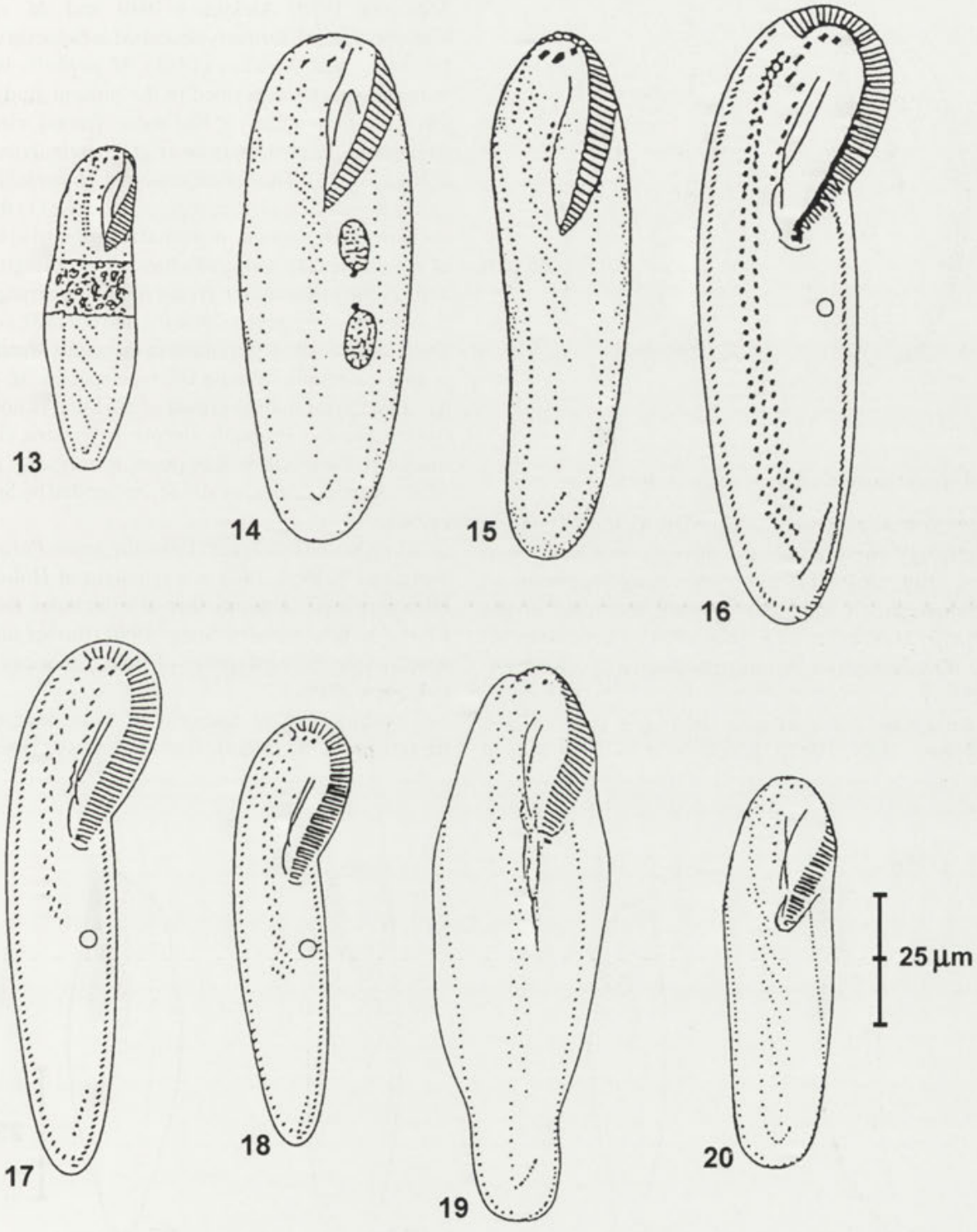

Figs. 13-20. Species of the genus *Bakuella* (13 - *Bakuella marina*, from Agamaliev and Alekperov, 1976; 14 - *Bakuella crenata*, from Agamaliev and Alekperov, 1976; 15 - *Bakuella imbricata*, from Alekperov, 1982; 16 - *Bakuella salinarum*, from Mihailowitsch and Wilbert, 1990; 17 - *Bakuella walibonensis*, from Mihailowitsch and Wilbert, 1990; 18 - *Bakuella kreuzcampii*, from Mihailowitsch and Wilbert, 1990; 19 - *Bakuella edaphoni*, from Song et al., 1992; 20 - *Bakuella pampinaria*, from Eigner and Foissner, 1992)

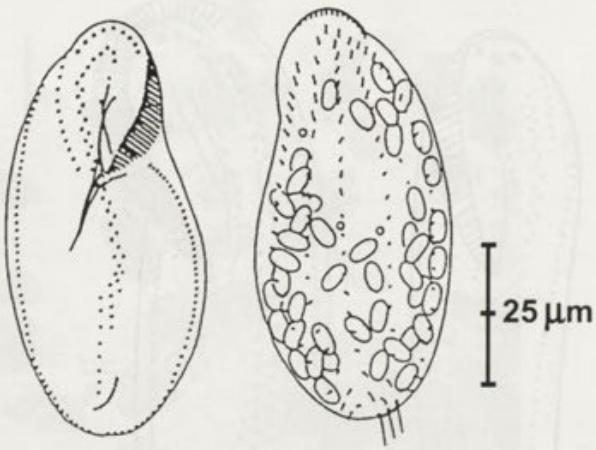

Fig. 21. *Keronella gracilis* from Wiackowski (1985)

genus *Eschaneustyla* has a complete different general morphology compared to the three genera mentioned above (Fig. 26). However, the morphogenesis of *Eschaneustyla* is identical to other members of the subfamily Bakuellinae (Eigner 1994). *Eschaneustyla* and *Metabakuella* are morphologically different (Table 3).

The genus *Metabakuella* includes two species (Alekperov 1989, 1992): *M. perbella* (Alekperov and Musayev, 1988) Alekperov 1989, and *M. variabilis* Alekperov, 1992, formerly described as *Bakuella variabilis* by Borror and Wicklow (1983). *M. perbella* is smaller than the species described in the present study (90 vs. 230 µm in length). It has more frontal cirri, more frontoterminal cirri, and more right marginal rows (Table 2, Figs. 27-28). The classification of *M. variabilis* in the genus *Bakuella* is not appropriate because (1) this genus is characterized by one marginal row of cirri at each side of the cell and *M. variabilis* has 2-5 left marginal rows; and (2) the midventral cirri are obliquely arranged in all the species of the genus *Bakuella*, and not in *M. variabilis*. The inclusion of *M. variabilis* in the genus *Metabakuella* is also uncertain, because the type species *M. perbella* has an anterior double crown of cirri that is not present in *M. variabilis*. Probably, the precise generic classification of *M. variabilis* will be possible only after the study of its morphogenesis, as already suggested by Song et al. (1992).

As proposed by Eigner (1994) the genus *Parabakuella* Song and Wilbert, 1988 is a synonym of *Holostichides* Foissner, 1987, a genus that also includes the former *Periholosticha wilberti* Song, 1990 (further taxonomic details of the different species of Bakuellinae can be found in Eigner, 1994).

The presence of bacteria in some macronuclear fragments of *M. bimarginata* sp. n. was observed in

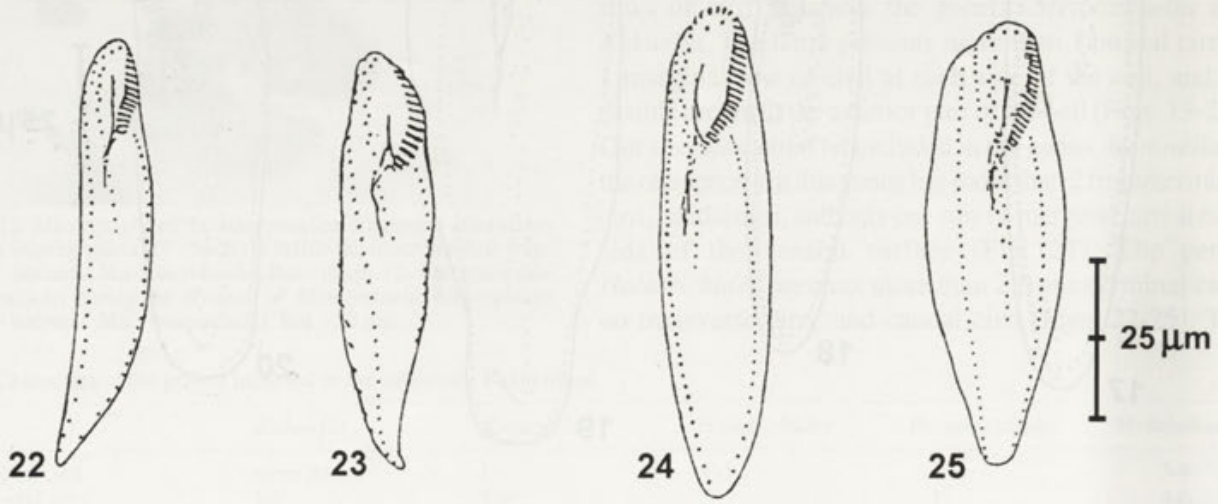

Figs. 22-25. Species of the genus *Holostichides* (22 - *Holostichides terricola*, from Foissner, 1988; 23 - *Holostichides wilberti*, from Song, 1990; 24 - *Holostichides chardezi*, from Foissner, 1987; 25 - *Holostichides typicus*, from Song and Wilbert, 1988)

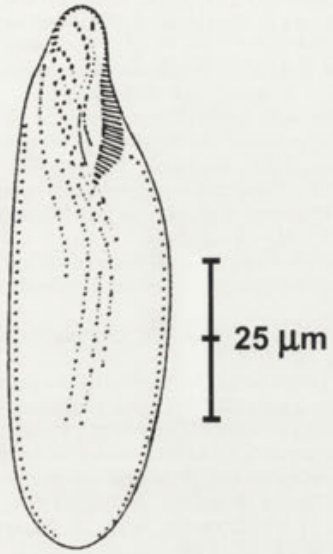

Fig. 26. *Eschaneustyla brachytona* (from Eigner, 1994)

wild and cultured cells. However, as mentioned above, further studies were not possible because the bacteria disappeared after some ciliate generations. Bacterial endosymbionts have been described in several ciliate species e.g., *Paramecium* (Beale et al. 1969, Görtz and Dieckmann 1980, Görtz 1983, Preer and Preer 1984, Görtz and Wiemann 1989, and references therein), *Vorticella* (Kirby 1942), *Metopus* (Jankowski 1964, Esteban et al. 1995), and *Euplotes* (Fauré-Fremiet 1952, Heckmann 1983, Heckmann et al. 1983, Rosati and Verni 1975). With the exception of *Euplotes crassus*, all endosymbionts in *Euplotes* are confined to the cytoplasm.

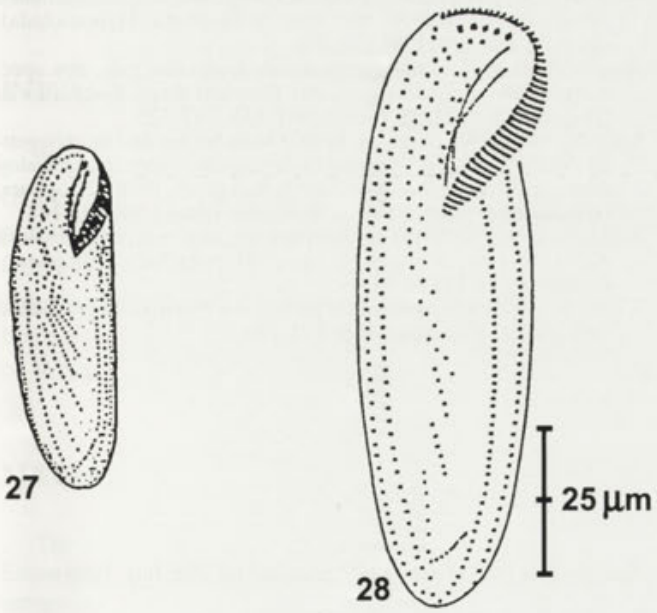

Figs. 27, 28. Species of the genus *Metabakuella* (27 - *Metabakuella perbella*, from Alekperov, 1992; 28 - *Metabakuella bimarginata* n. sp.)

Key to the Genera and Species of the Subfamily *Bakuellinae*

1. With caudal cirri **2**
- Without caudal cirri **4**
2. With transverse cirri ..... *Keronella*(single species, *K.gracilis*)
- Without transverse cirri **3**
3. With several short rows of more than 2 cirri in the anterior part of the cell ..... *Eschaneustyla* (single species, *E. brachytona*)
- With a double midventral row ..... *Holostichides* (several species)
4. The anterior part of the midventral cirri is single, and forms a bicorona ..... *Metabakuella* (several species)
- Without bicorona in the anterior part ..... *Bakuella* (several species)

Genus *Bakuella*
Revised and completed after Song et al. (1992)

1. Species from terrestrial habitats **2**
- Species from limnic or marine habitats **3**
2. More than 5 frontoterminal cirri and less than 5 transverse cirri ..... *B.pampinaria* Eigner and Foissner, 1992 (Fig. 20)
- Less than 5 frontoterminal cirri and more than 5 transverse cirri ..... *B. edaphoni* Song, Wilbert and Berger, 1992 (Fig. 19)
3. Two macronuclear segments ..... *B. crenata* Agamaliev and Alekperov, 1976 (Fig. 14)
- Many macronuclear segments **4**
4. Posteriormost ventral row terminates roughly in the middle or at the end of the 2nd third of the cell; ventral rows with only about 3-4 cirri **5**
- Posteriormost ventral row terminates at about the level of the transverse cirri; ventral rows with up to 13 cirri **6**
5. One buccal cirrus; an additional row between the anterior end of the midventral row and the right marginal row ..... *B. kreuzcampii* Song, Wilbert and Berger, 1992 (Fig. 18)
- A row of buccal cirri; additional row absent ..... *B. walibonensis* Song, Wilbert and Berger, 1992 (Fig. 17)
6. More than 3 frontal cirri ..... *B. salinarum* Mihailowitsch and Wilbert, 1990 (Fig. 16)
- Three frontal cirri **7**
7. More than 10 pairs of midventral cirri and more than 10 midventral rows of cirri ..... *B. marina* Agamaliev and Alekperov, 1976 (Fig. 13)
- Less than 10 pairs of midventral cirri and less than 10 midventral rows of cirri ..... *B. imbricata* Alekperov, 1982 (Fig. 15)

Genus *Holostichides*

1. Two dorsal kineties **2**
- Four dorsal kineties **3**
2. With cortical granules ..... *H. terricola* Foissner, 1988 (Fig. 22)
- Without cortical granules ..... *H. wilberti* (Song, 1990) Eigner, 1994 (Fig. 23)
3. One midventral row ..... *H. chardezi* Foissner, 1987 (Fig. 24)
- More than 1 midventral row (2-5) ..... *H. typicus* (Song and Wilbert, 1988) Eigner, 1994 (Fig. 25)

Genus *Metabakuella*

1. With a row of more than 2 frontoterminal cirri and more than 2 left marginal rows ..... *M. perbella* (Alekperov and Musayev, 1988) Alekperov, 1989 (Fig. 27)
- With 2 frontoterminal cirri; 2 left marginal rows of cirri ..... *M. bimarginata* sp. n. (Fig. 28)

Acknowledgements. CF received financial support from Consejo Superior de Investigaciones Científicas (Spain). This research was done within the project PB91-0384 granted by the DGICYT, Ministerio de Educación y Ciencia (Spain). Financial assistance from the Natural Environment Research Council (U.K.) supported the work of GFE.

REFERENCES

Agamaliev F. G., Alekperov I. H. (1976) A new genus *Bakuella* (Hypotrichida) from the Caspian Sea and the Djeiranbatansky water reservoir. *Zool. Zh.* **55:** 128-131 (in Russian)

Alekperov I. H. (1982) *Bakuella imbricata* sp. n. (Ciliophora, Hypotrichida) from the Djeiranbatansky water reservoir. *Zool. Zh.* **61:** 1253-1255 (in Russian)

Alekperov I. H. (1989) Revision of the genera *Bakuella* Agamaliev et Alekperov 1976 and *Keronella* Wiackowski 1985 (Hypotrichida, Ciliophora). In: Ecology of marine and freshwater protozoans (Eds. G. I. Poljansky, B. F. Zhukov and I. B. Raikov). Proceedings of the II Symposium. Academy of Sciences of the USSR. The All-Union Society of Protozoologists, Yaroslavl, p. 7, Abstract (in Russian)

Alekperov I. H. (1992) Revision of the Family Bakuellidae (Hypotrichidae, Ciliophora). *Zool. Zh.* **71:** 5-10 (in Russian)

Alekperov I. H., Musayev M. A. (1988) New and rare free-living infusoria from freshwater and soil of the Apsheron Peninsula. *Zool. Zh.* **67:** 1904-1908 (in Russian)

Beale G. H., Jurand A., Preer J. R. Jr. (1969) The classes of endosymbiont of *Paramecium aurelia*. *J. Cell. Sci.* **5:** 65-91

Borror A. C. (1972) Revision of the Order Hypotrichida (Ciliophora, Protozoa). *J. Protozool.* **19:** 1-23

Borror A. C., Wicklow B. J. (1983) The Suborder *Urostylina* Jankowski (Ciliophora, Hypotrichida): Morphology, Systematics and Identification of species. *Acta. Protozool.* **22:** 97-126

Eigner P. (1994) Divisional morphogenesis and reorganization in *Eschaneustyla brachytona* Stokes, 1886 and revision of the Bakuellinae (Ciliophora, Hypotrichida). *Europ. J. Protistol.* **30:** 462-475

Eigner P., Foissner, W. (1992) Divisional morphogenesis in *Bakuella pampinaria* nov. spec. and reevaluation of the classification of the Urostylids (Ciliophora, Hypotrichida). *Europ. J. Protistol.* **28:** 460-470

Esteban G., Fenchel T., Finlay B. J. (1995) Diversity of free-living morphospecies in the ciliate genus *Metopus*. *Arch. Protistenkd.* **146:** 137-164

Fauré-Fremiet E. (1952) Symbionts bacteriens des ciliès du genre *Euplotes*. *C. R. Acad. Sci.* **235:** 402-403

Fernández-Galiano D. (1994) The ammoniacal silver carbonate method as a general procedure in the study of protozoa from sewage (and other) waters. *Wat. Research.* **28:** 495-496

Foissner W. (1987) Neue und wenig bekannte hypotriche und colpodide Ciliaten (Protozoa: Ciliophora) aus Böden und Moosen. *Zool. Beitr. (N. F.)* **31:** 187-282

Foissner W. (1988) Gemeinsame Arten in der terricolen Ciliatenfauna (Protozoa: Ciliophora) von Australien und Afrika. *Stapfia, Linz,* **17:** 85-133

Görtz H-D. (1983) Endonuclear symbionts in ciliates. *Int. Rev. Cytol.* **Suppl. 14:** 145-176

Görtz H-D., Dieckmann J. (1980) Life cycle and infectivity of *Holospora elegans* Hafkine, a micronucleus-specific symbiont of *Paramecium caudatum* (Ehrenberg). *Protistologica* **16:** 591-603

Görtz H-D., Wiemann M. (1989) Route of infection of the bacteria *Holospora elegans* and *H. obtusa* into the nuclei of *Paramecium caudatum*. *Eur. J. Protistol.* **24:** 101-109

Heckmann K. (1983) Endosymbionts of *Euplotes*. *Int. Rev. Cytol.* **Supplement 14:** 111-144

Heckmann K., Ten Hagen R., Görtz H-D. (1983) Freshwater *Euplotes* species with a 9 type 1 cirrus pattern depend upon endosymbionts. *J. Protozool.* **30:** 284-289

Jankowski A. W. (1964) Morphology and evolution of ciliophora. III. Diagnosis and phylogenesis of 53 sapropelebionts, mainly of the order Heterotrichida. *Arch. Protistenkd.* **107:** 185-294

Kirby H., Jr. (1942) A parasite of the macronucleus of *Vorticella*. *J. Parasit.* **28:** 311-314

Mihailowitsch V. B., Wilbert N. (1990) *Bakuella salinarum* nov. spec. und *Pseudokeronopsis ignea* nov. spec. (Ciliata, Hypotrichida) aus einem solebelasteten Fließgewässer des129 östlichen "Münsterland", FRG. *Arch. Protistenkd.* **138:** 207-219

Preer J. R. Jr., Preer L. B. (1984) Endosymbionts of protozoa. p: 795-811. In: Bergey's manual of systematic bacteriology 4, Vol 1 (Ed. N. R. Krieg). Williams and Wilkins, Baltimore

Rosati G., Verni F. (1975) Macronuclear symbionts in *Euplotes crassus* (Ciliata, Hypotrichida). *Boll. Zool.* **42:** 231-232

Song W. (1990) Morphologie und morphogenese des Bodenciliaten *Periholosticha wilberti* nov. spec. (Ciliophora, Hypotrichida). *Arch. Protistenkd.* **138:** 221-231

Song W., Wilbert N. (1988) *Parabakuella typica* nov. gen., nov. spec. (Ciliata, Hypotrichida) aus dem Edaphon eines Standortes in Qingdao, China. *Arch. Protistenkd.* **135**: 319-325

Song W., Wilbert N., Berger H. (1992) Morphology and morphogenesis of the soil ciliate *Bakuella edaphoni* nov. spec. and revision of the genus *Bakuella* Agamaliev & Alekperov, 1976 (Ciliophora, Hypotrichida). *Bull. Br. Mus. Nat. Hist. (Zool.)* **58:** 133-148

Wiąckowski K. (1985) The morphology and morphogenesis of *Keronella gracilis* n. gen., n. spec. (Hypotrichida, Ciliophora). *Protistologica* **21:** 81-91

Wilbert N. (1975) Eine verbesserte Technik der Protargol-Imprägnation für Ciliaten. *Mikrokosmos* **6:** 171-179

Received on 25th March, 1996; accepted on 29th July, 1996

Acta Protozoologica (1996) 35: 331 - 334

ACTA
PROTOZOOLOGICA

Zschokkella pseudosciaena sp.n. and *Myxoproteus cujaeus* sp.n. (Myxozoa: Myxosporea) from Sciaenid Fish of Hooghly Estuary, West Bengal, India

Nirmal Kumar SARKAR

Department of Zoology, Rishi Bankim Chandra College, Naihati, West Bengal, India

Summary. Two new Myxosporidia (Myxozoa: Myxosporea) namely *Zschokkella pseudosciaena* sp.n. and *Myxoproteus cujaeus* sp.n. have been described from the kidney tubules and ureter of *Pseudosciaena coibor* (Ham.) and urinary bladder of *Macrospinosa cuja* (Ham.) (both of Sciaenidae), respectively. The salient features of *Zschokkella pseudosciaena* sp.n. (Myxidiidae): trophozoite disporous; spore cylindro-ellipsoidal, suture elongated S-shaped, not ridged, 11.48 x 5.9 µm; a pair of equal, spherical and subterminal polar capsules, 3.58 µm in diam., 3 to 4 coils of polar filament in each capsule; coelozic. *Myxoproteus cujaeus* sp. n. (Sinuolineidae): trophozoite disporous; spore triangular or inversely pyramidal, 10.45 x 5.9 µm, suture moderately thick and bent at the middle; a pair of spherical and equal polar capsules towards the anterior surface, set wide apart, 3 to 4 coils of polar filament in each capsule, 3.27 µm in diameter.

Key words: Hooghly estuary, Myxidiidae, *Myxoproteus cujaeus* sp.n., Sciaenidae, Sinuolineidae, urinary system, *Zschokkella pseudosciaena* sp.n.

INTRODUCTION

The sciaenid fishes constitute one of the major food fish of India and are often parasitised by Myxosporean pathogenic protozoa. During this investigation on Indian fish, two myxosporean parasites of the genera *Zschokkella* Auerbach, 1910 and *Myxoproteus* Doflein, 1898 have been obtained from two Sciaenid fish of Hooghly estuary of West Bengal, India.

MATERIALS AND METHODS

The host fish were obtained from the landing places of Hooghly Estuary in South 24-parganas, West Bengal and preserved in ice. All autopsies were done in frozen fish in the laboratory. Fresh preparations of parasites were studied from wet smears treated with Lugol's iodine (2%) and from air-dried smears stained with Giemsa (1:20) after fixation in absolute Methanol. Various concentrations of potassium hydroxide (2-10%) solution and saturated Urea solution were tested for the extrusion of polar filament. The India ink method (Lom and Vávra 1963) was employed to detect the presence of mucous envelope associated with the spore. All measurements were made in micrometers (µm). The figures were drawn with the aid of a camera lucida (Mirror type).

Address for correspondence: Nirmal Kumar Sarkar, Department of Zoology, Rishi Bankim Chandra College, Naihati 743 165, West Bengal, India

OBSERVATIONS

Zschokkella pseudosciaena sp.n.

Early trophozoites were not seen. Some oval to rectangular disporous trophozoites with two developing spores were found (Fig. 1a). These forms measured 18.0-25.0 x 11.00-14.0 µm. The mature spores were almost cylindrical to ellipsoidal with rounded poles (Fig. 1b). The upper surface of each spore was slightly arched or rarely flat or

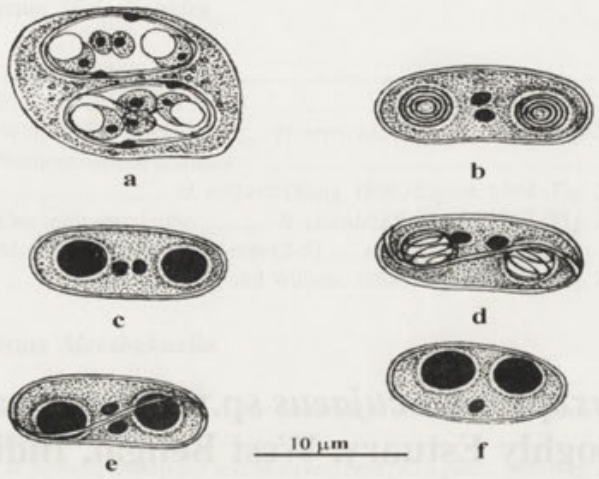

Fig. 1a - f. Trophozoite and spores of *Zschokkella pseudusciaena* sp.n. a - oval, disporous trophozoite with developing spores-Lugol's iodine. b - a fresh spore in valvular view showing arched anterior surface and concave posterior surface-Lugol's iodine. c - a cylindrical spore with rounded ends-Giemsa. d - a fresh spore in sutural view -Lugol's iodine. e - a fresh spore in sutural view -Giemsa. f - an unusual spore with unequal polar capsules towards the anterior surface-Giemsa

straight. The opposite surface of the spore was slightly concave but rarely straight. The two shell valves were thin-walled, smooth and symmetrical. The suture was moderately broad, oblique and elongated S-shaped but not ridged (Fig. 1d,e). The two spherical polar capsules were situated subterminally on either end of the spore. These two polar capsules were equal but sometimes appeared unequal because they opened in opposite direction (Fig. 1d) The polar filament in each polar capsule formed 3 to 4 coils. The extra-capsular spore cavity was completely filled with fine granular, binucleated mass of sporoplasm. There was no iodinophilous vacuole in the sporoplasm and no mucous envelope around the spore.

Measurements. Based on twenty five fresh spores from one frozen host; range is given with mean and standard deviation in the parentheses :

Spore length: 9.5-13.0 (11.48 ± 0.7413)
Spore width: 5.0-7.0 (5.90 ± 0.5477)
Polar capsule diameter: 3.5-4.5 (3.58 ± 0.3587)
Infection locus: kidney tubules and ureters.
Incidence: 3/46 (6.5%)
Pathogenecity: not apparent.
Host: *Pseudosciaena coibor* (Ham.)
Period of examination (infection): Aug.'93-Dec.'95 (November'94-February'95)
Locality: Hooghly estuary, West Bengal, India.
Material: syntypes on slide no. Mxz.-20, deposited to the Department of Zoology, Rishi Bankim Chandra College, Naihati, West Bengal, India.

***Myxoproteus cujaeus* sp.n.**

Early plasmodia or trophozoites were not seen. But some spore-producing trophozoites (plasmodia) were observed. These were usually elongated triangular with a broader end having two developing spores and a lobose pseudopodium at the opposite narrow end (Fig. 2a). A peripheral layer of hyaline non-granular ectoplasm enclosed the inner endoplasm of coarser granules. The trophozoites or plasmodia were disporous and measured 20.5-23.5 x 10.5-12.5 µm.

The mature spores were inversely pyramidal to triangular (Fig. 2 b-d)) with anterior flat ends and posterior narrow rounded ends. The occasional presence of pointed ends were also observed. The two shell valves were smooth and non-appendiculate. The two polar capsules were spherical, equal and placed wide apart at the flat ends. Usually one end of the anterior flat surface was more or less rounded while the other end was pointed (Fig. 2c,d). The suture was moderately thick but not ridged, weakly sinuous and bent in the middle but not twisted on its axis. The extra-capsular spore cavity was partly filled with finely granular, binucleated, oval, small mass of sporoplasm.

Measurements. Based on twenty-two fresh spores from single frozen host; range is given with mean and standard deviation within the parentheses :

Spore length: 9.0-12.0 (10.45 ± 0.7674)
Spore width: 8.0-10.0 (9.16 ± 0.76)
Polar capsule diameter: 3.0-4.0 (3.27± 0.3608)
Infection locus: urinary bladder.
Incidence: 2/46 (4.3%)
Pathogenicity: not apparent.
Host : *Macrospinosa cuja* (Ham.)

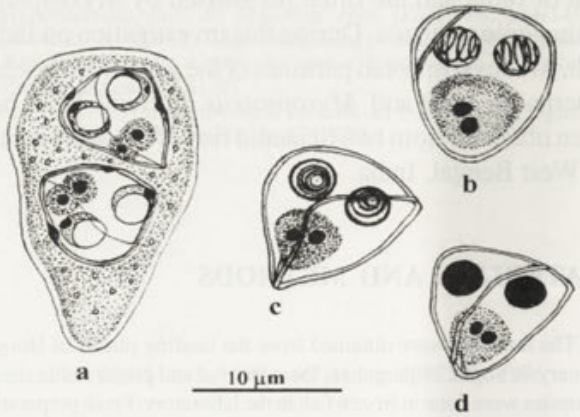

Fig. 2 a - d. Trophozoite and spores of *Myxoproteus cujaeus* sp.n. a - a disporous trophozoite with lobose pseudopodium-Lugol's iodine. b - a fresh spore in valvular view-Lugol's iodine. c - a fresh spore in sutural view-Lugol's iodine. d - a spore in slightly oblique view-Giemsa

Period of examination (infection): Aug.'93 to Dec.'95 (Nov.'94 to Feb.'95)

Locality: Hooghly estuary, West Bengal, India

Material: syntypes on slide no. MPT.-12, deposited to the Department of Zoology, Rishi Bankim Chandra College, Naihati, West Bengal, India.

DISCUSSION

Lom and Noble (1984) while proposing a new classification of the class Myxosporea Bütschli, 1881, considered the features such as disporous and polysporous trophozoites; ellipsoidal to semicircular spores with rounded or bluntly pointed ends; almost spherical and subterminal polar capsules; one binucleate sporoplasm and coelozoic as diagnostic of the genus *Zschokkella* Auerbach, 1910. Since most of the above features conform with the features of the myxosporean species obtained from *Pseudosciaena coibor* (Ham.), it has been assigned to the genus *Zschokkella* Auerbach, 1910.

The present *Zschokkella* sp. resembles superficially with *Zschokkella parasiluri* Fujita, 1927 (cited from Shulman 1966), *Z. ambiotocidis* Moser and Haldorson, 1976; *Z. tilapae* Chen and Hsieh, 1984. The spore of the present species also resembles the spores of *Z. globulosa* Davis, 1917, *Z. ophiocephalae* Chen and Hsieh, 1960, *Z. striata* Shulman, 1962, *Z. acheilognathi* Kudo, 1916 (cited from Kudo 1919) and *Z. orientalis* Konovalov and Shulman, 1966 (cited from Shulman 1966) in their mensural data. The comparison of the present species with its *Zschokkella* spp. mentioned above reveal that the trophic stages of *Z. parasiluri* are polysporous and its spores and polar capsule are much larger (Sp.-11.0-15.0 µm, Pc.-3.7-5.0 µm of *Z. parasiluri*) and the shape of its spore (elongated oval) and the polar capsule (spherical or slightly pyriform) are markedly different from the present species. Again, although the spore of the present species show similarity with the spore of *Z. embiotocidis* in smooth shell valves, the dimensions of the spore of the later species are always larger (Sp. 13.0-17.0 x 9.0-13.0 µm of *Z. embiotocidis*) and therefore, is distinct from the present species. Besides, the spores of *Z. tilapiae* and *Z. manhiensis* have longitudinally striated shellvalves and these striations are absent in the shellvalves of the present species in addition to the differences of their mensural data. Among the other *Zschokkella* spp. mentioned here except the species described from India, show almost similar dimensions of spores with the spore of the present species. However, the spore of *Z. globulosa* is flattened at capsular side and rounded at post-capsular side; sutural plane is twisted on its axis and sutural line is a distinct sinuate ridge. These features are absent in the spore of the present species: The spores of *Z. ophiocephalae* are elongated oval and the shellvalves are sometimes considerably swollen while in the present species the spores are almost cylindro-ellipsoidal and the polar capsules are smaller than *Z. ophiocephalae* (Pc. 4.5-5.6 µm in diam. of *Z. ophiocephali*). The spores of *Z. striata, Z. acheilognathi* and to some extent *Z. orientalis* have distinctly striated or faintly striated shell valves and therefore, are different from the smooth shell valves of the myxosporean in study. Moreover, the spores of *Z. orientalis* are pointed at poles while the poles are rounded in the present species.

Furthermore, the nature of trophozoite and the dimensions of spore of the present species resemble a few *Zschokkella* spp. namely, *Z. ilishae* Chakravarty, 1943, *Z. platistomusi* Sarkar, 1987, *Z. glosogobidii* Kalavati and Vaidehi, 1991 and *Z. gobidiensis* Sarkar and Ghosh, 1991 described from India. However, the shape of the spores of the above *Zschokkella* spp. i.e. semicircular, broadly ellipsoidal, dumbell-shaped to fusiform and broadly oval with flat truncate ends respectively, are quite different from the cylindro-ellipsoidal spore of the present species. In view of such differences with the related species, the present myxosporean has been considered as a new species and designated as *Zschokkella pseudosciaena* sp.n. after the name of the host.

Doflein (1898) transferred a myxosporean species *Myxosoma ambiguus* Thelohan, 1895 to a new genus *Myxoproteus* and designated *Myxoproteus ambiguus* (Thelohan, 1895) as its type species. The diagnostic features of the genus *Myxoproteus* (Thelohan,1895) as proposed by Lom and Noble (1984) are spores inversely pyramidal or triangular in sutural view with rounded outlines, anterior ends broad and more or less flattened, thick spore valves sometimes with various projections, sutural line straight or sinuous; polar capsules are set well apart, binucleate sporoplasm, trophozoite monosporous and disporous, coelozoic in the urinary system of marine fishes. Since most of the features of the present species conform with the above features, the present myxosporean, therefore, warrants its placement to *Myxoproteus* Doflein 1898.

The present *Myxoproteus* sp., in the shape of its spore shows similarity with the spores of *Myxoproteus ambiguus* (Thelohan, 1895) Doflein, 1898, *M. caudatus* Shulman, 1953, *M. elongatus* Shulman, 1953, *M. abyssus* Yoshino and Moser, 1974, *M. hubbs*i Moser and Noble, 1977 and *M. rosenblatti* Moser and Noble, 1977.

However, the spores of *M. caudatus* (11.0-21.6 x 8,5-14.0 µm) and *M. ambiguus* (25.0 x 18.0-20.0 µm) are much larger than the spore of the present species. Moreover, the filiform caudal appendage of *M. caudatus* is absent in the present species. Again, the posterior end of *M. elongatus* is always round while it is roundly pointed in the present species. The spore of *M. abyssus* occasionally appears concave or convex towards the anterior end but in the spore of the present species the broader anterior end is always convex or straight but never concave. Moreover, the posterior end of spore of the present species is roundly pointed while it is rounded in *M. abyssus*. Furthermore, the spore and the polar capsule of *M. hubbsi* are much smaller (Sp. 5.8 x 5.2 µm and Pc.1.4 µm in diam.) than the myxosporean species in study. Similarly, the spore of *M. rosenblatti* is much larger (17.0 x 10.5 µm) than the present species.

The present species also shows similarity in the mensural data of its spore with the spores of *M. cordiformis* Davis, 1917, *M. cornutus* Davis, 1917, *M. meridionalis* Evdokimova, 1977 and *M. moseri* Kovaleva and Gaevskaya, 1982. However, the spores of *M. cordiformis* and *M. cornutus* are heart shaped and possess wing-like processes which are absent in the spore of the present *Myxoproteus* sp.. This species also differs from *M. meridionalis* by triangular or inversely pyramidal spore (elongated spore in *M. meridionalis*), suture bent in the middle (suture not sinuate in *M. meridionalis*) and spherical polar capsules set wide apart at the broader flat end (ovoidal polar capsules 2.66 x 3.32 µm, placed side by side in *M. meridionalis*). The present species also differs from *M. moseri* by the shape of its spore and a pair of spherical and equal polar capsules (oval spore and spherical but unequal polar capsules-2.2-2.7 µm and 2.66-3.32 µm in *M. moseri*). In view of such differences with the related species, the present *Myxoproteus* sp. has been considered a new species and designated as *Myxoproteus cujaeus* sp.n., after the name of the host.

Acknowledgements. Author is grateful to Dr A. K. Roy, Teacher-in-charge and Professor S. Roy Chaudhury, Head, Department of Zoology for providing necessary facilities. Thanks are due to Sri Anupam Mazumder, M.Sc.(Stat.) for statistical calculation and Professor K.K Goswami for computer printing and Dr K.K. Misra for sincere co-operation.

REFERENCES

Auerbach M. (1910) Die Sporenbildung Von *Zschokkella* and das System der Myxospridien. *Zool. Anz.* **35:** 240-256

Chakravarty M. (1943) Studies on Myxosporidia from the common food fishes of Bengal. *Proc. Ind. Acad. Sci.* **18 B:** 21-35

Chen C.-L., Hsieh S.-R. (1960) Studies on Sporozoa from the fresh-water fishes *Ophiocephalus maculatus* and *O. argus* of China. *Acta Hydrobiol. Sin.* **2:** 171-196 (In Chinese with English Trans.)

Chen C.-L., Hsieh S.-R. (1984) New myxosporidian from the fresh water fishes of China. Ed. Inst.Hydrobiol., Acad. Sin., Beijing. (English Abst.) 13-14

Davis H. S. (1917) Structure and development of a myxosporidien parasite of the squeteague *Cynoscion regalis. J. Morphol.* **27:** 333-377

Doflein F. (1898) Studien zur Naturgeschichte der Protozoa. III. Uber Myxosporidien. *Zool. Jahrb. Abt. Anat.* **11:** 281-350

Evdokimova E.B. (1977) Miksosporidii kostistyh ryb Patagonskogo selfa (Atlanticeskoe pobereze Argentiny). *Parasitologia.* **11:** 166-178

Fujita T. (1927) Studies on Myxosporidia of Japan. V. On Myxosporidia in fishes of lake Biwa. *J. Coll. Agric. Hokkaido Univ.* **16:** 229-247

Kalavati C., Vaidehi J. (1991) Two New Species of Myxosporidians from Fishes of Chilka Lake. Genus *Sphaeromyxa* Thelohan and Genus *Zschokkella* Auerbach. *Uttar Pradesh J. Zool.* **11:** 146-150

Kovaleva A.A., Gaevskaya A.A. (1982) New data on Myxosporidia from the south-western Atlantic Ocean. *Parasitologia.* **16:** 353-359

Kudo R. (1919) Studies on Myxosporidia. A synopsis of genera and species of Myxosporidia. *Ill. Biol. Monogr.* **5:** 1-265

Lom J., Noble E.R.(1984) Revised classification of the class Myxosporea Bütschli, 1881. *Folia Parasitol. (Praha)* **31:** 193-205

Lom J., Vávra J. (1963) Mucous envelope of spores of the subphylum Cnidospora (Doflein, 1901). Vest. Cs. Spol. Zool. **27:** 4-6

Moser M., Haldorson L. (1976) *Zschokkella embiotocidis* sp.n. (Protozoa, Myxosporida) from California pile perch, *Damalichthys vacca* and striped perch *Embiotoca lateralis. Can. J. Zool.* **54:** 1403-1405

Moser M., Noble E. R. (1977) The genus *Myxoproteus* (Protozoa: Myxosporida) in macrourid Fishes. *Intl. J. Parasitol.* **7:** 253-255

Sarkar N.K. (1987) Studies on Myxosporidian Parasites (Myxozoa: Myxosporea) from Marine Fishes in West Bengal, India. II. Description of two new species from *Tachysurus platistomus* (Day). *Arch. Protistenkd.* **133:**151-155.

Sarkar N.K., Ghosh S. (1991) Two New Myxosporida (Myxozoa : Myxidiidae) from Fresh water fishes of West Bengal, India. *Uttar Pradesh J. Zool.* **11:** 54-58

Shulman S.S. (1953) New and little studied Myxosporidis. *Zool. Zhurn.* **32:** 384-393 (In Russian)

Shulman S.S. (1962) Key to myxosporidian fauna of USSR, no. 80. In: Key to Parasites of fresh water fishes of the USSR (Ed I.E. Bykhovskaya-Pavlovskaya). Nauka, Moskow-Lelingrad 55-155 (English Trans.)

Shulman S.S. (1966) Myxosporidia of the USSR (Ed. A.A. Strelkow) Emerind Publishing Co., New Delhi, (English Trans.)

Thelohan P. (1895) Recherches sur less Myxosporidies. *Bull. Sci. Fr. Belg.* **26:** 100-394

Yoshino T.P., Moser M. (1974) Myxosporidia (Protozoa) in Macrourid fishes (*Coryphaenoides* spp.) of the northeastern Pacific. *J. Parasit.* **60:** 655-659

Received on 13th October,1995 ; accepted on 13th May, 1996

Acta Protozoologica (1996) 35: 335 - 338

ACTA
PROTOZOOLOGICA

Kudoa cascasia sp.n. (Myxosporea: Kudoidae) Parasitic in the Mesentery of *Sicamugil cascasia* (Ham.) from Hooghly Estuary of West Bengal, India

Nirmal Kumar SARKAR and Saibal RAY CHAUDHURY

Department of Zoology, Rishi Bankim Chandra College, Naihati, West Bengal, India

Summary. A new myxosporean *Kudoa cascasia* sp.n. (Myxosporea: Kudoidae) is described from the mesentery associated with the anterior intestine of *Sicamugil cascasia* (Hum.), a mugilid fish of the Hooghly estuary of West Bengal, India. The new Myxosporean species forms cream colour cysts in the mesentery; spores are quadrate in basal or apical view but triangular or pyramidal in side view with a truncate apex; sutures are distinct only at the periphery; shell valves are smooth and symmetrical with no lateral inflation; four small, equal and pyriform polar capsules converging towards the apex; dimensions of the spore and the polar capsule are 6.6 x 8.2 x 7.6 μm and 3.11 x 1.62 μm, respectively.

Key words: Hooghly estuary, *Kudoa cascasia* sp.n., Kudoidae, mesentery, Mugilidae, Myxosporea, *Sicamugil cascasia* (Ham.).

INTRODUCTION

During the course of investigation about the parasitic protozoa of fish, we came across some myxosporean species from some mugilid fish. Since the spore of this myxosporean species are quadrate, four shell valves with corresponding number of pyriform polar capsules that converged anteriorly, it is described under *Kudoa* Meglitsch, 1947.

MATERIALS AND METHODS

All necropsies were conducted on frozen fish. The myxosporean parasite obtained from the mesentery was studied in detail at 1500x from wet smears treated with Lugol's iodine solution and from dry smears stained with Giemsa after fixation in absolute Methanol. Various concentrations of potassium hydroxide solutions (2-10%) and a saturated solution of urea were used to extrude the polar filament of the spores. The India ink method (Lom and Vávra 1963) was employed to detect the mucous envelope of the spore. All the measurements were given in micrometer (μm). The illustrations were drawn with the aid of a camera lucida and the photomicrographs were made with VFB Carl Zeiss, Jena, Photomicroscope III.

Address for correspondence: Nirmal Kumar Sarkar, Department of Zoology, Rishi Bankim Chandra College, Naihati, 743165, West Bengal, India

OBSERVATIONS

Kudoa cascasia sp.n. (Figs. 1,2)

While necropsies were conducted on the frozen hosts, a few large (1.0 to 1.5 mm in diameter) cream colour cysts were isolated from the mesentery associated with the anterior part of the intestine. There were no developmental stages in the content of the ruptured cysts except spores. The mature spores were quadrate in basal and apical view (Fig. 1a,b,d,e) while in side view, the spores were triangular or pyramidal with a turncate apex and had

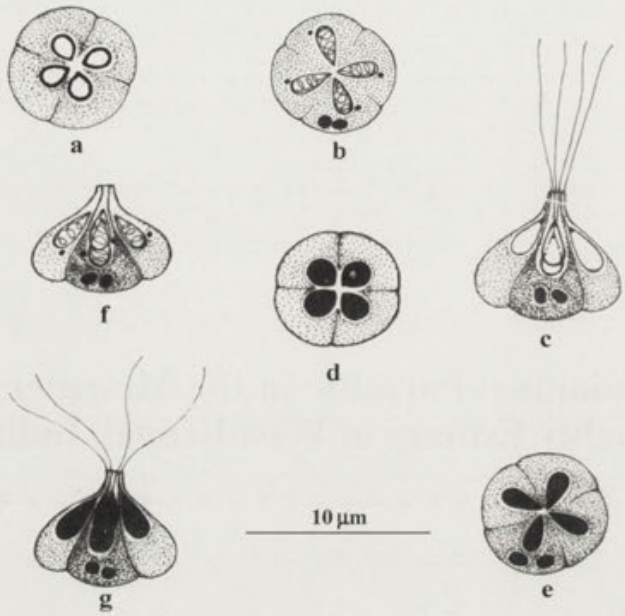

Fig. 1 a - g. Spores of *Kudoa cascasia* sp.n. a,b - fresh spores in basal and apical view respectively (Lugol's iodine). c - fresh spore in side view with extruded polar filament (Lugol's iodine). d,e - stained spores in basal and apical view respectively (Giemsa). f - fresh spore in side view (Lugol's iodine). g - stained spore in side view with extruded polar filaments (Giemsa)

a posterior wavy surface (Fig. 1 b,c,f,g). Each of the four shell valves showed a posterior swelling and had a small, elongately pyriform polar capsule (Fig. 1 b,d,f,g). The four shell valves were thin-walled, symmetrical, smooth and tender and had no lateral inflation. The four polar capsules were small, equal, elongately pyriform and converged towards the truncate apex (Fig. 1 c,f,g). The width of the spore was always greater than its length. The polar filament in the polar capsule was discernible; four polar filaments were extruded from each spore when treated with the saturated solution of urea. Each polar filament was short and thread-like (Fig. 1 c,g). The sutures were fine and visible only at periphery between the two adjacent shell valves of the quadrate spore but were obscured at the centre. The extra-capsular cavity of the quadrate spore was filled with a mass of binucleated granular sporoplasm behind the polar capsules. There was no iodinophilous vacuole in the sporoplasm and no mucous envelope around the spore.

Measurement. Based on twenty five fresh spores from one frozen host; range is given with mean and standard deviation in the parentheses:

Spore:

Length	6.0-8.0 (6.6 ± 0.6324)
Width	7.0-9.0 (8.2 ± 0.5075)
Thickness	7.0-8.0 (7.6 ± 0.3723)

Polar capsule:

Length	2.5-3.5 (3.1 ± 0.3643)
Width	1.2-2.04 (1.62 ± 0.327)

Infection locus : mesentery

Incidence : 1/30 (3.33%)

Pathogenicity: not apparent.

Host : *Sicamugil cascasia* (Ham.)

Period of infection : July - August, 1994

Locality : Hooghly estuary, West Bengal, India

Material : syntypes on slide No. MzK - 10, deposited to the Department of Zoology, Rishi Bankim Chandra College, Naihati, West Bengal, India.

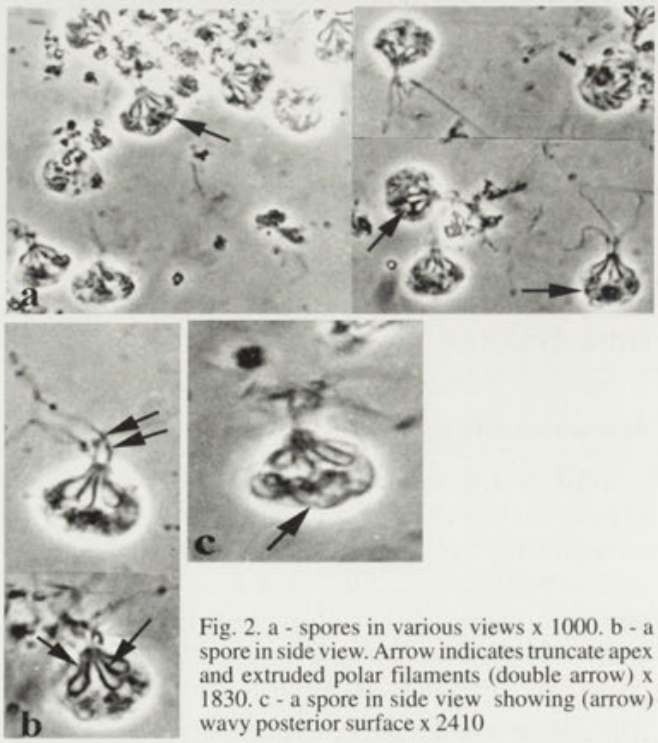

Fig. 2. a - spores in various views x 1000. b - a spore in side view. Arrow indicates truncate apex and extruded polar filaments (double arrow) x 1830. c - a spore in side view showing (arrow) wavy posterior surface x 2410

DISCUSSION

Of the thirty five species of *Kudoa* Meglitsch, 1947 to-date (Lom et al. 1992) seven species of *Kudoa* are reported from India (Tripathi 1951; Narasimhamurti and Kalavati 1979a,b; Sarkar and Mazumder 1983; Sandeep et al. 1986; Sarkar and Ghosh 1991). Among the *Kudoa* spp. recorded from the countries other than India, the spore of the present species both in basal and apical view, appears quadrate in shape, and resembles the spores of *Kudoa clupeidae* (Hahn, 1917) Meglitsch, 1947, *K. quadratum* (Thelohan, 1895) Meglitsch, 1947, *K. funduli* (Hahn, 1915) Meglitsch, 1948, *K. crumena* Iversen and Van Meter, 1967, *K. alliaria* Shulman and

Table 1. A comparative account of the related *Kudoa* spp. with the present species :

Parasite (Host)	Spore	Polar capsule	Infection site
Kudoa clupeidae (Hahn) Meglisch, 1947 (*Brevoortia tyrannus*)	Oval, sharply attenuated anterior end, lateral inflation of shell valve low, near capsular surface; 5.1 x 7.4 µm	Pyriform, equal, 5.1µm x 1.0 µm	Body musculature
K. quadratum (Thelohan) Meglitsch, 1947 (*Myxocephalus scorpius*)	Quadrate, lateral inflation low, near the base of the spore, posterior edge pointed; 6.0 - 7.0 x 7.4 µm	Pyriform, equal, 2.0 µm in length	Muscle
K. funduli (Hahn) Meglitsch, 1948 (*Fundulus heteroclitus*)	Pyramidal, sharply attenuated anterior end, lateral inflation low, near the capsular end; 8.4 x 6.7 µm	Pyriform, equal 3.3 x 1.5 µm	Muscle and fins
K. crumena Iversen & Van Meter, 1967 (*Scomberomorus maculatus*)	Quadrate, apical end truncate, no lateral inflation, 7.5 x 9.9 µm	Pyriform, equal 4.0 x 2.5 µm	Muscle
K. alliaria Shulman & Kovaleva, 1979; in Kovaleva et al 1979 (*Micromesticus australis*)	Quadrate, sutural lines distinct, no lateral inflation, 7.0 - 8.0 x 8.0 - 9.0 x 9.0 - 10.0 µm	Pyriform, equal, 2.4 x 1.8 µm	Muscle
K. ciliatae Lom et al., 1992 (*Sillago ciliata*)	Rounded, rectangular in apical view, rounded, pyramidal in side view, sutural line rarely visible, lateral inflation present, 5.5 x 5.4 x 6.6 µm	Pyriform, 'not quite equal', 2.4 x 1.4 µm	Smooth muscle of intestine wall
Kudoa cascasia sp.n. (*Sicamugil cascasia*)	Quadrate in apical view, triangular or pyramidal in side view, sutures distinct at periphery, apical end truncate, no lateral inflation, 6.6 x 8.2 x 7.6 µm	Pyriform, equal, 3.11 x 1.62 µm	Mesentery near intestine

Table 2. A Comparison of the present species with other *Kudoa* spp. described from India:

Parasite (Host)	Spore	Polar capsule	Infection site
Kudoa chilkaensis Tripathi, 1951 (*Strongilura strongilura*)	Rectangular in anterior view, lateral inflation low, 5.5 x 7.3 µm	Pyriform, equal, 3.5 x 1.0 - 1.5 µm, polar filament 10.0 µm	Muscle
K. tetraspora Narasimhamurti & Kalavati, 1979a (*Mugil cephalus*)	Quadrate in polar view, deep notches at the sutural lines, 9.0 x 9.0 µm	Club-shaped, equal, 3.4 - 4.0 x 1.5 - 1.8 µm, polar filament thick, 10.0 - 12.0 µm	Tissue around the optic lobe
K. sphyraeni Narasimhamurti & Kalavati, 1979b (*Splryraena jello*)	Quadrate in polar view, sutural lines faint, no lateral inflation, 9.4 x 9.8 µm	Club-shaped, equal, 3.6 x 1.0 - 1.6 µm, polar filament thick, 20.0 - 28.0 µm	Muscle of the gut
K. tachysurae Sarkar & Mazumder, 1983 (*Tachysurus tenuispines*)	Quadrate, notches at sutural lines, lateral inflations unequal, 4.87 x 7.55 x 5.5 µm	Pyriform, unequal, 3.25 x 2.45 µm and 1.45 x 1.4 µm	Gallbladder

Table 2. (con)

K. bengalensis Sarkar & Mazumder, 1983 (*Tachysurus platystomus*)	Stellate with four equal lateral inflations, small notches at indistinct sutures, 7.85 x 8.44 µm	Tubular, equal, 3.8 x 1.95 µm	Skeletal muscle
K. atropi Sandeep et al., 1986 (*Atropus atropus*)	Quadrate with deep notches, sutural lines distinct, no lateral inflation, 10.0 x 10.0 x 9.0 µm occasional presence of five shell valves, mucous envelope present	Pyriform, equal 3.3 x 1.7 µm polar filament 10.0 µm long, occasional presence of five polar capsules	Gill
K. haridasae Sarkar & Ghosh, 1991 (*Mugil parsina*)	Stellate with well developed lateral inflations, suture indistinct, 5.0 x 10.07 µm	Pyriform, equal, 1.75 x 1.11 µm, polar filament 10.0 µm long	Gallbladder
Kudoa cascasia sp.n. (*Sicamugil cascasia*)	Quadrate in apical view, triangular or pyramidal in side view, suture distinct at periphery, no lateral inflation, apical end truncate, 6.6 x 8.2 x 7.6 µm	Pyriform, equal, 3.11 x 1.62 µm	Mesentery near the intestine

Kovaleva, 1979 (cited from Kovaleva et al. 1979), and *K. ciliatae* Lom et al., 1992. However, except for the spore of *K. crumena*, none of the *Kudoa* spp. mentioned above, possess a narrow truncate apex. Moreover, the spores of those *Kudoa* spp. also differ markedly from the spore of the present species by their mensural data (Table 1) as well as by the presence of lateral inflations of the shell valves which are absent in the spore of the present species. Further, the spore of *K. crumena* has a truncate apex in side view like the spore of the present species. However, the spore of the *Kudoa* sp. in study, is smaller than that of *K. crumena* (7.5, 9.9 µm) and it has narrower neck. A comparison of the present species with the seven *Kudoa* spp. recorded from India also reveals that the present *Kudoa* sp. having a truncate apex, absence of lateral inflations of shell valves and different mensural data (Table 2) is conspicuously distinct from the other *Kudoa* spp. The myxosporean species in study is, therefore, considered as a new species and is designated as *Kudoa cascasia* sp.n. after the specific name of its host.

Acknowledgements. We are grateful to Dr A. K. Roy, Teacher-in-charge, Rishi Bankim Chandra Collage, Naihati for laboratory facilities, to Professor Dr A. K. Duttagupta, University of Calcutta for microphotography, to Sri A. Mazumder for statistical analysis, Professor K. Goswami for computer and Dr K. K. Misra for sincere cooperation.

REFERENCES

Iversen E.S., Van Meter N. N. (1967) A new Myxosporian (Sporozoa) infecting the Spanish Mackerel. *Bull. Mar. Sci.* **17:** 268 - 273

Kovaleva A.A., Shulman S.S., Yakovlev B.N. (1979) Systematic and Ecology of Cnidosporidian spores. *Proc. Zool. Inst. USSR.* **87:** 42 - 64

Lom J., Vávra J. (1963) Mucous envelopes of spores of the Subphylum Cnidospora (Doflein, 1901). *Vest. Cs. Zool. Spol.* **27:** 4 - 6

Lom J., Rohde K., Dyková I. (1992) Protozoan parasites of Australian fishes I. New species of the genera *Coccomyxa* Leger et Hesse, 1907, *Ortholinea* Shulman, 1962 and *Kudoa* Meglitsch, 1947 (Myxozoa, Myxosporea). *Folia Parasitol.* **39:** 289 - 306

Meglitsch P.A. (1947) Studies on Myxosporidia from the Beaufort region. II Observations on *Kudoa clupeidae* (Hahn) gen. nov. *J. Parasitol.* **33:** 271 - 277

Meglitsch P.A. (1948) On *Kudoa funduli* (Hahn). *Trans. Amer. Micros. Soc.* **67:** 272 - 274

Narasimhamurti C.C., Kalavati C. (1979a) *Kudoa tetraspora* n.sp.(Protozoa : Myxosporidia) parasitic in the brain tissue of *Mugil ceplialus. Proc. Ind. Acad. Sci.* **88B:** 85-89

Narasimhamurti C.C., Kalavati C. (1979b) Kudoa sphyraeni n.sp.(Protozoa: Myxosporidia) parasitic in the muscles of the gut of the estuarine fish *Sphyraena jello* Cuv. *Proc. Ind. Acad, Sci.* **88B:** 265-269

Sandeep B.V., Kalavati C., Narasimhamurti C.C. (1986) *Kudoa atropi* sp.n. (Myxosporea: Multivalvulida) a myxosporidian parasite from the gills of *Atropus atropus. Vest. Cs.Spol, Zool.* **50:** 132 - 135

Sarkar N. K., Ghosh S. (1991) Two new myxosporida (Myxozoa : Myxosporea) from estuarine teleost fishes (Mugilidae) of West Bengal, India. *Proc. Zool. Soc. Calcutta* **44:** 131 - 135

Sarkar N.K.Mazumder S. (1983) Studies on myxosporidian parasites (Myxozoa: Myxosporea) from marine fishes in West Bengal, India. I. Description of three news species from *Tachysurus* spp. *Arch. Protistenkd.* **127:** 59 - 63

Tripathi Y.R. (1951) Studies on parasites of Indian fishes, I. Protozoa: Myxosporidia together with a cheek list of parasitic protozoa described from Indian fishes. *Rec. Indian Mus.* **50:** 63 - 89

Received on 13th October, 1995 ; accepted on 13th May,1996

Acknowledgement

The editors wish to acknowledge the help of the following colleagues who have served as reviewers for one or more manuscripts submitted for publication in our journal.

Andre Adoutte
Sally L. Allen
Charles F. Austerberry
Sihem Bahri
Tilly Bakker-Grunwald
G. B. Bouck
Gaylen Bradley
C. Graham Clark
Giuliano Colombetti
John O. Corliss
Peter Daszak
Isabelle Desportes-Livage
Jean Dragesco
Donald W. Duszynski
Flemming Ekelund
Marc T. Elskens
Stanisław Fabczak
Tom Fenchel
Wilhelm Foissner
Agnes K. Fok
Zbigniew Gaciong
Andrzej Grębecki
Juan C. Gutiérrez
Klaus Hausmann
Donat-P. Häder
Fred G. Hochberg
Kazumi Hoshide
J. van Houten
John Janovy, Jr.
Jan-Owe Josefsson
Włodzimierz Korohoda
Hans-Werner Kuhlmann
Jan H. Landsberg
H. Norbert Lanners
J. I. Ronny Larsson
John J. Lee
Vagn Leick
Ewa Lenartowicz
Ryszard Ligowski
Barbara Machnicka
Tadao Matsuoka
Jean-Pierre Mignot
Ojvind Moestrup
Kalman Molnar
Alan Musqrave
Miklós Müller
Jytte R. Nilsson
Gianfranco Novarino
Klaus Odening
David J. Patterson
Malcolm Potts
Sarah L. Poynton
Igor B. Raikov
Nicola Ricci
Siegfried Scherer
Joachim E. Schultz
Robert E. Sinden
Ariadna Sitjá Bobadilla
Humphrey G. Smith
Wilhelm Schönborn
Milena Svobodová
Nicole Tandeau-de-Marsac
Arno Tiedtke
Steve J. Upton
Jiri Vávra
Patricia Walne
Alan Warren
Barry J. Wicklow
Norbert Wilbert

Author Index: Acta Protozoologica 35 (1-4) 1996

Subject Index: Acta Protozoologica 35 (1-4) 1996

ACTA PROTOZOOLOGICA

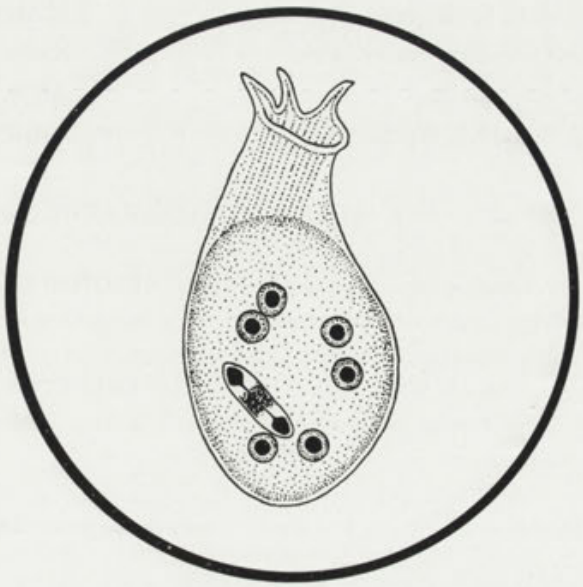

NENCKI INSTITUTE OF EXPERIMENTAL BIOLOGY
WARSAW, POLAND
1996
VOLUME 35
ISSN 0065-1583

Polish Academy of Sciences
Nencki Institute of Experimental Biology

ACTA PROTOZOOLOGICA

International Journal on Protistology

ACTA PROTOZOOLOGICA appears quarterly.

The price (including Air Mail postage) of subscription to ACTA PROTOZOOLOGICA at 1997 is: US $ 180.- by institutions and US $ 120.- by individual subscribers. Limited number of back volumes at reduced rate are available. TERMS OF PAYMENT: Cheque, money oder or payment to be made to the Nencki Institute of Experimental Biology. Account Number: 370044-3522-2700-1-73 at Państwowy Bank Kredytowy XIII Oddz. Warszawa, Poland. WITH NOTE: ACTA PROTOZOOLOGICA! For matters regarding ACTA PROTOZOOLOGICA, contact Managing Editor, Nencki Institute of Experimental Biology, ul. Pasteura 3, 02-093 Warszawa, Poland; Fax: 48-22 225342; E-mail: jurek@ameba.nencki.gov.pl

Front cover: *Stephanopogon colpoda.* In: I. B. Raikov - Kariologiya prosteishikh. Izd. Nauka, Leningrad 1967

Printed at the MARBIS, ul. Kombatantów 60, 05-070Sulejówek, Poland

Contents of Volume 35 (1-4) 1996

Number 1

Number 2

Number 3

Number 4

INSTRUCTIONS FOR AUTHORS

ACTA PROTOZOOLOGICA publishes original papers embodying the results of experimental or theoretical research in all fields of protistology with the exception of faunistic notices of local character and purely clinical reports. Short (rapid) communications are acceptable but also long review articles. The papers should be as concise as possible, be written in English. Submission of a manuscript to ACTA PROTOZOOLOGICA implies that it has not been submitted for publication elsewhere and that it contains unpublished, new information. There are no page charges except colour illustration. Names and addresses of suggested reviewers will be appreciated. In case of any question please do not hesitate to contact Editor. Authors should submit papers to:

Miss Małgorzata Woronowicz
Managing Editor of ACTA PROTOZOOLOGICA
Nencki Institute of Experimental Biology,
ul. Pasteura 3
02-093 Warszawa, Poland
Fax:48- 22 225342

Organization of Manuscripts

Submissions

Please enclose three copies of the text, one set of original of line drawings (without lettering!) and three sets of copies with lettering, four sets of photographs (one without lettering). In case of photographs arranged in the form of plate, please submit one set of original photographs unmounted and without lettering, and three sets of plates with lettering.

The ACTA PROTOZOOLOGICA prefers to use the author's word-processor disks (3.5"and 5.25" format IBM or IBM compatible, and MacIntosh 6 or 7 system on 3.5" 1.44 MB disk only) of the manuscripts instead of rekeying articles. If available, please send a copy of the disk with your manuscript. Preferable programs are Word or Wordperfect for Windows and DOS Wordperfect 5.1. Disks will be returned with galley proof of accepted article at the same time. Please observe the following instructions:

1. Label the disk with your name: the word processor/computer used, e.g. IBM; the printer used, e.g. Laserwriter; the name of the program, e.g. Word for Windows or Wordperfect 5.1.
2. Send the manuscript as a single file; do not split it into smaller files.
3. Give the file a name which is no longer than 8 characters.
4. If necessary, use only italic, bold, underline, subscript and superscript. Multiple font, style or ruler changes, or graphics inserted the text, reduce the usefulness of the disc.
5. Do not right-justify and use of hyphen at the end of line.
6. Avoid the use of footnotes.
7. Distinguish the numerals 0 and 1 from the letters O and l.

Text (three copies)

The text must be typewritten, doublespaced, with numbered pages. The manuscript should be organized into Summary, Key words, Abbreviations used, Introduction, Materials and Methods, Results, Discussion, Acknowledgments, References, Tables and Figure Legends. The Title Page should include the full title of the article, first name(s) in full and surname(s) of author(s), the address(es) where the work was carried out, page heading of up to 40 characters. The present address for correspondence, Fax, and E-mail should also be given.

Each table must be on a separate page. Figure legends must be in a single series at the end of the manuscript. References must be listed alphabetically, abbreviated according to the World List of Scientific Periodicals, 4th ed. (1963). Nomenclature of genera and species names must agree with the International Code of Zoological Nomenclature, third edition, London (1985) or International Code of Botanical Nomenclature, adopted by XIV International Botanical Congress, Berlin, 1987. SI units are preferred.

Examples for bibliographic arrangement of references:

Journals:

Häder D-P., Reinecke E. (1991) Phototactic and polarotactic responses of the photosynthetic flagellate, *Euglena gracilis*. *Acta Protozool.* **30:** 13-18

Books:

Wichterman R. (1986) The Biology of Paramecium. 2 ed. Plenum Press, New York

Article's from books:

Allen R. D. (1988) Cytology. In: Paramecium, (Ed. H.-D. Görtz). Springer-Verlag, Berlin, Heidelberg, 4-40

Zeuthen E., Rasmussen L. (1972) Synchronized cell division in protozoa. In: Research in Protozoology, (Ed. T. T. Chen). Pergamon Press, Oxford, **4:** 9-145

Illustrations

All line drawings and photographs should be labeled, with the first author's name written on the back. The figures should be numbered in the text as arabic numerals (e.g. Fig. 1). Illustrations must fit within either one column (86 x 231 mm) or the full width and length of the page (177 x 231 mm). Figures and legends should fit on the same page. Lettering will be inserted by the printers and should be indicated on a tracing-paper overlay or a duplicate copy.

Line drawings (three copies + one copy without lettering)

Line drawings should preferably be drawn about twice in size, suitable for reproduction in the form of well-defined line drawings and should have a white background. Avoid fine stippling or shading. Computer printouts of laser printer quality may be accepted, however *.TIF, *.PCX, *.BMP graphic formats on disk are preferred.

Photographs (three copies + one copy without lettering)

Photographs at final size should be sharp, with a glossy finish, bromide prints. Photographs grouped as plates (in size not exceeding 177 x 231 mm **including legend**) must be trimmed at right angles accurately mounted and with edges touching and mounted on firm board. The engraver will then cut a fine line of separation between figures. Magnification should be indicated. Colour illustration on transparent positive media (slides 60 x 45mm, 60 x 60mm or transparency) are preferred.

Proof sheets and offprints

Authors will receive one set of page proofs for correction and are asked to return these to the Editor within 48-hours. Fifty reprints will be furnished free of charge. Orders for additional reprints have to be submitted with the proofs.

Indexed in Chemical Abstracts Service, Current Contents (Agriculture, Biology and Environmental Sciences), LIBREX-AGEN, Protozoological Abstracts. POLISH SCIENTIFIC JOURNALS CONTENTS - AGRIC.& BIOL. SCI. data base is available in INTERNET under URL (UNIFORM RESOURCE LOCATOR) address: http://saturn.ci.uw.edu.pl /psjc/ or http://ciuw.warman.org.pl /alf/psjc/ any WWW browser; in graphical operating systems: MS Windows, Mac OS, X Windows - mosaic and Netscape programs and OS/2 - Web Explorer program; in text operating systems: DOS, UNIX, VM - Lynx and www programs.

ACTA
PROTOZOOLOGICA

ORIGINAL ARTICLES

1996 NOVEMBER
VOLUME 35 NUMBER 4